THE MULTI-SPAN MITOCHONDRIAL OUTER MEMBRANE PROTEIN OM14 FOLLOWS DIFFERENT BIOGENESIS PATHWAYS

Dissertation
der Mathematisch-Naturwissenschaftlichen Fakultät
der Eberhard Karls Universität Tübingen
zur Erlangung des Grades eines
Doktors der Naturwissenschaften
(Dr. rer. nat.)

vorgelegt von
Jialin Zhou
aus Weihai, China

Tübingen
2022

THE MULTI-SPAN MITOCHONDRIAL OUTER MEMBRANE PROTEIN OM14 FOLLOWS DIFFERENT BIOGENESIS PATHWAYS

Dissertation
der Mathematisch-Naturwissenschaftlichen Fakultät
der Eberhard Karls Universität Tübingen
zur Erlangung des Grades eines
Doktors der Naturwissenschaften
(Dr. rer. nat.)

vorgelegt von
Jialin Zhou
aus Weihai, China

Tübingen
2022

Gedruckt mit Genehmigung der Mathematisch-Naturwissenschaftlichen Fakultät
der Eberhard Karls Universität Tübingen.

Tag der mündlichen Qualifikation:	22.04.2022
Dekan der Math.-Nat. Fakultät:	Prof. Dr. Thilo Stehle
1. Berichterstatter:	Prof. Dr. Doron Rapaport
2. Berichterstatterin:	Prof. Dr. Gabriele Dodt

Erklärung / Declaration: Ich erkläre, dass ich die zur Promotion eingereichte Arbeit mit dem Titel:

"The multi-span mitochondrial outer membrane protein Om14 follows different biogenesis pathways "

selbständig verfasst, nur die angegebenen Quellen und Hilfsmittel benutzt und wörtlich oder inhaltlich übernommene Stellen als solche gekennzeichnet habe. Ich versichere an Eides statt, dass diese Angaben wahr sind und dass ich nichts verschwiegen habe. Mir ist bekannt, dass die falsche Abgabe einer Versicherung an Eides statt mit Freiheitsstrafe bis zu drei Jahren oder mit Geldstrafe bestraft wird.

I hereby declare that I have produced the work entitled ***"The multi-span mitochondrial outer membrane protein Om14 follows different biogenesis pathways "***, submitted for the award of a doctorate, on my own (without external help), have used only the sources and aids indicated and have marked passages included from other works, whether verbatim or in content, as such. I swear upon oath that these statements are true and that I have not concealed anything. I am aware that making a false declaration under oath is punishable by a term of imprisonment of up to three years or by a fine.

Tübingen, den ....

Datum / Date Unterschrift / Signature

CONTENTS

1

LIST OF ABBREVIATIONS

AAC	ADP/ATP carrier
ATP	adenosine triphosphate
CE	carbonate extraction
CS	carrier signature
FL	full-length
GFP	green fluorescent protein
Hsp70	heat shock protein 70
IMM	inner mitochondrial membrane
IMS	intermembrane space
MIM	mitochondrial import
MAM	mitochondrialen Außenmembranen
mtDNA	mitochondrial DNA
OMM	outer mitochondrial membrane
PA	phosphatidic acid
tRNA	transfer RNA
TPR	tetratricopeptide repeat
TMD	transmembrane domain
TIM	translocase of the inner membrane
TOM	translocase of the outer membrane
VDAC	voltage-dependent anion channel
WT	wild type
WCL	whole cell lysate

2

SUMMARY

Mitochondria are essential eukaryotic organelles for energy production as well as various cellular activities. Dysfunction of mitochondria is closely related to cell death and can result in severe human diseases such as neurodevelopmental and metabolic disorders. The maintenance of proper mitochondrial function is achieved by proteins located in different mitochondrial sub-compartments.

Proteins embedded in the outer mitochondrial membrane (OMM) with several transmembrane segments are defined as multi-span proteins and considerable efforts have been made to understand their biogenesis. Newly synthesized precursors of these proteins are believed to be recognized by the receptor Tom70 on the surface of mitochondria. However, the precise contribution of Tom70 to this process is poorly understood. In this study, I analyzed the involvement of the Tom70 cytosolic domain in the recognition of different substrates. I found that Tom70 could directly interact with multi-span OMM proteins as well as function as a docking site for precursor-bound chaperones. The relative importance of the two functions of Tom70 varies from substrate to substrate.

After the initial recognition, multi-span outer membrane precursor proteins are passed on to the MIM complex which further facilitate their integration into the outer membrane. Nevertheless, little is known about the targeting signal within such substrates and the involvement of other potential factors in their biogenesis. Interestingly, another theory suggested that the integration of multi-span OMM proteins is only lipid-regulated and can occur spontaneously without the help of any import factors. In my study, I tried to reconcile this apparent discrepancy and obtain a deep knowledge of the biogenesis of these proteins using the yeast multi-span OMM protein Om14 as a model protein.

I first examined the targeting behavior of different truncation variants and found out that multiple targeting signals collectively contributes to the perfect mitochondrial targeting specificity.

Next, I employed a specific import assay to test the effect of different elements on the insertion efficiency of Om14. The results suggest that none of the cytosolic exposed domain of proteinaceous factors is essential for the Om14 biogenesis process. In contrast, I could demonstrate that both Mim1 and Porin are involved in the optimal membrane integration of Om14.

In addition, I analyzed the influence of the unfolding of newly synthesized Om14, the hydrophobicity of its transmembrane segments, and an increased membrane fluidity on the efficiency of its membrane integration. I observed that unfolding of the substrate protein and elevated temperature increased the import efficiency of Om14 whereas reduced hydrophobicity of the second transmembrane segment decreased it.

Collectively, my results provide a novel insight into the biogenesis of the multi-span OMM protein Om14, suggesting the coexistence of many alternative routes in which both proteinaceous factors and membrane behavior contribute to varying degrees to the combined insertion efficiency.

3

ZUSAMMENFASSUNG

Mitochondrien sind wichtige eukaryontische Organellen für die Energieerzeugung sowie für verschiedene zelluläre Aktivitäten. Eine Funktionsstörung der Mitochondrien steht in engem Zusammenhang mit dem Zelltod und kann beim Menschen zu schweren Krankheiten wie neurologischen Entwicklungsstörungen und Stoffwechselstörungen führen. Die Aufrechterhaltung der ordnungsgemäßen mitochondrialen Funktion wird durch Proteine aus verschiedenen mitochondrialen Subkompartimenten gewährleistet.

Proteine, die sich in der mitochondrialen Außenmembranen (MAM) befinden und mehrere Transmembrandomänen aufweisen, werden als „multispan"-Proteine bezeichnet. Zahlreiche Forschungsarbeiten haben versucht, die Biogenese von Multispan MAM-Proteinen zu verstehen. Es wird angenommen, dass die neu synthetisierten MAM Vorläuferproteine vom Rezeptor Tom70 auf der Oberfläche der Mitochondrien erkannt werden. Der genaue Beitrag von Tom70 zu diesem Prozess ist jedoch nur unzureichend bekannt. In dieser Studie habe ich die Rolle, die die zytosolische Domäne von Tom70 bei der Erkennung verschiedener Substrate spielt untersucht. Hierbei konnte ich nachweisen, dass Tom70 direkt mit Multispan MAM-Proteinen interagieren kann und auch als Andockstelle für an Vorläufer-gebundene Chaperone fungiert.

Nach der Erkennung werden die Multispan Vorläufer der Außenmembran an den MIM-Komplex weitergeleitet, der ihre Integration in die Außenmembran weiter erleichtert. Dennoch ist wenig über das Zielsignal innerhalb solcher Substrate und die Beteiligung anderer potenzieller Faktoren an ihrer Biogenese bekannt. Eine andere Theorie besagt, dass die Integration von Multispan MAM-Proteinen nur durch Lipide reguliert wird und spontan ohne die Hilfe von Importfaktoren erfolgen kann. In meiner Studie habe ich versucht, diese Diskrepanz auszugleichen und die Biogenese dieser Proteine anhand des Multispan Hefe MAM-Proteins Om14 als Modellprotein zu erforschen.

Ich habe zunächst das Targeting-Verhalten verschiedener Trunkierungsvarianten untersucht und dabei herausgefunden, dass mehrere Targeting-Signale gemeinsam zu einer perfekten mitochondrialen Targeting-Spezifität beitragen.

Als Nächstes habe ich einen spezifischen Importtest durchgeführt, um die Auswirkungen verschiedener Elemente auf die Insertionseffizienz von Om14 zu testen. Die Ergebnisse deuten darauf hin, dass keine der zytosolisch ex-

ponierten Domänen der Proteinös-Faktoren für den Om14-Biogeneseprozess wesentlich ist. Gleichzeitig wurde nachgewiesen, dass Mim1 und Porin beide an der optimalen Membranintegration von Om14 beteiligt sind.

Darüber hinaus analysierte ich den Einfluss der Entfaltung von neu synthetisiertem Om14, der Hydrophobizität seiner Transmembransegmente und einer erhöhten Membranfluidität auf die Effizienz seiner Membranintegration. Ich beobachtete, dass die Entfaltung des Substratproteins und eine erhöhte Temperatur die Importeffizienz von Om14 erhöhten, während eine verringerte Hydrophobizität des zweiten Transmembransegments diese reduzierte.

Insgesamt bieten meine Ergebnisse einen neuen Einblick in die Biogenese des Multispan MAM-Proteins Om14 und deuten auf die Koexistenz zahlreicher alternativer Wege hin, bei denen sowohl proteinhaltige Faktoren als auch das Membranverhalten in unterschiedlichem Maße zur kombinierten Insertionseffizienz beitragen.

4

LIST OF PUBLICATIONS CONTAINED IN THIS THESIS

1. Sandra Backes, Yury S. Bykov, Tamara Flohr, Markus Räschle, **Jialin Zhou**, Svenja Lenhard, Lena Krämer, Timo Mühlhaus, Chen Bibi, Cosimo Jann, Justin D. Smith, Lars M. Steinmetz, Doron Rapaport, Zuzana Storchová, Maya Schuldiner, Felix Boos, and Johannes M. Herrmann (2021). The chaperone-binding activity of the mitochondrial surface receptor Tom70 protects the cytosol against mitoprotein-induced stress. *Cell Reports*, 35(1), 108936.
doi: 10.1016/j.celrep.2021.108936.

2. **Jialin Zhou**, Martin Jung, Kai Dimmer, and Doron Rapaport (2022). The multi-factor modulated biogenesis of the mitochondrial multi-span protein Om14. *Journal of Cell Biology*, 221(4), e202112030.
doi: 10.1083/jcb.202112030.

5

PERSONAL CONTRIBUTION TO THE PUBLICATIONS CONTAINED IN THIS THESIS

1. Sandra Backes, Yury S. Bykov, Tamara Flohr, Markus Räschle, **Jialin Zhou**, Svenja Lenhard, Lena Krämer, Timo Mühlhaus, Chen Bibi, Cosimo Jann, Justin D. Smith, Lars M. Steinmetz, Doron Rapaport, Zuzana Storchová, Maya Schuldiner, Felix Boos, and Johannes M. Herrmann (2021). The chaperone-binding activity of the mitochondrial surface receptor Tom70 protects the cytosol against mitoprotein-induced stress. *Cell Reports*, 35(1), 108936.
doi: 10.1016/j.celrep.2021.108936.

I isolated mitochondria from wild type + pYX142, *tom70/71*Δ + pYX142, *tom70/71*Δ + pYX142-mtTah1, and *tom70/71*Δ + pYX142-mtTah1(K8A) cells and analyzed by Western blotting the steady levels of their proteins (Fig. 6A and B).

2. **Jialin Zhou**, Martin Jung, Kai Dimmer, and Doron Rapaport (2022). The multi-factor modulated biogenesis of the mitochondrial multi-span protein Om14. *Journal of Cell Biology*, 221(4), e202112030.
doi: 10.1083/jcb.202112030.

I first examined the mitochondrial targeting capacity of full-length Om14 and its truncated variants through fluorescence microscopy and subcellular fractionation (Fig. 1). To analyze the involvement of Tom70 and other substitutive receptors in the biogenesis of Om14, I performed peptide scan assay and *in vitro* import experiments (Fig. 2 and Fig. S2). Next, I tested the contribution of the transmembrane hydrophobicity to the membrane integration capacity of Om14 both *in vivo* and *in vitro* (Fig. 3 and Fig. S4). To investigate the effect of membrane properties and the protein structure on the biogenesis of Om14, I performed *in vitro* import experiments using increased import temperature or urea-denatured proteins (Fig. 4). Then I isolated mitochondria from wild type, *mim1*Δ*, por1*Δ, *om45*Δ*, and mim1*Δ*por1*Δ cells and I performed several *in vitro* import experiments, BN-PAGE, and carbonate extractions to show the role of Mim1, Porin, and Om45 in the biogenesis of Om14 (Figs. 5 and 6, Figs. S1 and S3). I participated in writing the manuscript and prepared all the figures.

6

INTRODUCTION

6.1 ORIGIN AND STRUCTURE OF MITOCHONDRIA

Mitochondria are double-membrane-bounded organelles, which possess their own circular mitochondrial DNA (mtDNA), ribosomes composed of 30S and 50S subunits, and several transfer RNA (tRNA). These characteristics support the endosymbiotic theory, proposing that mitochondria originated from α-proteobacteria engulfed by either eukaryotic ancestors cells or by anaerobic archaebacteria (Dyall, Brown, and Johnson, 2004; Gray, 2012; Zimorski et al., 2014).

Mitochondria contain around 1000 proteins in yeast and 1500 in humans, of which 99 % are nuclear-encoded and produced by cytosolic ribosomes before being directed to their respective mitochondrial sub-compartment (Drwesh and Rapaport, 2020; Neupert and Herrmann, 2007; Pfanner, Warscheid, and Wiedemann, 2019; Walther and Rapaport, 2009). The remaining 1% of proteins are encoded by mtDNA and include proteins of the oxidative phosphorylation machinery (8 in yeast and 13 in human) (Lee and Han, 2017). In addition, mtDNA encodes also for several tRNAs and 2 ribosomal RNAs for the translation inside mitochondria (Epler, Shugart, and Barnett, 1970; Galper and Darnell, 1969; Lee and Han, 2017). The outer mitochondrial membrane which harbors channels for ion trafficking and protein import serves as a fence between the inner compartments of the organelle and the surrounding cellular environment. The inner mitochondrial membrane (IMM) forms cristae and separates the intermembrane space (IMS) from the matrix. Although mitochondria can exhibit variable morphologies in different types of cells, they usually form tubular shaped networks (Sogo and Yaffe, 1994), which are highly dynamic through constant fission and fusion events (Cohen et al., 2009; Friedman et al., 2011; Hermann et al., 1998).

6.2 FUNCTION OF MITOCHONDRIA

Mitochondria are mostly known as the cellular powerhouse that can metabolize nutrients to produce most of the energy needed by cells (Osellame, Blacker,

and Duchen, 2012; Spinelli and Haigis, 2018). A series of respiratory chain complexes in the IMM can efficiently generate adenosine triphosphate (ATP) through oxidative phosphorylation. Additionally, mitochondria serve as a hub for the biosynthesis of multiple biomolecules such as fatty acids, hormones, nucleotides, amino acids and heme (Spinelli and Haigis, 2018).

The proteins residing in the OMM are indispensable for the maintenance of normal cell activities. These membrane proteins are largely involved in protein biogenesis, the formation of contact sites with the endoplasmic reticulum (ER) and the nucleus, as well as mitochondrial morphology and dynamics. Dysfunction of these proteins may cause severe human neurodevelopmental disorders (Ghosh et al., 2019; Wei et al., 2020).

In higher eukaryotes, mitochondria also participate in programmed cell death (apoptosis). Several apoptogens in mitochondria promotes cell death when released into the cytosol after the permeabilization of the OMM, which further triggers the mitochondria-induced apoptosis (Osellame, Blacker, and Duchen, 2012; Wang and Youle, 2009). Furthermore, mitochondria play an essential role in many cellular activities such as calcium hemeostasis, innate immunity, autophagy, and aging (Murphy et al., 2016; Osellame, Blacker, and Duchen, 2012; West, Shadel, and Ghosh, 2011).

6.3 PROTEIN IMPORT INTO MITOCHONDRIA

As the majority of mitochondria proteins are encoded in the nucleus, a well-established import system is necessary for the transport of proteins to keep the normal morphology and proper function of mitochondria (Palmer, Anderson, and Stojanovski, 2021). Such a system in mitochondria consists of multiple protein import complexes located at both outer and inner mitochondrial membranes. The import of a single protein can follow either a unique pathway or a combination of multiple pathways (Pfanner, Warscheid, and Wiedemann, 2019; Vitali et al., 2020; Walther and Rapaport, 2009).

6.3.1 *Translocase of the outer membrane (TOM) complex*

The translocase of the outer membrane (TOM) complex is the main entrance gate on the OMM, which is involved in the biogenesis of nearly all the nuclear encoded mitochondrial proteins except some OMM proteins (Palmer, Anderson, and Stojanovski, 2021). The TOM complex is composed of three receptors (Tom70, Tom20 and Tom22), β-barrel protein Tom40, and three small

structural subunits (Tom5, Tom6, and Tom7), which possess a single α-helical transmembrane domain (TMD) (Araiso et al., 2019; Bausewein et al., 2017; Pitt and Buchanan, 2021).

The receptors Tom70 and Tom20

The receptors Tom70 and Tom20 are only transiently associated with the core complex. Besides, both of them are anchored to the OMM by a single TMD in their N-terminal (Drwesh and Rapaport, 2020; Walther and Rapaport, 2009). However, Tom20 and Tom70 have partially different substrate binding specificities (Brix et al., 1999).

Tom70 preferentially binds to mitochondrial proteins that possess an internal targeting information (Brix et al., 1999; Kreimendahl and Rassow, 2020; Kreimendahl et al., 2020). It contributes largely to the biogenesis of multi-span proteins on OMM such as Ugo1, Scm4 (Becker et al., 2011; Papić et al., 2011). It was also reported that the phosphorylation of Tom70 stimulates its interaction with the main TOM translocase (Walter et al., 2021), which further facilitates the import of carrier family proteins (Brix et al., 1999; Kreimendahl et al., 2020; Söllner et al., 1990). The cytosolic part of Tom70 contains multiple tetratricopeptide repeats tetratricopeptide repeats (TPRs). The three N-terminal TPR motifs in Tom70 and its paralog Tom71 form a dicarboxylate clamp domain and can thus interact with the C-terminus of cytosolic chaperones such as heat shock protein 70 (Hsp70) and Hsp90 (Panigrahi et al., 2015). The TPR motifs in the C-terminus, however, constitute a core binding domain for preproteins (Chan et al., 2006; Wu and Sha, 2006).

In comparison, Tom20 recognizes mainly presequence containing mitochondrial preproteins. The hydrophilic C-terminal domain exposed to the cytosol recognizes the targeting signal in the presequence and further enhances the import efficiency of preproteins by tethering the presequence to the TOM40 complex (Abe et al., 2000; Brix et al., 1999; Yamamoto et al., 2011; Yamano et al., 2008). Nevertheless, it has been observed that Tom20 can also interact with precursor proteins lacking presequence (Brix et al., 1999), suggesting that Tom20 and Tom70 might have overlapping substrates. Deficiency of either Tom20 or Tom70 does not affect the fermentative growth of yeast, however the double deletion is lethal (Ramage et al., 1993). The compromised respiration caused by the deletion of Tom20 can be restored by overexpressing Tom70 (Ramage et al., 1993), which further indicate that both receptors can function as substitutes for each other.

Tom40 forms the core protein-conducting channel

The β-barrel protein Tom40 constitutes a channel which allows the transport of preproteins across the OMM. According to the recently solved cryo-EM structure, two molecules of Tom40 can form a dimer which is stabilized by two molecular of Tom22 and one phospholipid molecule residing in-between the two monomers (Araiso et al., 2019; Bausewein et al., 2017). The structure of Tom40 central pore provides two exit sites for different substrate groups. For presequence-containing preproteins, the intermembrane space domain of Tom22 forms a presequence-binding site together with Tom40 and Tom7 near the middle of the dimeric TOM structure. Preproteins exit the Tom40 channel at this trans site and are further transferred to the receptor Tim50 of the translocase of the inner membrane (TIM) complex on the IMM (Araiso et al., 2019). For proteins lacking a presequence such as Mia substrates, carrier proteins, as well as β-barrel proteins, the N-terminal extension of Tom40 functions together with Tom5 in guiding these substrates to exit at the periphery of the dimer (Araiso et al., 2019; Becker et al., 2010).

6.3.2 *Mitochondria import (MIM) complex*

The mitochondrial import (MIM) complex represents the main translocase for α-helical substrate proteins on the OMM. The complex functions in an oligomeric form of ~200 kDa, which is assumed to consist of multiple copies of Mim1 (13 kDa) and one or two copies of Mim2 (10 kDa)(Dimmer et al., 2012; Popov-Čeleketić, Waizenegger, and Rapaport, 2008). Mim1 possesses a single α-helix with the N- terminus in the cytosol and the C-terminus in the IMS. MIM complex has a wide range of substrates. Single span proteins including both signal-anchored and tail-anchored proteins were found to be directly regulated by Mim1 (Doan et al., 2020; Vitali et al., 2020). Moreover, Mim1 also interact with Tom70 and mediates the insertion of multi-span proteins such as Ugo1 in a Tom70-dependent manner (Becker et al., 2011; Coonrod, Karren, and Shaw, 2007; Papić et al., 2011). In the biogenesis of Mcp3, MIM was found to facilitate its integration into OMM from the IMS side (Sinzel et al., 2017; Wenz et al., 2014).

In addition, Mim1 associates with the sorting and assembly machinery on the OMM to facilitate the assembly of TOM complex (Waizenegger et al., 2005). A combination of Blue-Native PAGE and import assay has suggested that Mim1 is involved in the membrane integration of the small TOM subunit Tom6 (Becker et al., 2008). In comparison, it does not affect the insertion of Tom5 and Tom7

but rather mediates their proper assembly into the TOM complex (Becker et al., 2010). Taken together, MIM plays a vital role in the biogenesis of proteins on the OMM. Its importance is supported by the fact that deletion of Mim1 can cause severe growth defect as well as morphological change of mitochondria in yeast (Dimmer et al., 2012). A functional analogue of Mim1 in Trypanosomes, named pATOM36, which lacks sequential or topological similarities with Mim1/2 has been uncovered (Vitali et al., 2018).

6.3.3 *Translocase of the inner membrane TIM22 complex*

The mitochondrial translocase TIM22 complex is one of the IMM import machineries that facilitate the translocation of non-cleavable multi-span proteins into the IMM (Neupert and Herrmann, 2007). Besides carrier proteins, it also mediates the biogenesis of other multi-span IMM proteins such as Tim17, Tim22 and Tim23. The complex is comprised of the main channel protein Tim22, a receptor like protein Tim54, the Tim9·10·12 chaperone complex and the Tim18-Sdh3 module (Kovermann et al., 2002). The large domain of Tim54 in the IMS provides a docking site for the Tim9·10·12 complex (Kerscher et al., 1997). The soluble Tim9·10 chaperones bind to the carrier precursors upon their exit from the Tom40 channel and further pass it to the Tim9·10·12 complex on the surface of the TIM22 complex (Endres, Neupert, and Brunner, 1999). This sophisticated system aims to prevent potential misfolding and aggregation of the hydrophobic carrier precursors. Tim22 contains four membrane-spanning segments that form a hydrophilic channel. This channel is activated by the membrane potential of the IMM and consequently releases the precursors into the IMM. Sdh3, the succinate dehydrogenase subunit 3, is dual localized in both TIM22 complex and in the respiratory complex II (Kulawiak et al., 2013; Pfanner, Warscheid, and Wiedemann, 2019). While Sdh3 mediates the electron transfer in complex II, as part of the TIM22 complex it can interact with Tim18 and functions in the assembly and stabilization of the complex (Wiedemann and Pfanner, 2017).

6.3.4 *Mitochondrial oxidase assembly protein1 (Oxa1)*

The insertase Oxa1 in the IMM belongs to the conserved Oxa1 superfamily which is evolutionarily related to the bacterial YidC insertase in the bacterial plasma membrane. It has been observed that Oxa1 and YidC can functionally substitute each other (Preuss et al., 2005). The Oxa1 superfamily includes in addition the protein Alb3 in the thylakoid membrane and the proteins GET1,

EMC3, and TMCO1 in ER. All these members catalyze the membrane integration of transmembrane segments of newly synthesized membrane proteins (Bonnefoy et al., 2009; Hennon et al., 2015). Oxa1 in the yeast IMM contains five TMDs with the N-terminus facing the IMS and a long C-terminus exposing to the mitochondrial matrix (Herrmann, Neupert, and Stuart, 1997; Yen et al., 2001). The positively charged C-terminus binds mitochondrial ribosomes and thus facilitate the co-translational insertion of mitochondrial encoded membrane proteins (Hell, Neupert, and Stuart, 2001; Szyrach et al., 2003). It is well documented that Oxa1 functions primarily for the assembly of protein complex involved in respiration (Bonnefoy et al., 2009). The insertion of cytochrome c oxidase 1 (Cox1) and Cox2 into IMM is largely dependent on Oxa1 (Hell, Neupert, and Stuart, 2001). Furthermore, Oxa1 is partially involved in the biogenesis of F_1F_0-ATP synthase complex (Jia, Dienhart, and Stuart, 2007).

Besides mtDNA encoded proteins, Oxa1 is also involved in the biogenesis of some nuclear-encoded proteins that have bacterial homologs such as ATP-dependent permease Mdl1, Oxa1 itself, and its homolog Oxa2/Cox18 (He and Fox, 1997; Saracco and Fox, 2002). Moreover, it is proposed that Oxa1 can also directly or indirectly regulate the biogenesis of carrier protein (Hildenbeutel et al., 2012).

6.4 MULTI-SPAN MEMBRANE PROTEINS

The outer mitochondrial membrane contains several types of proteins with different topologies (Fig.1). Multi-span proteins are membrane proteins that process two or more α-helical transmembrane domains. In mitochondria, this type of proteins is found in both the outer and inner membranes. The number of multi-span OMM proteins known so far is limited. The most studied model protein in yeast is the mitochondrial fusion-related protein Ugo1. Similarly, another fusion mediator Fzo1 (mitofusin Mfn1 and Mfn2 in mammalian) also possesses two TMDs with both N- and C- terminus facing the cytosol (Rojo et al., 2002). Another example is the Mdm10 complementing protein 3 (Mcp3) that has an unknown function (Sinzel et al., 2017). In addition, the yeast proteins Om14 and Scm4 are also multi-span OMM proteins whose function remains uncertain. In higher eukaryotes, human peripheral benzodiazepine receptor (PBR, known also as TSPO) and members of the Bcl-2 family belong to this protein type as well (Chipuk et al., 2010; Otera et al., 2007). In the IMM, all members of the carrier protein family share remarkable structural similarities with three pairs of transmembrane segments linked by loops at the matrix side

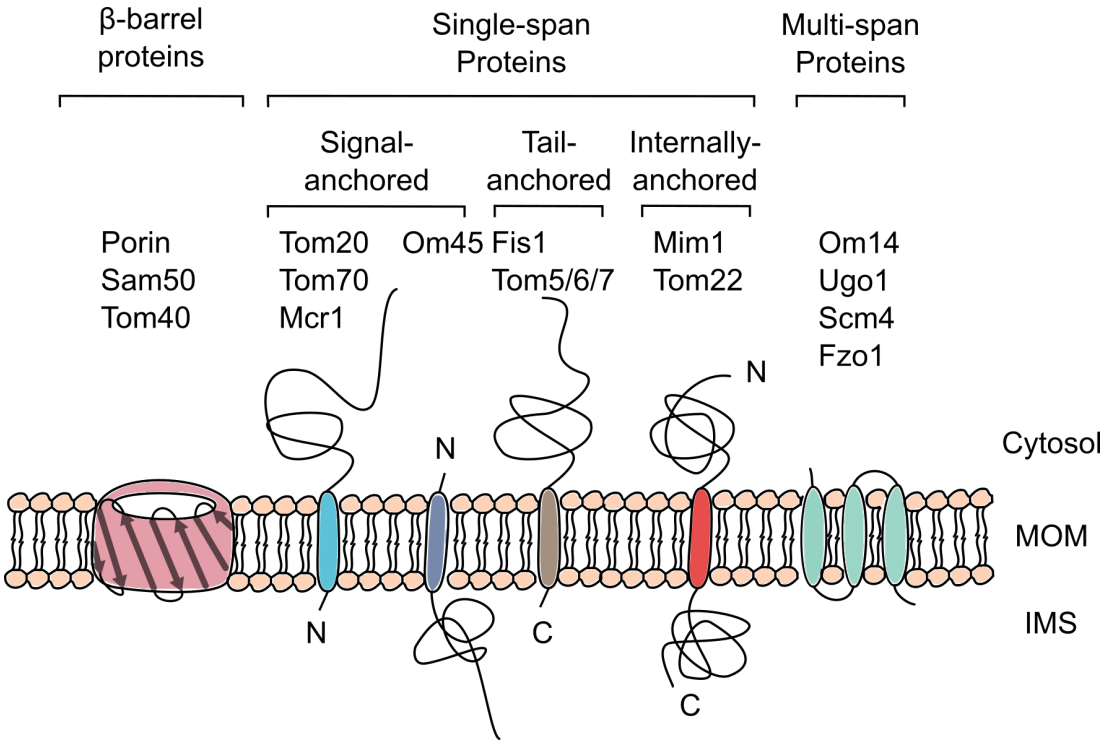

Figure 1: **Topologies of proteins in the outer mitochondrial membrane.** According to their topologies, mitochondrial outer membrane proteins can be divided into those that contain transmembrane α-helices and β-barrel proteins that consist of a series of anti-parallel β-strands. The α-helical proteins can be further sorted according to their structure and topologies. Signal-anchored proteins are embedded into the mitochondrial outer membrane by a single N-terminal transmembrane segment with a large domain exposing either to the cytosol or the intermembrane space. In contrast, tail-anchored proteins possess a C-terminal transmembrane domain, exposing the N-terminal to the cytosol. Another group of single-span proteins contains a transmembrane domain flanked by two soluble domains facing both the cytosol and the intermembrane space. Unlike single-span proteins, multi-span proteins on the outer mitochondrial membrane contain more than one transmembrane α-helices.

(Palmieri, 2013; Zara et al., 2007). There are about 35 carrier proteins in yeast and more than 50 proteins in humans (Wohlrab, 2006). The carrier proteins are crucial for the transport of metabolites across the inner membrane as well as for many cellular processes such as oxidative phosphorylation, amino acid catabolism, fatty acid oxidation, and citric acid cycle (Ruprecht and Kunji, 2020).

In the past decades, studies have provided multiple insights into the various stages of the biogenesis of multi-span mitochondrial proteins involving cytosolic synthesis, mitochondrial targeting, membrane integration, and functional maturation.

6.4.1 *Biogenesis of multi-span proteins in the IMM*

The biogenesis of multi-span IMM proteins is dissected into five stages (Endres, Neupert, and Brunner, 1999; Söllner et al., 1990). Similar to multi-span proteins in the OMM, the recognition of multi-span inner membrane proteins is supported by the receptor Tom70 (Brix et al., 2000; Wiedemann, Pfanner, and Ryan, 2001; Zara et al., 2007). The interaction between Tom70 and chaperones is essential for the import of inner membrane multi-span preproteins. Whereas the ATP-dependent chaperone Hsp90 contributes to the import of multi-span IMM proteins mainly in mammals, the chaperone Hsp70 mediates the import of Tom70-dependent proteins in both mammals and yeast (stage I) (Young, Hoogenraad, and Hartl, 2003). Precursor-bound chaperones can interact with Tom70 and deliver the precursors to the C-terminal binding domain of Tom70 (stage II). Substrate proteins are then transported across the OMM through the Tom40 pore by the help of the Tom40 N-terminal helix and a hexameric complex formed by small chaperone proteins (Tim9 and Tim10) in the IMS (stage III)(Araiso et al., 2019). This Tim9·10 complex further conducts the substrate proteins across the IMS to the surface of TIM22 complex, where the carrier precursors are integrated into the IMM lipid bilayer with the help of membrane potential (stage IV). Another factor that might be involved in the biogenesis of carrier proteins is the translocase Oxa1. According to an *in vitro* import assay (Hildenbeutel et al., 2012), the import of carrier proteins into isolated mitochondria was severely impaired in the absence of Oxa1, whereas no significant effect was observed for the import of matrix proteins under the same condition. Although the underlying mechanism is poorly known, Oxa1 is presumably required to help the folding of newly imported carrier precursors. After being released from TIM22 to the inner membrane, carrier proteins are finally assembled into a dimeric form to fulfill their function (stage V)(Neupert and Herrmann, 2007).

All carrier proteins have their both termini in the IMS and contain three homologous modules, each possessing two TMDs. A highly conserved motif (PX[D/E]XX[K/R]) is found on the matrix side of each module, just after the odd-numbered TMDs (Pebay-Peyroula, 2003). This motif, also known as carrier signature (CS), was initially suggested to facilitate the transport of precursors across the OMM (Zara et al., 2007), but later was suggested to be mainly important for the function of these proteins (Ruprecht and Kunji, 2020). The charged residues in CS form charge-pair networks to facilitate the specific transport of metabolites (Nelson, Felix, and Swanson, 1998).

The internal targeting information of carrier proteins should be decrypted at three stages: the initial targeting from cytosol to mitochondria, the interaction with Tim9·Tim10 complex in the IMS, and the recognition by the TIM22 translocase. All three modules are apparently involved in the specific recognition of carrier proteins by Tom70 and Tim9·10 complex and all three homologous modules can be independently driven across the OMM (Brix et al., 1999, 2000). However, only the last module in the C-terminus of both ADP/ATP carrier (AAC) (Endres, Neupert, and Brunner, 1999) and dicarboxylate carrier (Brandner, Rehling, and Truscott, 2005) was found to be properly localized in the IMM in a strictly membrane potential dependent manner. Nevertheless, the targeting information in the third module has not been identified yet.

Similar to the multi-span OMM proteins, the biogenesis and function of carrier proteins are also largely dependent on the mitochondria-specific lipid cardiolipin (Claypool et al., 2008; Dyall et al., 2003; Jiang et al., 2000; Sauerwald et al., 2015). Surprisingly, it has been reported that AAC can integrated into liposomes containing a IMM-mimetic lipid composition (Long, O'Brien, and Alder, 2012).

6.4.2 *Biogenesis of multi-span proteins in the OMM*

In the cytosol, a variety of molecular chaperones and cochaperones function corporately in preventing their substrates from misfolding and aggregation. The multi-span protein Om14 has been reported to directly interact with ATP-dependent chaperones of the Hsp90 and Hsp70 families and some of their cochaperones (like Ydj1 and Sis1) (Jores et al., 2018). It is therefore assumed that chaperones might support the precise targeting of cytosolic synthesized multi-span precursors to the surface of mitochondria.

Unlike preseuquence-containing proteins, no N-terminal targeting sequence was found in multi-span proteins of both mitochondrial membranes. In contrast, previous studies hinted on the internal targeting information. The last 50 residues in the C-terminal of Ugo1 were reported to be sufficient for its mitochondrial targeting (Coonrod, Karren, and Shaw, 2007), whereas both the C-terminus and the coiled-coil domains upstream and downstream of the TMD in Mfn2 function together for its specific mitochondrial targeting (Rojo et al., 2002). The recognition of freshly synthesized multi-span proteins is promoted by the Tom70 receptor (Doan et al., 2020; Papić et al., 2011; Sinzel et al., 2017). However, it remains unclarified whether Tom70 can interact directly with the precursor proteins, or it may act as a docking site for chaperones that attach to

the newly synthesized proteins. Naturally, these two options are not mutually exclusive.

In addition, many studies have reported that the MIM complex, especially Mim1, is heavily involved in the biogenesis of multi-span OMM proteins in yeast. According to research, the receptor Tom70 cooperate with MIM complex in facilitating the integration of multi-span precursors into the outer membrane (Becker et al., 2011; Dimmer et al., 2012; Doan et al., 2020). However, the precise role of MIM complex and the underlying mechanism remain to be identified.

Besides the proteinaceous factors mentioned above, the lipid composition of OMM can also affect the biogenesis of multi-span OMM proteins. It has been observed that the deficient synthesis of cardiolipin resulted in reduced steady-stated levels of multi-span but not single-span proteins in the OMM (Sauerwald et al., 2015). Moreover, freshly synthesized Ugo1 can be integrated *in vitro* into pure lipid vesicles and the integration process can be enhanced by the increased level of phosphatidic acid (PA) in the lipid vesicles (Vögtle et al., 2015).

Om14

Om14 is one of the most abundant proteins in the OMM and it contains three predicted α-helical transmembrane segments (Burri et al., 2006). According to proteolytic assays, the N-terminus of Om14 is exposed towards the cytosol and the C-terminus towards the IMS (Burri et al., 2006). Even though the precise function of Om14 has yet to be determined, several hypotheses have been made. It was reported that Om14 forms a complex together with Porin, the yeast voltage-dependent anion channel (VDAC), and Om45 in the OMM, which might facilitate the transport of metabolites (Lauffer et al., 2012). In addition, Om14 was proposed to function as a receptor for cytosolic ribosomes and to contribute to the co-translational import of mitochondrial proteins (Lesnik et al., 2014).

In comparison to Ugo1, the biogenesis of Om14 is largely unclear. Even though certain common factors such as Tom70 and the MIM complex appear to aid the biogenesis of both Om14 and Ugo1, it is currently unclear what roles other parameters such as protein folding, TMD hydrophobicity, and lipid composition play. It is possible that multi-span proteins follow rather individual biogenesis routes, as was described for single-span proteins (Vitali et al., 2020).

Ugo1

Ugo1 is a 56 kDa protein residing on the OMM. It is assumed to have three or more TMDs with a cytosolic N-terminal and a C-terminal facing the IMS (Coonrod, Karren, and Shaw, 2007; Papić et al., 2011). During mitochondrial fusion, Ugo1 forms a functional complex with the two GTPases Fzo1 (OMM) and Mgm1 (IMS) to promote the fusion of both inner and outer membranes (Hoppins et al., 2009). The dysfunction of any member of the fusion apparat can cause mitochondria fragmentation, mtDNA loss, and respiratory defect. Ugo1 was previously classified as a member of the carrier protein family since it contains two motifs similar to the highly conserved carrier signature in carrier proteins. It was reported that the reversal mutation of charged residues in the second motif of Ugo1 disrupt mitochondrial fusion (Hoppins et al., 2009). However, unlike carrier proteins, there is so far no evidence for the function of Ugo1 as a transporter.

7

RESEARCH OBJECTIVES

Considerable research has been done to understand the underlying mechanism of the biogenesis of multi-span mitochondrial outer membrane proteins. So far, we already gained some insights about the potential receptor, the involvement of the MIM complex, and the contribution of membrane lipid components. However, many details of the process remain unclear, including the early cytosolic targeting event, the undiscovered targeting signals, potential determinative factors, and the specificity of the biogenesis pathway.

To characterize the biogenesis of multi-span outer membrane mitochondrial proteins, I used Om14 as a model protein and combined *in vitro* and *in vivo* approaches.

The main questions addressed in this study are:

1. How does Tom70 contribute to the biogenesis of mitochondrial proteins especially multi-span proteins?

The crucial function of Tom70 was investigated in the article “The chaperone-binding activity of the mitochondrial surface receptor Tom70 protects the cytosol against mitoprotein-induced stress” (Backes et al., 2021).

2. What are the main factors that are involved in the biogenesis of the multi-span mitochondrial protein Om14 and are alternative pathways coexist for its biogenesis?

This aim was addressed in the article “The multi-factor modulated biogenesis of the mitochondrial multi-span protein Om14” (Zhou et al., 2022).

8

SUMMARY OF THE RESULTS

8.1 THE CHAPERONE-BINDING ACTIVITY OF THE MITOCHONDRIAL SURFACE RECEPTOR TOM70 PROTECTS THE CYTOSOL AGAINST MITOPROTEIN-INDUCED STRESS (BACKES ET AL. 2021)

Previous studies have shown that Tom70 can function as the main receptor for multi-span proteins of both OMM and IMM (Brix et al., 2000; Doan et al., 2020; Papić et al., 2011; Sinzel et al., 2017; Wiedemann, Pfanner, and Ryan, 2001; Zara et al., 2007). Tom70 contains 11 tetratricopeptide repeats (TPRs), some of which form a groove that can specifically bind to Hsp70 (Young, Hoogenraad, and Hartl, 2003), one of the major cytosolic chaperones in yeast. In addition, it is suggested that preproteins can directly interact with the TPRs in the C-terminal of Tom70 (Brix et al., 2000). It therefore raises our interest to understand the exact function of Tom70 in the targeting process of protein precursors. To address this question, we isolated mitochondria from *tom70/71*Δ strains expressing a construct where the TMD of Tom70 was linked to Tah1 in the C-terminus, thus anchoring the latter protein to the OMM. In the following, this variant is indicated as mtTah1. According to previous publications, Tah1 contains two TRP motifs which can interact with Hsp70 (Jiménez et al., 2012). The mutant Tah1(K8A) was used as a control since the mutation K8A was shown to abolish its Hsp70 binding capacity (Jiménez et al., 2012).

To examine whether such mitochondrially localized Tah1 can restore the function of Tom70, we isolated pure mitochondria from the *tom70/71*Δ double deletion strain transformed with an empty vector (ø), or expressing the mitochondrial versions of either Tah1 or Tah1(K8A). Mitochondria from wild type (WT) stains were also isolated to serve as a control. We first tested the steady-state levels of different Tom70 substrates in these mitochondria and observed that while the levels of Ugo1, Oxa1 and Aac2 (Pet9) dropped significantly in the absence of Tom70/71 (Backes et al. 2021, Fig. 6A, B), substrates such as Pic2 and Om14 were only moderately affected. By replacing Tom70 with mtTah1, the levels of Oxa1, Aac2 and Ugo1 were partially restored but still less than in the WT (Backes et al. 2021, Fig. 6A, B). Importantly, the recovery effect from mtTah1 was abolished by the mutation K8A. Since Tah1 does not

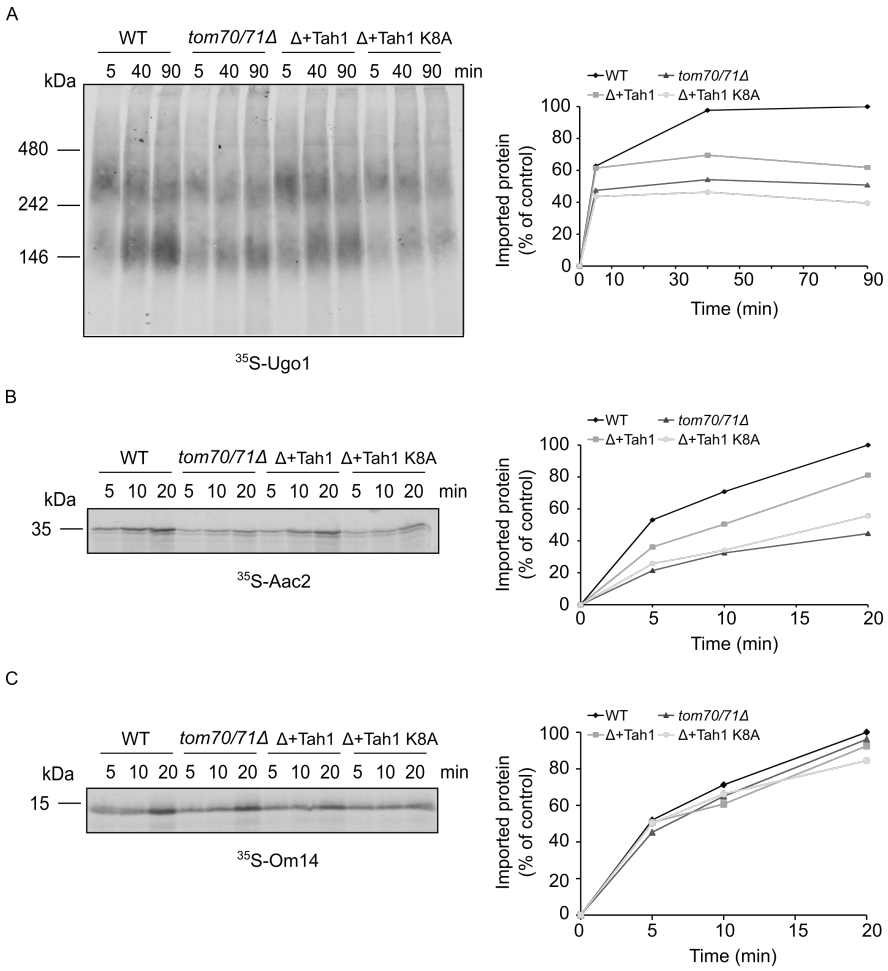

Figure 2: **mtTah1 partially rescue the import of substrates in mitochondria from *tom70/71*Δ cells.** Radiolabeled Ugo1 (A), Aac2 (B), or Om14 (C) were imported into mitochondria isolated from WT cells or from *tom70/71*Δ cells transformed with either mtTah1 or mtTah1(K8A). After import of Ugo1, mitochondria were solubilized in 1% digitonin in a protein:detergent ratio of 1:6 and Ugo1 complexes were analyzed by BN-PAGE. For Aac2 and Om14, carbonate extraction (CE) was conducted after import and the pellets fractions were analyzed using SDS-PAGE. In all cases, proteins were detected by autoradiography. Right panes: For all three proteins, the band representing import for 20 min into WT mitochondria was set as 100%. The average of three independent experiments is plotted.

interact with preproteins directly, these findings indicate that the recovery shown in the samples with mtTah1 results from a restored interaction with Hsp70. To further verify this assumption, we analyzed the in vitro import capacity of Ugo1, Aac2 and Om14 into these isolated mitochondria (Fig. 2). In agreement with the steady-state levels, the import of both Aac2 and Ugo1 was impaired in the absence of Tom70/71 and this impairment was partially restored by expressing

mtTah1 but not mtTah1(K8A). In contrast, both the steady-state levels and the import efficiency of Om14 showed only a minor dependence on Tom70.

Since the expression of mtTah1 did not fully rescue the steady-state levels of these substrates to the extent of WT, a sub-portion of these substrates is assumed to directly interact with Tom70. To examine this possibility, we analyzed the interaction between Tom70 and Ugo1 using a peptide scan assay (Fig. 3). Each dot on the cellulose membrane represents a peptide of 20 amino acid residues with a shift of three amino acids and the membrane, which was prepared by Dr. Martin Jung (Homburg), covers the whole sequence of Ugo1. By incubating the membrane with purified GST-Tom70, we observed that several parts of Ugo1, especially those near the putative transmembrane domains, have a strong Tom70 binding capacity.

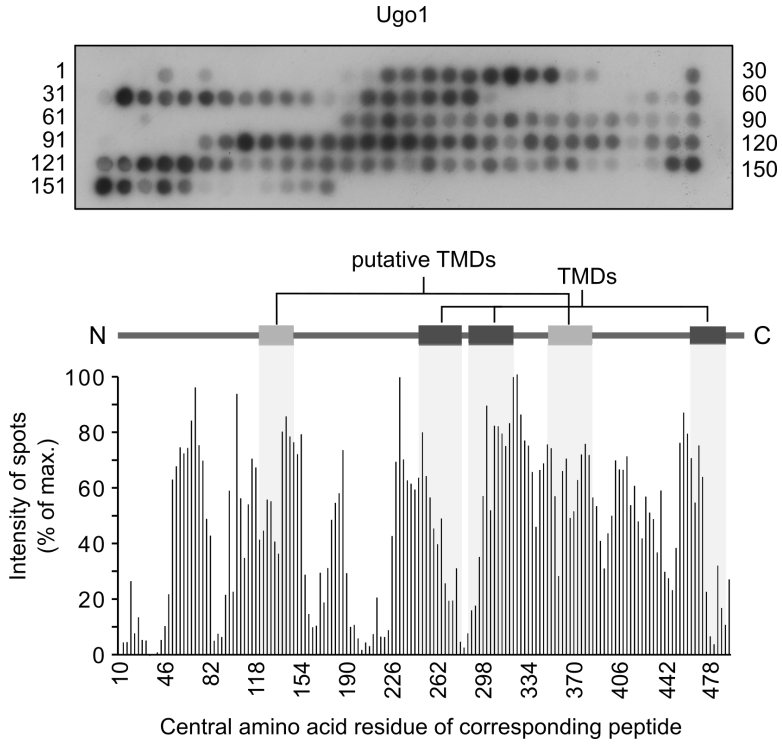

Figure 3: **Ugo1 segments interact with the Tom70 cytosolic domain.** Upper panel: Purified recombinant protein GST-Tom70(cytosolic domain) was incubated with a nitrocellulose membrane that contains 20-mer peptides covering the whole sequence of Ugo1. The interaction was visualized using antibody against GST. The serial numbers of the peptides were indicated by the numbers flanking the panel. Lower panel: The intensity of each dot was quantified from three independent experiments and the average were plotted. The intensity of the dot representing the strongest signal was set as 100%. The numbers of the central amino acid residue of each peptide are plotted on the X-axis.

Next, we also examined the direct interaction between Tom70 and Aac2 using GST pull-down assay (Fig. 4). Full-length radiolabeled Aac2 and its truncated variants were translated *in vitro* and were pulled-down with either GST alone (as a control) or GST-Tom70(cytosolic domain). According to the results, the full-length Aac2 shows the most specific binding to Tom70, whereas the truncated variants also show direct Tom70 interaction but with a sub-portion unspecifically bound to the GST or the beads. Collectively, our data suggest that Tom70 can

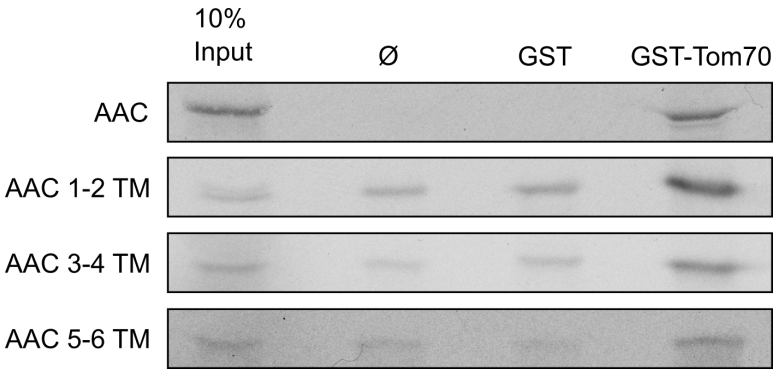

Figure 4: **All three domains of AAC can independently interact with Tom70.** Radiolabeled Aac2 full-length and its truncated variants were incubated and pulled-down together with the recombinant fusion proteins GST alone or GST-Tom70 which were pre-bound to Sepharose beads. No recombinant protein was added to a mock sample (ø). The eluted proteins were analyzed using SDS-PAGE and were detected via autoradiography.

recruit cytosolic precursor-binding chaperones to the mitochondrial surface. In addition, it can also directly interact with precursor proteins for an efficient protein targeting. Of note, different substrates show variable dependence on the dual functions of Tom70.

8.2 THE MULTI-FACTOR MODULATED BIOGENESIS OF THE MITOCHONDRIAL MULTI-SPAN PROTEIN OM14 (ZHOU ET AL. 2022)

So far, the majority of studies investigating the biogenesis of multi-span proteins was done using Ugo1 as a model protein. In contrast, the knowledge about the biogenesis of Om14 is limited. Although Om14 is one of the most abundant proteins in the yeast OMM, the null mutation of Om14 does not cause any growth defect. Due to its considerable quantity, we questioned ourselves how strongly the import machineries on the OMM are required for the biogenesis of Om14 and whether multiple pathways contribute collectively to its biogenesis as described for single-span proteins (Vitali et al., 2020).

8.2.1 *The existence of multiple targeting signals*

As the initial step to dissect this question, I first decided to investigate the potential targeting information inside Om14. To this aim, I created green fluorescent protein (GFP) fused full-length (FL) Om14 and four GFP fused constructs, each containing at least one of the three TMDs and its flanking region. To investigate whether these constructs can successfully target to mitochondria, I monitored the *in vivo* localization of these constructs using fluorescence microscopy. As expected, the full-length Om14 was clearly co-localized with mitochondrial targeted RPF fusion protein (Zhou et al., Fig. 1B). Mitochondria co-localization was also observed for all the truncated Om14 variants, although in these variants cytosolic GFP signals were detected as well. These cytosolic signals could result from proteolytic cleaved Om14 or GFP alone. In addition, I observed some peri-nuclear fluorescence signals in the variant containing the first TMD of Om14(1-62), which might indicate a possible mislocalization to the ER.

To further examine the intracellular localization of all the GFP fusion constructs, sub-cellular fractionation was performed and these constructs were detected in the different cell fractions via immunodecoration using antibody against GFP. Consistent with the fluorescence microscopy results, the full-length Om14 was fully localized in the mitochondria (Zhou et al., Fig. 1C), whereas all the truncated variants were primarily localized to mitochondria but with a subpopulation mis-localized to the ER. Of note, a band slightly smaller than the intact GFP-Om14(1-62) was found only in the whole cell lysate (WCL) and cytosol fractions. This band which might result from a C-terminal degradation of the construct indicates the importance of the C-terminal region of Om14(1-62) for the specific mitochondria targeting (Zhou et al., Fig. 1C). The integration capacity of single Om14 TMDs was further supported by *in vitro* import assay followed by alkaline extraction. All the Om14 constructs containing a single TMD can properly integrate into mitochondria (Zhou et al., Fig. S1A-C). Intriguingly, the import efficiency of all single-TMD constructs was hardly affected in *mim1*Δ *cells*, indicating that the intact structure of Om14 contributes to the dependency on Mim1.

8.2.2 *The minor function of Tom70 and other substitutive receptors*

Tom 70 was previously found to facilitate the recognition of multi-span OMM proteins (Doan et al., 2020; Papić et al., 2011; Sinzel et al., 2017). I therefore studied the involvement of Tom70 or other potential receptors in the biogenesis

of Om14. To this aim, I analyzed the Tom70-interaction site in Om14 via peptide scan assay. Membranes that contain peptides covering the whole sequence of Om14, which were prepared by Dr. Martin Jung (Homburg), were incubated with recombinant GST-tagged cytosolic domain of Tom70 purified from *E. coli* cells. I observed multiple moderate interaction sites inside or close to the predicted first two transmembrane domains of Om14 and a strong interaction in its C-terminal region (Zhou et al., Fig. 2A).

Next, I examined the physiological relevance of Tom70 by importing *in vitro* synthesized radiolabeled Om14 into mitochondria isolated from either WT or *tom70/71*Δ cells. A proteolytic assay using Trypsin was performed after the import to distinguish the properly integrated Om14 from the aggregated one (Burri et al., 2006). According to preliminary experiment, a 13 kDa characteristic fragment (F') can be used as an indicator of properly embedded Om14 after digesting the isolated mitochondria with 50 µg/ml Trypsin (Zhou et al., Fig. S2A). Compared to WT, the integration capacity of Om14 into organelles lacking Tom70/71 was moderately reduced by less than 20% (Zhou et al., Fig. 2B). Since human TOM70 and yeast Tom70 share functional similarities, I also performed the same import assay in mitochondria from TOM70 knock down cells (kindly provided by Klaudia Maruszczak; Zhou et al, Fig. S2B). Although no homolog of Om14 was found in the human genome, Om14 can be properly inserted into these organelles as indicated by the formation of the typical F' fragment after trypsin treatment. Moreover, the import of Om14 exhibit a slightly higher dependence on mammalian TOM70, which was reflected by a 30% reduction of imported Om14 when TOM70 was depleted.

To further investigate the substitutive effect of other receptor such as Tom20, I removed the cytosolic exposed domain of both Tom70 and Tom20 by incubating isolated mitochondria with trypsin prior to the import reactions (Zhou et al., Fig. 2D). Nevertheless, similar amounts of Om14 were imported into both intact and pre-trypsinized WT mitochondria. These findings indicate a nonessential role of the cytosolic domains of both receptors Tom70 and Tom20.

Although Mim1 is known to be heavily involved in the biogenesis of multi-span OMM proteins, its precise function in the process is still unclear. Since Mim1 remained intact during the aforementioned trypsinization, I wondered whether the cytosolic part of Mim1 might function as a receptor for Om14. To address this question, I introduced a plasmid-encoded native Mim1 or variant possessing only the central TMD of Mim1 (residues 35-75, Mim1-TMD) into *mim1*Δ cells. Previous report has revealed that the overexpression of Mim1-TMD rescued the growth phenotype caused by deletion of native Mim1 (Popov-

Čeleketić, Waizenegger, and Rapaport, 2008). By checking the steady-state levels of different Mim1 substrates including Om14, we observed that the overexpression of Mim1-TMD could rescue the levels of these substrates to the same extent as overexpression of native Mim1 (Zhou et al., Fig. S3A). Moreover, the overexpression of Mim1-TMD in *mim1*Δ cells could facilitate the assembly of newly synthesized Om14 to the same extent as overexpressing native Mim1 (Zhou et al., Fig. S3B). To examine whether the cytosolic part of Mim1 functions only as a substitute in the absence of other receptors, we imported Om14 into pre-trypsinized *mim1*Δ (Zhou et al., Fig. 2C). However, the removal of the cytosolic domain of both Tom20 and Tom70 in the absence of Mim1 did not cause further impairment compared to the import of Om14 into organelles lacking only Mim1. Hence, these results indicate a minor involvement of Tom70, Tom20, or the cytosolic region of Mim1 in the biogenesis of Om14.

8.2.3 *The influence of TMD hydrophobicity on the membrane integration capacity of Om14*

According to Wimley and White hydrophobicity scale (Wimley and White, 1996), Om14 possesses three TMDs with the hydrophobicity values of 1.0, 1.5, 1.5, respectively. To better understand the integration capacity of Om14, I created two constructs containing either an increased hydrophobicity of the 1st TMD (Om14-3I) or a decreased hydrophobicity of the 2nd TMD (Om14-4A). I first conducted carbonate extraction to monitor the integration efficiency. It is worth to mention that a sub-population of native Om14 was repeatedly found in the supernatant fraction as reported in previous publications (Burri et al., 2006; Sauerwald et al., 2015). According to our preliminary experiment, a better separation between peripheral and integral Om14 can be obtained in a solution with pH of 10.5 (Fig. 5). Upon carbonate extraction (pH 10.5), the Om14-3I variant showed a similar behavior as the original Om14, whereas decreased amount of Om14-4A with a larger portion in the supernatant fraction was detected, indicating an impaired integration capacity as well as an enhanced turn-over of Om14 after decreasing the hydrophobicity of its 2nd TMD (Zhou et al., Fig. 3B, C). To elaborate whether the deficient integration of Om14-4A is Mim1-dependent, we examined the import efficiency of Om14-4A into mitochondria isolated from either WT or *mim1*Δ *cells*. In line with previous findings, the import efficiency of Om14-4A dropped drastically as compared to native Om14 (Zhou et al., Fig. 3D). In the absence of Mim1, the import of Om14-4A was further compromised, which suggests that the deficient membrane

integration of Om14-4A was not a consequence of reduced interaction with Mim1. These findings revealed the involvement of the 2nd TMD of Om14 in the membrane integration steps in a MIM-independent manner.

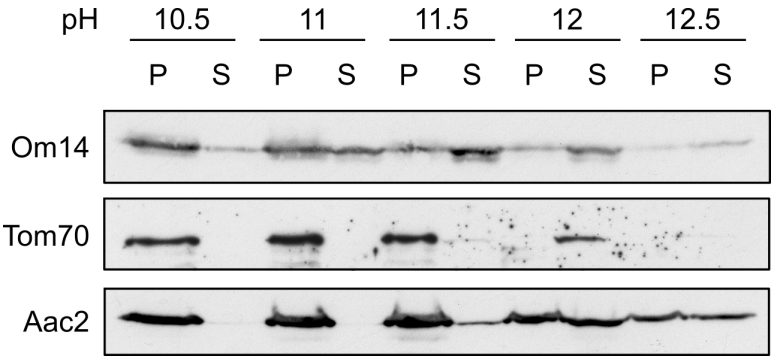

Figure 5: **Carbonate extraction of Om14 under different pH environment.** Isolated mitochondria were subjected to carbonate extraction with a solution with the indicated pH value. Both pellet (P) and supernatant (S) samples were analyzed using SDS-PAGE.

8.2.4 *The accelerated import of Om14 under unfolding states or increased temperature*

Since the hydrophobicity (Zhou et al., Fig. 3) and the intact structure (Zhou et al., Fig. 1, Fig. S1) were proved to regulate the biogenesis of Om14, I further asked whether the folding state of the newly synthesized protein is important for the import of Om14. I therefore denatured *in vitro* translated Om14 using 6 M urea prior to the import reaction. To our surprise, the import capacity of denatured Om14 was enhanced by four-fold compared to untreated Om14 (Zhou et al., Fig. 4A). Such enhancement is apparently unrelated to Mim1, as similar increase was also observed while importing denatured Om14 into mitochondria lacking Mim1. These results indicate that unfolded Om14 is integrated into OMM better than partially folded specie.

This conclusion leads us to the question whether membrane behavior is involved in the biogenesis of Om14. To this goal, I monitored the import efficiency of Om14 at the normal import temperature of 25℃ or at 37℃. The elevated temperature, which increases the fluidity of membranes, considerably enhanced the import efficiency of Om14 (Zhou et al., Fig. 4B). To test whether such behavior was specific for Om14, we also imported two other OMM proteins, Ugo1 and Porin (Zhou et al., Fig. 4C). Similar to Om14, we observed a slightly enhanced import efficiency of Ugo1 only after 20 min. In contrast, less Porin was able to be imported into organelle when the temperature was elevated. We therefore

speculated that membrane fluidity can facilitate the membrane integration of Om14, although we cannot exclude the possibility that the enhanced integration results from partially unfolding of Om14 at the elevated temperature.

8.2.5 *Different involvement of Porin, Mim1 and Om45 in the biogenesis of Om14*

The aforementioned results suggested that at least 70% of Om14 can properly integrated into membranes in the absence of Mim1, Tom20 and Tom70. We therefore assumed that additional proteinaceous factors might regulate the biogenesis of Om14. According to previous report, Om14 can form stable complex with Porin and Om45 (Lauffer et al., 2012). To shed light on the function of Porin or Om45 in the biogenesis of Om14, I first conducted carbonate extraction to check the integration capacity of Om14 in mitochondria lacking either of these proteins (Zhou et al., Fig. 5A, B). We observed a significantly increase of Om14 in the supernatant fraction in the absence of Om45, indicating that the membrane integration of Om14 was compromised. In contrast, Om14 behavior was not affected in mitochondria lacking Porin. Next, I examined by BN-PAGE the assembly of Om14 complex in the absence of either Porin or Om45 (Zhou et al., Fig. 5C). I observed that the migration of Om14-containing oligomeric complexed changed drastically to a smaller species in mitochondria isolated from *om45*Δ cells.

In additional, radiolabeled Om14 was imported *in vitro* into organelles isolated from either *por1*Δ or *om45*Δ cells (Zhou et al., Fig. 5D). We observed a 20% and 30% decrease of the import efficiency in mitochondria lacking Om45 and Porin, respectively. Hence, it seems that both Porin and Om45 are involved in the biogenesis of Om14 and Om45 contributes more to the assembly of Om14 complexes and to its stability.

Since we observed compromised Om14 import in both *por1*Δ and *mim1*Δ mitochondria (Zhou et al., Fig. 2C and Fig. 5D), we asked whether Mim1 and Porin can compensate the function of each other in the early biogenesis of Om14. To address this question, I monitored the steady-state level of Om14 in *por1*Δ*mim1*Δ double deletion strain (generated by Dr. Kai Dimmer, Zhou et al., Fig. 6A,6B). Compared to mitochondria isolated from WT or single deletion strain *por1*Δ or *mim1*Δ, the levels of Om14 dropped significantly in mitochondria from the double deletion strain *por1*Δ*mim1*Δ. In comparison, the levels of other MIM substrates such as Tom20 and Tom70 were also reduced in the absence of Mim1 but no further reduction was observed upon the co-deletion of Porin.

To better understand in which step the Om14 levels were affected in *por1*Δ*mim1*Δ cells, *in vitro* synthesized radiolabeled Om14 was imported into mitochondria isolated from the four strains mentioned above (Zhou et al., Fig. 6C). Although the import efficiency of Om14 was impaired in all the three mutated organelles, no further impairment was observed in *por1*Δ*mim1*Δ compared to the single deletions. To further examine whether Mim1 and Porin function together in mediating the membrane integration of Om14, I monitored the integration capacity of Om14 using carbonate extraction (Zhou et al., Fig. 6D). Although the steady-state level of Om14 dropped drastically in mitochondria lacking both proteins, the majority of Om14 molecules was still able to integrate into OMM in the double deletion strain. Taken together, these observations indicate that Mim1 and Porin function separately in the early biogenesis of Om14 and are both not involved in maintaining the stability of Om14 oligomeric complex within the membrane.

In conclusion, my results provide new insights on a variety of elements that potentially contribute to the biogenesis of Om14, supporting the hypothesis about the coexistence of different Om14 biogenesis pathways.

9

DISCUSSION

9.1 THE CHAPERONE-BINDING ACTIVITY OF THE MITOCHONDRIAL SURFACE RECEPTOR TOM70 PROTECTS THE CYTOSOL AGAINST MITOPROTEIN-INDUCED STRESS.

The receptor Tom70 facilitates the targeting of a wide range of substrates from some single-span proteins to multi-span proteins located in both the outer and inner mitochondrial membranes.

The peptide scan assay of Ugo1 as well as the pull-down assay suggest its ability to directly interact with substrates, which is consistent with previous reports (Brix et al., 2000). However, recent studies have highlighted its potential function to serve as a chaperone-binding factor (Opaliński et al., 2018; Young, Hoogenraad, and Hartl, 2003). According to the steady-states levels and in vitro import assays, Ugo1, Aac2 and Oxa1 show strong dependence on Tom70. In the absence of Tom70/71, the compromised biogenesis of these proteins can be rescued by a chaperone-binding TPR protein Tah1 which is artificially tethered to the mitochondrial surface, even though the endogenous Tah1 is completely uninvolved in the biogenesis of mitochondria. The rescuing effect was abolished when the chaperon-binding activity was inhibited by the Tah1 K8A mutation, which further suggests that the chaperone binding capacity on the surface of mitochondria is relevant to the biogenesis of these substrates.

In comparison, the mtTah1 rescuing effect was not dominant for some other Tom70 substrates such as Om14 and Pic2. In this case, we assumed that a direct interaction with Tom70 is required for their proper mitochondrial targeting and recognition. Taken together, we demonstrate that Tom70 plays dual functions in the biogenesis of mitochondrial membrane proteins and the dependence on these dual functions of Tom70 is substrate specific.

9.2 THE MULTI-FACTOR MODULATED BIOGENESIS OF THE MITOCHONDRIAL MULTI-SPAN PROTEIN OM14.

Newly synthesized OMM multi-span proteins are believed to be integrated into the membrane by the help of the receptor Tom70 and the MIM complex

(Fig. 6, pathway I)(Drwesh and Rapaport, 2020; Neupert and Herrmann, 2007; Pfanner, Warscheid, and Wiedemann, 2019; Walther and Rapaport, 2009). However, a different theory proposes that such a protein namely, Ugo1 can integrate into the lipid phase without the assistance of proteinaceous import factors through a process that is enhanced by phosphatidic acid (Vögtle et al., 2015). To investigate whether the two contradicted mechanisms mentioned above coexist, we examined the effect of multiple cis and trans factors on the biogenesis of the model protein Om14.

9.2.1 *Several targeting information contributes additively to the specific mitochondria localization*

Multi-span proteins are known to target to mitochondria via internal targeting signals rather than a canonical N-terminal sequence. In AAC, each homologous repeat contains sufficient information for its independent targeting to mitochondria, although the last repeat at its C-terminus is necessary for its proper integration into the IMM (Endres, Neupert, and Brunner, 1999; Kreimendahl et al., 2020). In Ugo1, the presence of the C-terminus reduces its mislocalization to the cytosol and support the localization to the mitochondria (Coonrod, Karren, and Shaw, 2007). In the current study, I assessed the targeting behavior of different truncated Om14 variants and found that all of them were capable of targeting to mitochondria while a subpopulation got mislocalized to the cytosol or ER. In sharp contrast, the full-length protein shows a perfect targeting to mitochondria. Intriguingly, the removal of several amino acid residues at the C-terminal flanking region of the first TMD, probably due to degradation, can sufficiently impede the mitochondrial targeting of this construct. Overall, I could demonstrate that each TMD of Om14 contains sufficient information to be targeted to mitochondria, although with compromised specificity. Only the collective contribution of all the local signals assures the specific mitochondrial targeting of the native protein. However, it is still unclear so far how the targeting information are decoded, and future studies are required to investigate the exact targeting signal, which is currently unidentified.

9.2.2 *Multiple proteinaceous factors regulate the early biogenesis of Om14*

Although the complete absence of Tom70, and its paralog Tom71, results in a moderate reduction of imported Om14, one cannot exclude the potential contribution of Tom70 in the biogenesis of Om14. The peptide scan assay

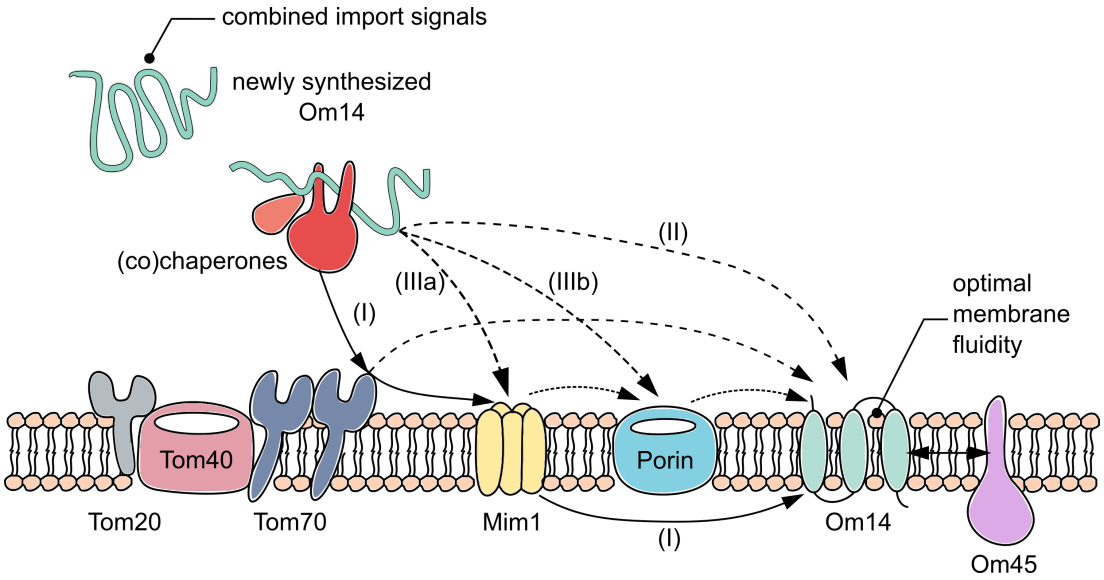

Figure 6: **Schematic figure showing different potential routes for the biogenesis of Om14.** This figure is published in the Zhou et al. Fig. 7.

indicated several specific Tom70-Om14 interaction sites. Moreover, a pull-down assay with newly synthesized Om14 suggested that it associates with the Hsp70 chaperones and the co-chaperones of the Hsp40 family (Jores et al., 2018). While the exact mechanism through which (co)chaperones facilitate protein targeting and insertion is unclear, it can be speculated that they shield the hydrophobic segments to avoid the misfolding and premature aggregation of the precursors. Taken together, we assume that Tom70 can, at least partially, contribute for the biogenesis of Om14 as the chaperon docking site on the membrane.

As reported previously, deletion of *TOM70* in yeast or knock-down of this protein in mammalian cells can cause varying degrees of reduction in the import efficiency of OMM multi-span proteins (Becker et al., 2011; Brix et al., 1999; Otera et al., 2007; Papić et al., 2011; Wan et al., 2016). In *tom70*Δ yeast cells, the moderate reduction of Om14 suggests that alternative routes might be available. Supporting this assumption, Om14 showed a higher Tom70 dependence in human cells. This difference might be due to the lack of optimal alternative pathways in the mammalian cells, as Om14 is not a natural substrate of these cells. In addition, an integrative organelle proteomics analysis defines Om14 as a very abundant protein in the OMM (Morgenstern et al., 2017). It is therefore possible that its minor dependence on Tom70 might be a mechanism for avoiding the over-occupation of Tom70 by Om14 while leaving a limited capacity for other substrates.

Tom20 can be considered as an attractive candidate for an alternative receptor for Tom70-substrates, as Tom20 and Tom70 partially share substrates and function (Brix et al., 1999). However, the proteolytic treatment of mitochondria prior to the import reactions, which removes the cytosolic domains of both Tom70 and Tom20, has a similar minor effect on the import efficiency of Om14. These observations suggest that Tom20 is not a major factor in the biogenesis of Om14 even in the absence of Tom70. Notably, a small amount of intact Tom20 remains detectable after the trypsin treatment as indicated by a longer exposure of the western blot. Thus, although unlikely, it cannot be ruled out that the remaining minor amounts of Tom20 can be sufficient for supporting optimal recognition of Om14.

Another candidate for the initial recognition of Om14 is the MIM complex which is thought to function as an OMM insertase. As Tom70 was proposed to relay its substrates to the MIM complex (Becker et al., 2011), we wondered whether OMM multi-span precursors can be directly recognized by the MIM complex (Fig. 6 pathway IIIa). However, previous study has shown that the expression of only the central TMD of Mim1 can rescue the growth phenotype caused by deletion of Mim1 (Popov-Čeleketić, Waizenegger, and Rapaport, 2008). Similarly, I observed that the steady-state levels of Mim1 substrates were recovered while expressing the TMD of Mim1 in *mim1*Δ cells. This finding argues against the proposal of a receptor-like function for Mim1. It should be noted that since the topology of Mim2 and the specific functions of its different parts are not resolved yet, it cannot be excluded that Mim2 might be involved in initial recognition.

Of note, the import of single-TMD-containing Om14 constructs showed only a moderate dependence on Mim1, suggesting that the optimal interaction with Mim1 requires an intact structure of Om14 or that the variants with a single TMD can easier employ MIM-independent routes. Eventually, the minimal requirement of Mim1 by these constructs might be explained by the fact that single-span proteins are usually easier and faster to be integrated into the membrane.

An additional option for a receptor for Om14 is the pore-forming protein Porin (Fig. 6 pathway IIIb), as a clear contribution of Porin was suggested by my observations. However, since porin exposes only short loops towards the cytosol, a receptor-like function for this protein is unlikely. Similar to Mim1, Porin has been found to be extensively involved in the biogenesis of different types of mitochondrial protein. It is reported to interact with newly synthesized Tom22 and further modulate the assembly of TOM complex (Sakaue et al., 2019). In addition, it is suggested to facilitate the transfer of the small TIM chaperone-

bound carrier precursors through the IMS to the TIM22 complex (Ellenrieder et al., 2019). The two-dimensional electrophoresis data from a previous study proposed that the deletion of Porin fully abolished the capacity of Om14 to form high molecular weight complex (Lauffer et al., 2012). In contrast, we still observed by BN-PAGE two different forms of Om14-containing complex in the absence of Porin, although they were both in lower amounts as compared to their amounts in control samples. Since in their study HA was tagged at the C-terminus of Om14 which is exposed to the IMS side (Burri et al., 2006), we assumed that the C-terminal tagged HA might interfere with the stability of the Om14 oligomeric complex in the absence of Porin. It would be an interesting topic to investigate the precise mechanism by which Porin can promote the Om14 integration into the OMM.

Intriguingly, the combined absence of both Mim1 and Porin resulted in a further reduction of the steady-state level of Om14 compared to the single deletions. This observation further supports the hypothesis that the biogenesis of Om14 can follow several alternative pathways. Furthermore, although both Mim1 and Por1 are proteinaceous elements that significantly influence the biogenesis of Om14, a substantial portion of Om14 molecules could still be correctly integrated into the OMM in the absence of both proteins. This remaining portion of Om14 indicates the existence of either a yet unknown pathway mediated by undiscovered proteinaceous factors or a lipid-relevant biogenesis pathway which has been described before (Fig. 6 pathway II)(Vögtle et al., 2015).

9.2.3 *Membrane fluidity, protein hydrophobicity and unfolding states influence the biogenesis of Om14*

Previous study has shown that the cardiolipin level affects the biogenesis of multi-span OMM proteins (Sauerwald et al., 2015). Our findings further highlight the role of substrate-lipid crosstalk, as unfolding of Om14 or maintenance of the hydrophobicity of the second TMD appears to promote the membrane integration of the protein. In addition, the import of Om14 is accelerated at elevated temperature. These observations can be explained by assuming that while the membrane fluidity is increased due to the elevated temperature, the hydrophobic segments of Om14 might easier integrate into the membrane. Notably, similar effect was also observed after 20 min import of Ugo1, whose membrane integration was reported to be dependent on the OMM phosphatidic acid (PA) level. This further support our assumption, since PA is known to induce

curvature of the membrane and hence to facilitate membrane protein integration. The somehow different behavior of Om14 and Ugo1 at increased temperature indicates that the dependence on membrane properties might be substrate specific. This is also in line with the observation that the integration of Porin into the membrane was compromised at higher temperature. This reduction is possibly due to the fact that the biogenesis of β-barrel proteins highly relies on the activity of multiple proteinaceous import elements like the TOM and TOB/SAM complexes. Collectively, my findings suggest that the membrane integration of Om14 has a higher dependence on the membrane behavior than other proteinaceous factors in comparison to Ugo1 and Porin.

9.2.4 *Om45 regulates the late stages of Om14 biogenesis*

In the carbonate extraction assay, a sub-portion of Om14 has always been found in the supernatant fractions not only in the current study but also in previous ones (Burri et al., 2006; Sauerwald et al., 2015). This portion of apparently membrane peripheral molecules might have stronger interactions with neighbor proteins than with the lipid bilayer. Om45 is one of the potential interactors that appears to mediate the final maturation of Om14. In the absence of Om45, Om14 became more extractable from the membrane and the ability of Om14 to form a high-molecular-weight oligomeric structure was severely impaired. As Om45 exposes its large domain into the IMS, I assumed that Om45 might facilitate the maturation of Om14 from the IMS side after Om14 is properly embedded in the membrane. In addition, the hydrophobicity of the second TMD of Om14 also seems to contribute to its stable membrane integration. Therefore, it is also possible that the putative N-terminal TMD of Om45 interacts with the second TMD of Om14 (or with the other TMDs) to promote the late stages of the biogenesis of Om14.

In summary, this study provides new insights into the variety of parameters that can be involved in the biogenesis of multi-span OMM proteins. For Om14, these parameters include cis elements like protein hydrophobicity and structure properties, and a combination of various trans factors such as proteinaceous elements, the membrane behavior and its lipid composition. Comparing the biogenesis of different model proteins, we cannot conclude that all the multi-span proteins fully share the same biogenesis routes. However, one can speculate that the biogenesis of different multi-span OMM proteins might be modulated by similar elements but to different extents.

The biogenesis of Om14 appears to be relatively robust as alteration of none of the investigated factors massively affected it. Thus, apparently multiple alternative pathways might coexist and contribute altogether to the biogenesis of Om14. My findings suggest that Om4 can follow different biogenesis pathways in which proteinaceous elements and membrane properties contribute to varying degrees to the biogenesis efficiency. Similarly, previous study suggested that single-span OMM proteins also follow multiple biogenesis pathways (Vitali et al., 2020). It is therefore tempting to assume that the multi-factor modulated biogenesis widely exists in many α-helical OMM proteins.

10

REFERENCES

1. Abe, Yoshito, Toshihiro Shodai, Takanori Muto, Katsuyoshi Mihara, Hisayoshi Torii, Shuh ichi Nishikawa, Toshiya Endo, and Daisuke Kohda (2000). "Structural Basis of Presequence Recognition by the Mitochondrial Protein Import Receptor Tom20." In: *Cell* 100.5, pp. 551–560. DOI: 10.1016/S0092-8674(00)80691-1.

2. Araiso, Yuhei et al. (2019). "Structure of the Mitochondrial Import Gate Reveals Distinct Preprotein Paths." In: *Nature* 575.7782, pp. 395–401. DOI: 10.1038/s41586-019-1680-7.

3. Bausewein, Thomas, Deryck J. Mills, Julian D. Langer, Beate Nitschke, Stephan Nussberger, and Werner Kühlbrandt (2017). "Cryo-EM Structure of the TOM Core Complex from Neurospora Crassa." In: *Cell* 170.4, 693–700.e7. DOI: 10.1016/j.cell.2017.07.012.

4. Becker, Thomas, Bernard Guiard, Nicolas Thornton, Nicole Zufall, David A. Stroud, Nils Wiedemann, and Nikolaus Pfanner (2010). "Assembly of the Mitochondrial Protein Import Channel: Role of Tom5 in Two-Stage Interaction of Tom40 with the SAM Complex." In: *Molecular Biology of the Cell* 21.18, pp. 3106–3113. DOI: 10.1091/mbc.E10-06-0518.

5. Becker, Thomas, Sylvia Pfannschmidt, Bernard Guiard, Diana Stojanovski, Dusanka Milenkovic, Stephan Kutik, Nikolaus Pfanner, Chris Meisinger, and Nils Wiedemann (2008). "Biogenesis of the Mitochondrial TOM Complex: Mim1 Promotes Insertion and Assembly of Signal-Anchored Receptors." In: *Journal of Biological Chemistry* 283.1, pp. 120–127. DOI: 10.1074/jbc.M706997200.

6. Becker, Thomas et al. (2011). "The Mitochondrial Import Protein Mim1 Promotes Biogenesis of Multispanning Outer Membrane Proteins." In: *Journal of Cell Biology* 194.3, pp. 387–395. DOI: 10.1083/jcb.201102044.

7. Bonnefoy, Nathalie, Heather L. Fiumera, Geneviève Dujardin, and Thomas D. Fox (2009). “Roles of Oxa1-related Inner-Membrane Translocases in Assembly of Respiratory Chain Complexes.” In: *Biochimica et Biophysica Acta - Molecular Cell Research* 1793.1, pp. 60–70. DOI: 10.1016/j.bbamcr.2008.05.004.

8. Brandner, Katrin, Peter Rehling, and Kaye N. Truscott (2005). “The Carboxyl-Terminal Third of the Dicarboxylate Carrier Is Crucial for Productive Association with the Inner Membrane Twin-Pore Translocase.” In: *Journal of Biological Chemistry* 280.7, pp. 6215–6221. DOI: 10.1074/jbc.M412269200.

9. Brix, Jan, Stefan Rüdiger, Bernd Bukau, Jens Schneider-Mergener, and Nikolaus Pfanner (1999). “Distribution of Binding Sequences for the Mitochondrial Import Receptors Tom20, Tom22, and Tom70 in a Presequence-Carrying Preprotein and a Non- Cleavable Preprotein.” In: *Journal of Biological Chemistry* 274.23, pp. 16522–16530. DOI: 10.1074/jbc.274.23.16522.

10. Brix, Jan, Gabriele A. Ziegler, Klaus Dietmeier, Jens Schneider-Mergener, Georg E. Schulz, and Nikolaus Pfanner (2000). “The Mitochondrial Import Receptor Tom70: Identification of a 25 kDa Core Domain with a Specific Binding Site for Preproteins.” In: *Journal of Molecular Biology* 303.4, pp. 479–488. DOI: 10.1006/jmbi.2000.4120.

11. Burri, Lena, Katherine Vascotto, Ian E. Gentle, Nickie C. Chan, Traude Beilharz, David I. Stapleton, Lynn Ramage, and Trevor Lithgow (2006). “Integral Membrane Proteins in the Mitochondrial Outer Membrane of Saccharomyces Cerevisiae.” In: *FEBS Journal* 273.7, pp. 1507–1515. DOI: 10.1111/j.1742-4658.2006.05171.x.

12. Chan, Nickie C., Vladimir A. Likić, Ross F. Waller, Terrence D. Mulhern, and Trevor Lithgow (2006). “The C-terminal TPR Domain of Tom70 Defines a Family of Mitochondrial Protein Import Receptors Found Only in Animals and Fungi.” In: *Journal of Molecular Biology* 358.4, pp. 1010–1022. DOI: 10.1016/j.jmb.2006.02.062.

13. Chipuk, Jerry E., Tudor Moldoveanu, Fabien Llambi, Melissa J. Parsons, and Douglas R. Green (2010). “The BCL-2 Family Reunion.” In: *Molecular Cell* 37.3, pp. 299–310. DOI: 10.1016/j.molcel.2010.01.025.

14. Claypool, Steven M., Yavuz Oktay, Pinmanee Boontheung, Joseph A. Loo, and Carla M. Koehler (2008). “Cardiolipin Defines the Interactome of the Major ADP/ATP Carrier Protein of the Mitochondrial Inner Membrane.” In: *Journal of Cell Biology* 182.5, pp. 937–950. DOI: 10.1083/jcb.200801152.

15. Cohen, Mickael M.J., Guillaume P. Leboucher, Nurit Livnat-Levanon, Michael H. Glickman, and Allan M. Weissman (2009). “Ubiquitin–Proteasome-dependent Degradation of a Mitofusin, a Critical Regulator of Mitochondrial Fusion.” In: *Molecular Biology of the Cell* 19.6. Ed. by Janet Shaw and Janet Shaw, pp. 2457–2464. DOI: 10.1091/mbc.e08-02-0227.

16. Coonrod, Emily M., Mary Anne Karren, and Janet M. Shaw (2007). “Ugo1p Is a Multipass Transmembrane Protein with a Single Carrier Domain Required for Mitochondrial Fusion.” In: *Traffic* 8.5, pp. 500–511. DOI: 10.1111/j.1600-0854.2007.00550.x.

17. Dimmer, Kai S., Dražen Papić, Benjamin Schumann, Desirée Sperl, Katrin Krumpe, Dirk M. Walther, and Doron Rapaport (2012). “A Crucial Role for Mim2 in the Biogenesis of Mitochondrial Outer Membrane Proteins.” In: *Journal of Cell Science* 125.14, pp. 3464–3473. DOI: 10.1242/jcs.103804.

18. Doan, Kim Nguyen, Alexander Grevel, Christoph U. Mårtensson, Lars Ellenrieder, Nicolas Thornton, Lena Sophie Wenz, Łukasz Opaliński, Bernard Guiard, Nikolaus Pfanner, and Thomas Becker (2020). “The Mitochondrial Import Complex MIM Functions as Main Translocase for α-Helical Outer Membrane Proteins.” In: *Cell Reports* 31.4. DOI: 10.1016/j.celrep.2020.107567.

19. Drwesh, Layla and Doron Rapaport (2020). “Biogenesis Pathways of α-Helical Mitochondrial Outer Membrane Proteins.” In: *Biological Chemistry* 401.6-7, pp. 677–686. DOI: 10.1515/hsz-2019-0440.

20. Dyall, Sabrina D., Stephanie C. Agius, Carine De Marcos Lousa, Véronique Trézéguet, and Kostas Tokatlidis (2003). “The Dynamic Dimerization of the Yeast ADP/ATP Carrier in the Inner Mitochondrial Membrane Is Affected by Conserved Cysteine Residues.” In: *Journal of Biological Chemistry* 278.29, pp. 26757–26764. DOI: 10.1074/jbc.M302700200.

21. Dyall, Sabrina D., Mark T. Brown, and Patricia J. Johnson (2004). “Ancient Invasions: From Endosymbionts to Organelles.” In: *Science* 304.5668, pp. 253–257. DOI: 10.1126/science.1094884.

22. Ellenrieder, Lars, Martin P. Dieterle, Kim Nguyen Doan, Christoph U. Mårtensson, Alessia Floerchinger, María Luisa Campo, Nikolaus Pfanner, and Thomas Becker (2019). “Dual Role of Mitochondrial Porin in Metabolite Transport across the Outer Membrane and Protein Transfer to the Inner Membrane.” In: *Molecular Cell* 73.5, 1056–1065.e7. DOI: 10.1016/j.molcel.2018.12.014.

23. Endres, Maxi, Walter Neupert, and Michael Brunner (1999). “Transport of the ADP/ATP Carrier of Mitochondria from the TOM Complex to the TIM22.54 Complex.” In: *EMBO Journal* 18.12, pp. 3214–3221. DOI: 10.1093/emboj/18.12.3214.

24. Epler, J. L., Lee R. Shugart, and W. Edgar Barnett (1970). “N-Formylmethionyl Transfer Ribonucleic Acid in Mitochondria from Neurospora.” In: *Biochemistry* 9.18, pp. 3575–3579. DOI: 10.1021/bi00820a011.

25. Friedman, Jonathan R., Laura L. Lackner, Matthew West, Jared R. DiBenedetto, Jodi Nunnari, and Gia K. Voeltz (2011). “ER Tubules Mark Sites of Mitochondrial Division.” In: *Science* 334.6054, pp. 358–362. DOI: 10.1126/science.1207385.

26. Galper, J B and J E Darnell (1969). “The Presence of N-formyl-methionyl-tRNA in HeLa Cell Mitochondria.” In: *Biochemical and biophysical research communications* 34.2, pp. 205–14.

27. Ghosh, Sagnika, Donna M. Iadarola, Writoban Basu Ball, and Vishal M. Gohil (2019). “Mitochondrial Dysfunctions in Barth Syndrome.” In: *IUBMB Life* 71.7. Ed. by Janet Shaw and Janet Shaw, pp. 791–801. DOI: 10.1002/iub.2018.

28. Gray, Michael W. (2012). “Mitochondrial Evolution.” In: *Cold Spring Harbor Perspectives in Biology* 4.9, a011403–a011403. DOI: 10.1101/cshperspect.a011403.

29. He, Shichuan and Thomas D. Fox (1997). “Membrane Translocation of Mitochondrially Coded Cox2p: Distinct Requirements for Export of N and C Termini and Dependence on the Conserved Protein Oxa1p.” In: *Molecular Biology of the Cell* 8.8, pp. 1449–1460. DOI: 10.1091/mbc.8.8.1449.

30. Hell, Kai, Walter Neupert, and Rosemary A. Stuart (2001). “Oxa1p Acts as a General Membrane Insertion Machinery for Proteins Encoded by Mitochondrial DNA.” In: *EMBO Journal* 20.6, pp. 1281–1288. DOI: 10.1093/emboj/20.6.1281.

31. Hennon, Seth W., Raunak Soman, Lu Zhu, and Ross E. Dalbey (2015). "YidC/Alb3/Oxa1 Family of Insertases." In: *Journal of Biological Chemistry* 290.24, pp. 14866–14874. DOI: 10.1074/jbc.R115.638171.

32. Hermann, Greg J., John W. Thatcher, John P. Mills, Karen G. Hales, Margaret T. Fuller, Jodi Nunnari, and Janet M. Shaw (1998). "Mitochondrial Fusion in Yeast Requires the Transmembrane GTPase Fzo1p." In: *Journal of Cell Biology* 143.2, pp. 359–373. DOI: 10.1083/jcb.143.2.359.

33. Herrmann, Johannes M., Walter Neupert, and Rosemary A. Stuart (1997). "Insertion into the Mitochondrial Inner Membrane of a Polytopic Protein, the Nuclear-Encoded Oxa1p." In: *The EMBO Journal* 16.9, pp. 2217–2226. DOI: 10.1093/emboj/16.9.2217.

34. Hildenbeutel, Markus, Melanie Theis, Melanie Geier, Ilka Haferkamp, H. Ekkehard Neuhaus, Johannes M. Herrmann, and Martin Ott (2012). "The Membrane Insertase Oxa1 Is Required for Efficient Import of Carrier Proteins into Mitochondria." In: *Journal of Molecular Biology* 423.4, pp. 590–599. DOI: 10.1016/j.jmb.2012.07.018.

35. Hoppins, Suzanne, Jennifer Horner, Cheng Song, J. Michael McCaffery, and Jodi Nunnari (2009). "Mitochondrial Outer and Inner Membrane Fusion Requires a Modifi Ed Carrier Protein." In: *Journal of Cell Biology* 184.4, pp. 569–581. DOI: 10.1083/jcb.200809099.

36. Jia, Lixia, Mary K. Dienhart, and Rosemary A. Stuart (2007). "Oxa1 Directly Interacts with Atp9 and Mediates Its Assembly into the Mitochondrial F 1 F o -ATP Synthase Complex." In: *Molecular Biology of the Cell* 18.5. Ed. by Janet Shaw and Janet Shaw, pp. 1897–1908. DOI: 10.1091/mbc.e06-10-0925.

37. Jiang, Feng, Michael T. Ryan, Michael Schlame, Ming Zhao, Zhiming Gu, Martin Klingenberg, Nikolaus Pfanner, and Miriam L. Greenberg (2000). "Absence of Cardiolipin in the Crd1 Null Mutant Results in Decreased Mitochondrial Membrane Potential and Reduced Mitochondrial Function." In: *Journal of Biological Chemistry* 275.29, pp. 22387–22394. DOI: 10.1074/jbc.M909868199.

38. Jiménez, Beatriz, Francisca Ugwu, Rongmin Zhao, Leticia Ortí, Taras Makhnevych, Antonio Pineda-Lucena, and Walid A. Houry (2012). “Structure of Minimal Tetratricopeptide Repeat Domain Protein Tah1 Reveals Mechanism of Its Interaction with Pih1 and Hsp90.” In: *Journal of Biological Chemistry* 287.8, pp. 5698–5709. DOI: 10.1074/jbc.M111.287458.

39. Jores, Tobias et al. (2018). “Cytosolic Hsp70 and Hsp40 Chaperones Enable the Biogenesis of Mitochondrial β-Barrel Proteins.” In: *Journal of Cell Biology* 217.9, pp. 3091–3108. DOI: 10.1083/jcb.201712029.

40. Kerscher, Oliver, Jason Holder, Maithreyan Srinivasan, Roxanne S. Leung, and Robert E. Jensen (1997). “The Tim54p-Tim22p Complex Mediates Insertion of Proteins into the Mitochondrial Inner Membrane.” In: *Journal of Cell Biology* 139.7, pp. 1663–1675. DOI: 10.1083/jcb.139.7.1663.

41. Kovermann, Peter, Kaye N. Truscott, Bernard Guiard, Peter Rehling, Naresh B. Sepuri, Hanne Müller, Robert E. Jensen, Richard Wagner, and Nikolaus Pfanner (2002). “Tim22, the Essential Core of the Mitochondrial Protein Insertion Complex, Forms a Voltage-Activated and Signal-Gated Channel.” In: *Molecular Cell* 9.2, pp. 363–373. DOI: 10.1016/S1097-2765(02)00446-X.

42. Kreimendahl, Sebastian and Joachim Rassow (2020). “The Mitochondrial Outer Membrane Protein Tom70—Mediator in Protein Traffic, Membrane Contact Sites and Innate Immunity.” In: *International Journal of Molecular Sciences* 21.19, pp. 1–32. DOI: 10.3390/ijms21197262.

43. Kreimendahl, Sebastian, Jan Schwichtenberg, Kathrin Günnewig, Lukas Brandherm, and Joachim Rassow (2020). “The Selectivity Filter of the Mitochondrial Protein Import Machinery.” In: *BMC Biology* 18.1, pp. 1–23. DOI: 10.1186/s12915-020-00888-z.

44. Kulawiak, Bogusz, Jan Höpker, Michael Gebert, Bernard Guiard, Nils Wiedemann, and Natalia Gebert (2013). “The Mitochondrial Protein Import Machinery Has Multiple Connections to the Respiratory Chain.” In: *Biochimica et Biophysica Acta - Bioenergetics* 1827.5, pp. 612–626. DOI: 10.1016/j.bbabio.2012.12.004.

45. Lauffer, Susann, Katrin Mäbert, Cornelia Czupalla, Theresia Pursche, Bernard Hoflack, Gerhard Rödel, and Udo Krause-Buchholz (2012). “Saccharomyces Cerevisiae Porin Pore Forms Complexes with Mitochondrial Outer Membrane Proteins Om14p and Om45p.” In: *Journal of Biological Chemistry* 287.21, pp. 17447–17458. DOI: 10.1074/jbc.M111.328328.

46. Lee, Sung Ryul and Jin Han (2017). “Mitochondrial Nucleoid: Shield and Switch of the Mitochondrial Genome.” In: *Oxidative Medicine and Cellular Longevity* 2017, pp. 1–15. DOI: 10.1155/2017/8060949.

47. Lesnik, Chen, Yifat Cohen, Avigail Atir-Lande, Maya Schuldiner, and Yoav Arava (2014). “OM14 Is a Mitochondrial Receptor for Cytosolic Ribosomes That Supports Co-Translational Import into Mitochondria.” In: *Nature Communications*. DOI: 10.1038/ncomms6711.

48. Long, Ashley R., Catherine C. O’Brien, and Nathan N. Alder (2012). “The Cell-Free Integration of a Polytopic Mitochondrial Membrane Protein into Liposomes Occurs Cotranslationally and in a Lipid-Dependent Manner.” In: *PLoS ONE* 7.9. DOI: 10.1371/journal.pone.0046332.

49. Morgenstern, Marcel et al. (2017). “Definition of a High-Confidence Mitochondrial Proteome at Quantitative Scale.” In: *Cell Reports* 19.13, pp. 2836–2852. DOI: 10.1016/j.celrep.2017.06.014.

50. Murphy, Elizabeth et al. (2016). *Mitochondrial Function, Biology, and Role in Disease: A Scientific Statement from the American Heart Association*. Vol. 118. Circulation Research. DOI: 10.1161/RES.0000000000000104.

51. Nelson, David R., Cherise M. Felix, and Joseph M. Swanson (1998). “Highly Conserved Charge-Pair Networks in the Mitochondrial Carrier Family.” In: *Journal of Molecular Biology* 277.2, pp. 285–308. DOI: 10.1006/jmbi.1997.1594.

52. Neupert, Walter and Johannes M. Herrmann (2007). “Translocation of Proteins into Mitochondria.” In: *Annual Review of Biochemistry* 76, pp. 723–749. DOI: 10.1146/annurev.biochem.76.052705.163409.

53. Opaliński, Łukasz, Jiyao Song, Chantal Priesnitz, Lena Sophie Wenz, Silke Oeljeklaus, Bettina Warscheid, Nikolaus Pfanner, and Thomas Becker (2018). “Recruitment of Cytosolic J-Proteins by TOM Receptors Promotes Mitochondrial Protein Biogenesis.” In: *Cell Reports* 25.8, 2036–2043.e5. DOI: 10.1016/j.celrep.2018.10.083.

54. Osellame, Laura D., Thomas S. Blacker, and Michael R. Duchen (2012). "Cellular and Molecular Mechanisms of Mitochondrial Function." In: *Best Practice and Research: Clinical Endocrinology and Metabolism* 26.6, pp. 711–723. DOI: 10.1016/j.beem.2012.05.003.

55. Otera, Hidenori, Yohsuke Taira, Chika Horie, Yurina Suzuki, Hiroyuki Suzuki, Kiyoko Setoguchi, Hiroki Kato, Toshihiko Oka, and Katsuyoshi Mihara (2007). "A Novel Insertion Pathway of Mitochondrial Outer Membrane Proteins with Multiple Transmembrane Segments." In: *Journal of Cell Biology* 179.7, pp. 1355–1363. DOI: 10.1083/jcb.200702143.

56. Palmer, Catherine S., Alexander J. Anderson, and Diana Stojanovski (2021). "Mitochondrial Protein Import Dysfunction: Mitochondrial Disease, Neurodegenerative Disease and Cancer." In: *FEBS Letters* 595.8, pp. 1107–1131. DOI: 10.1002/1873-3468.14022.

57. Palmieri, F. (2013). "Mitochondrial Metabolite Carrier Protein Family." In: *Encyclopedia of Biological Chemistry: Second Edition*, pp. 149–158. DOI: 10.1016/B978-0-12-378630-2.00149-3.

58. Panigrahi, Rashmi, Szymon Kubiszewski-Jakubiak, James Whelan, and Alice Vrielink (2015). "The Design and Structure of Outer Membrane Receptors from Peroxisomes, Mitochondria, and Chloroplasts." In: *Structure* 23.10, pp. 1783–1800. DOI: 10.1016/j.str.2015.08.005.

59. Papić, Dražen, Katrin Krumpe, Jovana Dukanovic, Kai S. Dimmer, and Doron Rapaport (2011). "Multispan Mitochondrial Outer Membrane Protein Ugo1 Follows a Unique Mim1-dependent Import Pathway." In: *Journal of Cell Biology* 194.3, pp. 397–405. DOI: 10.1083/jcb.201102041.

60. Pebay-Peyroula, Eva (2003). "Structure of Mitochondrial ADP/ATP Carrier in Complex with Carboxyatractyloside." In: 426, p. 6.

61. Pfanner, Nikolaus, Bettina Warscheid, and Nils Wiedemann (2019). "Mitochondrial Proteins: From Biogenesis to Functional Networks." In: *Nature Reviews Molecular Cell Biology* 20.5, pp. 267–284. DOI: 10.1038/s41580-018-0092-0.

62. Pitt, Ashley S. and Susan K. Buchanan (2021). "A Biochemical and Structural Understanding of Tom Complex Interactions and Implications for Human Health and Disease." In: *Cells* 10.5. DOI: 10.3390/cells10051164.

63. Popov-Čeleketić, Jelena, Thomas Waizenegger, and Doron Rapaport (2008). “Mim1 Functions in an Oligomeric Form to Facilitate the Integration of Tom20 into the Mitochondrial Outer Membrane.” In: *Journal of Molecular Biology* 376.3, pp. 671–680. DOI: 10.1016/j.jmb.2007.12.006.

64. Preuss, Marc, Martin Ott, Soledad Funes, Joen Luirink, and Johannes M. Herrmann (2005). “Evolution of Mitochondrial Oxa Proteins from Bacterial YidC: Inherited and Acquired Functions of a Conserved Protein Insertion Machinery.” In: *Journal of Biological Chemistry* 280.13, pp. 13004–13011. DOI: 10.1074/jbc.M414093200.

65. Ramage, L., T. Junne, K. Hahne, T. Lithgow, and G. Schatz (1993). “Functional Cooperation of Mitochondrial Protein Import Receptors in Yeast.” In: *EMBO Journal* 12.11, pp. 4115–4123. DOI: 10.1002/j.1460-2075.1993.tb06095.x.

66. Rojo, Manuel, Frédéric Legros, Danielle Chateau, and Anne Lombès (2002). “Membrane Topology and Mitochondrial Targeting of Mitofusins, Ubiquitous Mammalian Homologs of the Transmembrane GTPase Fzo.” In: *Journal of cell science* 115.Pt 8, pp. 1663–74. DOI: 10.1111/j.1467-968X.1858.tb01122.

67. Ruprecht, Jonathan J. and Edmund R.S. Kunji (2020). “The SLC25 Mitochondrial Carrier Family: Structure and Mechanism.” In: *Trends in Biochemical Sciences* 45.3, pp. 244–258. DOI: 10.1016/j.tibs.2019.11.001.

68. Sakaue, Haruka et al. (2019). “Porin Associates with Tom22 to Regulate the Mitochondrial Protein Gate Assembly.” In: *Molecular Cell* 73.5, 1044–1055.e8. DOI: 10.1016/j.molcel.2019.01.003.

69. Saracco, Scott A. and Thomas D. Fox (2002). “Cox18p Is Required for Export of the Mitochondrially Encoded Saccharomyces Cerevisiae Cox2p C-tail and Interacts with Pnt1p and Mss2p in the Inner Membrane.” In: *Molecular Biology of the Cell* 13.4, pp. 1122–1131. DOI: 10.1091/mbc.01-12-0580.

70. Sauerwald, Julia, Tobias Jores, Michal Eisenberg-Bord, Silvia Gabriela Chuartzman, Maya Schuldiner, and Doron Rapaport (2015). “Genome-Wide Screens in Yeast Highlight a Role for Cardiolipin in Biogenesis of Mitochondrial Outer Membrane Multispan Proteins.” In: *Molecular and Cellular Biology* 35.18, MCB.00107–15. DOI: 10.1128/mcb.00107-15.

71. Sinzel, Monika, Tao Tan, Philipp Wendling, Hubert Kalbacher, Cagakan Özbalci, Xenia Chelius, Benedikt Westermann, Britta Brügger, Doron Rapaport, and Kai Stefan Dimmer (2017). “Mcp3 Is a Novel Mitochondrial Outer Membrane Protein That Follows a Unique IMP -dependent Biogenesis Pathway.” In: *EMBO reports* 18.10, pp. 1869–1869. DOI: 10.15252/embr.201745020.

72. Sogo, L. Farah and Michael P. Yaffe (1994). “Regulation of Mitochondrial Morphology and Inheritance by Mdm10p, a Protein of the Mitochondrial Outer Membrane.” In: *Journal of Cell Biology* 126.6, pp. 1361–1373. DOI: 10.1083/jcb.126.6.1361.

73. Söllner, Thomas, Rupert Pfaller, Gareth Griffiths, Nikolaus Pfanner, and Walter Neupert (1990). “A Mitochondrial Import Receptor for the ADP/ATP Carrier.” In: *Cell* 62.1, pp. 107–115. DOI: 10.1016/0092-8674(90)90244-9.

74. Spinelli, Jessica B. and Marcia C. Haigis (2018). “The Multifaceted Contributions of Mitochondria to Cellular Metabolism.” In: *Nature Cell Biology* 20.7, pp. 745–754. DOI: 10.1038/s41556-018-0124-1.

75. Szyrach, Gregor, Martin Ott, Nathalie Bonnefoy, Walter Neupert, and Johannes M. Herrmann (2003). “Ribosome Binding to the Oxa1 Complex Facilitates Co-Translational Protein Insertion in Mitochondria.” In: *EMBO Journal* 22.24, pp. 6448–6457. DOI: 10.1093/emboj/cdg623.

76. Vitali, Daniela G., Layla Drwesh, Bogdan A. Cichocki, Antonia Kolb, and Doron Rapaport (2020). “The Biogenesis of Mitochondrial Outer Membrane Proteins Show Variable Dependence on Import Factors.” In: *iScience* 23.1, p. 100779. DOI: 10.1016/j.isci.2019.100779.

77. Vitali, Daniela G., Sandro Käser, Antonia Kolb, Kai S. Dimmer, Andre Schneider, and Doron Rapaport (2018). “Independent Evolution of Functionally Exchangeable Mitochondrial Outer Membrane Import Complexes.” In: *eLife* 7, pp. 1–22. DOI: 10.7554/eLife.34488.

78. Vögtle, F. Nora et al. (2015). “The Fusogenic Lipid Phosphatidic Acid Promotes the Biogenesis of Mitochondrial Outer Membrane Protein Ugo1.” In: *Journal of Cell Biology* 210.6, pp. 951–960. DOI: 10.1083/jcb.201506085.

79. Waizenegger, Thomas, Simone Schmitt, Jelena Zivkovic, Walter Neupert, and Doron Rapaport (2005). “Mim1, a Protein Required for the Assembly of the TOM Complex of Mitochondria.” In: *EMBO Reports* 6.1, pp. 57–62. DOI: 10.1038/sj.embor.7400318.

80. Walter, Corvin et al. (2021). “Global Kinome Profiling Reveals DYRK1A as Critical Activator of the Human Mitochondrial Import Machinery.” In: *Nature Communications* 12.1, pp. 1–12. DOI: 10.1038/s41467-021-24426-9.

81. Walther, Dirk M. and Doron Rapaport (2009). “Biogenesis of Mitochondrial Outer Membrane Proteins.” In: *Biochimica et Biophysica Acta - Molecular Cell Research* 1793.1, pp. 42–51. DOI: 10.1016/j.bbamcr.2008.04.013.

82. Wan, Jijun et al. (2016). “Loss of Function of SLC25A46 Causes Lethal Congenital Pontocerebellar Hypoplasia.” In: *Brain* 139.11, pp. 2877–2890. DOI: 10.1093/brain/aww212.

83. Wang, Chunxin and Richard J. Youle (2009). “The Role of Mitochondria in Apoptosis.” In: *Annual Review of Genetics* 43, pp. 95–118. DOI: 10.1146/annurev-genet-102108-134850.

84. Wei, Xiujuan et al. (2020). “Mutations in TOMM70 Lead to Multi-OXPHOS Deficiencies and Cause Severe Anemia, Lactic Acidosis, and Developmental Delay.” In: *Journal of Human Genetics* 65.3, pp. 231–240. DOI: 10.1038/s10038-019-0714-1.

85. Wenz, Lena Sophie et al. (2014). “The Presequence Pathway Is Involved in Protein Sorting to the Mitochondrial Outer Membrane.” In: *EMBO Reports* 15.6, pp. 678–685. DOI: 10.1002/embr.201338144.

86. West, A. Phillip, Gerald S. Shadel, and Sankar Ghosh (2011). “Mitochondria in Innate Immune Responses.” In: *Nature Reviews Immunology* 11.6, pp. 389–402. DOI: 10.1038/nri2975.

87. Wiedemann, Nils and Nikolaus Pfanner (2017). “Mitochondrial Machineries for Protein Import and Assembly.” In: *Annual Review of Biochemistry* 86, pp. 685–714. DOI: 10.1146/annurev-biochem-060815-014352.

88. Wiedemann, Nils, Nikolaus Pfanner, and Michael T. Ryan (2001). “The Three Modules of ADP/ATP Carrier Cooperate in Receptor Recruitment and Translocation into Mitochondria.” In: *EMBO Journal* 20.5, pp. 951–960. DOI: 10.1093/emboj/20.5.951.

89. Wimley, William C and Stephen H White (1996). “At Membrane Interfaces.” In: *Nature Strutural Biology* 3.10, pp. 842–848.

90. Wohlrab, Hartmut (2006). “The Human Mitochondrial Transport/Carrier Protein Family. Nonsynonymous Single Nucleotide Polymorphisms (nsSNPs) and Mutations That Lead to Human Diseases.” In: *Biochimica et Biophysica Acta - Bioenergetics* 1757.9-10, pp. 1263–1270. DOI: 10.1016/j.bbabio.2006.05.024.

91. Wu, Yunkun and Bingdong Sha (2006). “Crystal Structure of Yeast Mitochondrial Outer Membrane Translocon Member Tom70p.” In: *Nature Structural & Molecular Biology* 13.7, pp. 589–593. DOI: 10.1038/nsmb1106.

92. Yamamoto, Hayashi et al. (2011). “Dual Role of the Receptor Tom20 in Specificity and Efficiency of Protein Import into Mitochondria.” In: *Proceedings of the National Academy of Sciences of the United States of America* 108.1, pp. 91–96. DOI: 10.1073/pnas.1014918108.

93. Yamano, Koji, Yoh Ichi Yatsukawa, Masatoshi Esaki, Alyson E. Aiken Hobbs, Robert E. Jensen, and Toshiya Endo (2008). “Tom20 and Tom22 Share the Common Signal Recognition Pathway in Mitochondrial Protein Import.” In: *Journal of Biological Chemistry* 283.7, pp. 3799–3807. DOI: 10.1074/jbc.M708339200.

94. Yen, Ming-Ren, Kevin T. Harley, Yi-Hsiung Tseng, and Milton H. Saier (2001). “Phylogenetic and Structural Analyses of the Oxa1 Family of Protein Translocases.” In: *FEMS Microbiology Letters* 204.2, pp. 223–231. DOI: 10.1111/j.1574-6968.2001.tb10889.x.

95. Young, Jason C, Nicholas J Hoogenraad, and F Ulrich Hartl (2003). “Molecular Chaperones Hsp90 and Hsp70 Deliver Preproteins to the Mitochondrial Import Receptor Tom70.” In: *Trends in Biochemical Sciences* 30.3, p. i. DOI: 10.1016/s0968-0004(05)00043-5.

96. Zara, Vincenzo, Alessandra Ferramosca, Loredana Capoblanco, Katrin M. Baltz, Olga Randel, Joachim Rassow, Ferdinando Palmieri, and Panagiotis Papatheodorou (2007). “Biogenesis of Yeast Dicarboxylate Carrier: The Carrier Signature Facilitates Translocation across the Mitochondrial Outer Membrane.” In: *Journal of cell science* 120.Pt 23, pp. 4099–4106. DOI: 10.1242/JCS.018929.

97. Zimorski, Verena, Chuan Ku, William F. Martin, and Sven B. Gould (2014). “Endosymbiotic Theory for Organelle Origins.” In: *Current Opinion in Microbiology* 22, pp. 38–48. DOI: 10.1016/j.mib.2014.09.008.

11

ACKNOWLEDGMENTS

First of all, I would like to sincerely thank Prof. Dr. Doron Rapaport, my supervisor for offering me the opportunity to do research in his lab. I am very grateful for his guidance, his patience and continuous support. He helped me develop the right attitude towards scientific research and his encouragement constantly boosts up my confidence during my PhD study.

I wish to extend my special thanks to Prof. Dr. Gabriele Dodt, my second supervisor, as well as Prof. Dr. Ralf Jansen and Prof. Dr. Samuel Wagner for their valuable participation as members of my doctoral examination committee.

I would extremely like to thank all my colleagues for being always supportive and considerate. Elena, for all the technical helps and her bright laughter, Kai for his advices and the kitten puzzle, Layla for sharing her rational life philosophy and healthy lifestyle, Fenja for being my hip-hop/swimming/Japanese food mate and all the encouragement and happiness she brought me, Klaudia for teaching me how to become a strong woman and for her Oma-feeding, Anasuya for being our lab databank and cheering me up with KitKat, Nitya for her best snack and game instigation, Vitasta for being my mobile dictionary and understanding my life anxiety, Roza for being my coffee friend and keeping the lab in order, Zac and John for being the new blood with full passion. I would also like to thank the former lab members Daniela, Janani, Diana, Bogdan, Tobias and Moni for helping me rapidly get used to the new working environment when I just joined. Furthermore, I would like to thank Prof. Dr. Martin Jung and Dr. Kai Dimmer for their contribution and advices for the manuscript.

I would like to thank all my friends for adding delight to my life and accompanying me through the hard times. Especially I would like to thank Kaidi for pulling me out of the pile of Latex errors and encouraging me untill the last moment. A very special thanks goes to my close family members. To my husband Yue for willing to follow me into the dark and showing me the scenery from such great heights. To my aunt, uncle and little Maya for bring optimism. To my parents, parents in low and my grandmothers for always believing in me and standing by me. Last but not least, a reduplicate gratitude to my Mom.

12

APPENDIX

Accepted papers

1. Sandra Backes, Yury S. Bykov, Tamara Flohr, Markus Räschle, **Jialin Zhou**, Svenja Lenhard, Lena Krämer, Timo Mühlhaus, Chen Bibi, Cosimo Jann, Justin D. Smith, Lars M. Steinmetz, Doron Rapaport, Zuzana Storchová, Maya Schuldiner, Felix Boos, and Johannes M. Herrmann (2021). The chaperone-binding activity of the mitochondrial surface receptor Tom70 protects the cytosol against mitoprotein-induced stress. *Cell Reports*, 35(1), 108936.
doi: 10.1016/j.celrep.2021.108936.

2. **Jialin Zhou**, Martin Jung, Kai Dimmer, and Doron Rapaport (2022). The multi-factor modulated biogenesis of the mitochondrial multi-span protein Om14. *Journal of Cell Biology*, 221(4), e202112030.
doi: 10.1083/jcb.202112030.

Cell Reports

Article

The chaperone-binding activity of the mitochondrial surface receptor Tom70 protects the cytosol against mitoprotein-induced stress

Graphical Abstract

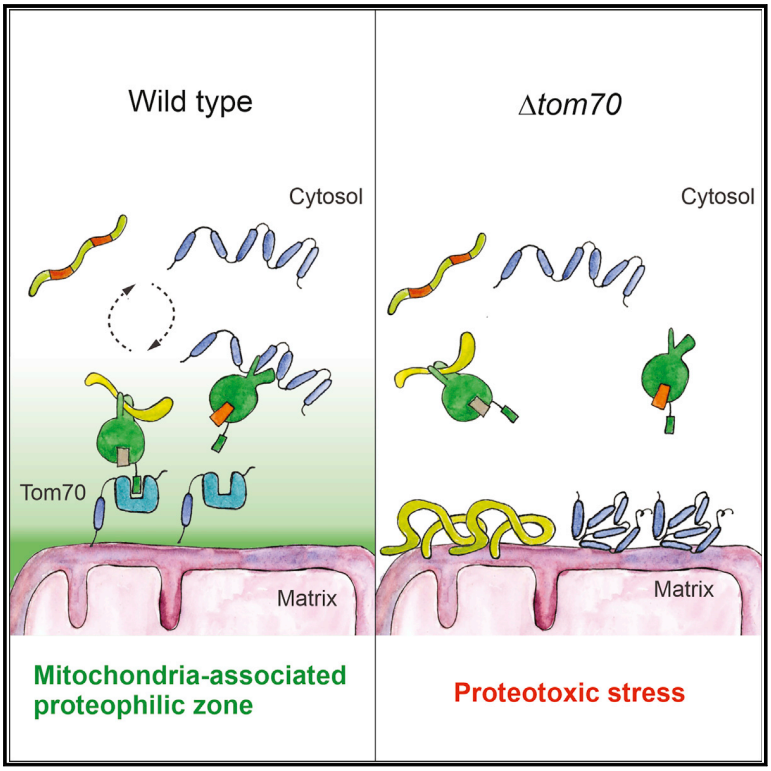

Authors

Sandra Backes, Yury S. Bykov, Tamara Flohr, ..., Maya Schuldiner, Felix Boos, Johannes M. Herrmann

Correspondence

hannes.herrmann@biologie.uni-kl.de

In brief

Backes et al. identify the spectrum of substrates of the mitochondrial Tom70 receptor. Many Tom70 clients are aggregation-prone and/or membrane proteins. *In vivo*, the critical function of Tom70 is the recruitment of chaperones to the mitochondrial surface, whereas its ability to directly bind precursor proteins is largely dispensable.

Highlights

- Tom70 supports the targeting of a wide range of precursor proteins to mitochondria
- *In vivo*, the main function of Tom70 is to recruit chaperones to the outer membrane
- Small inner membrane proteins are highly toxic in the absence of Tom70
- Tom70 protects the cytosol against toxic effects of mitochondrial precursors

Backes et al., 2021, Cell Reports *35*, 108936
April 6, 2021
https://doi.org/10.1016/j.celrep.2021.108936

CellPress

Cell Reports

CellPress
OPEN ACCESS

Article

The chaperone-binding activity of the mitochondrial surface receptor Tom70 protects the cytosol against mitoprotein-induced stress

Sandra Backes,[1] Yury S. Bykov,[2] Tamara Flohr,[1] Markus Räschle,[3] Jialin Zhou,[4] Svenja Lenhard,[1] Lena Krämer,[1] Timo Mühlhaus,[5] Chen Bibi,[2] Cosimo Jann,[6,7] Justin D. Smith,[8,9] Lars M. Steinmetz,[6,8,9] Doron Rapaport,[4] Zuzana Storchová,[3] Maya Schuldiner,[2] Felix Boos,[1] and Johannes M. Herrmann[1,10,*]

[1]Cell Biology, University of Kaiserslautern, 67663 Kaiserslautern, Germany
[2]Department of Molecular Genetics, Weizmann Institute of Science, Rehovot 7610001, Israel
[3]Molecular Genetics, University of Kaiserslautern, 67663 Kaiserslautern, Germany
[4]Interfaculty Institute of Biochemistry, University of Tübingen, 72076 Tübingen, Germany
[5]Computational Systems Biology, University of Kaiserslautern, 67663 Kaiserslautern, Germany
[6]Genome Biology Unit, EMBL, Meyerhofstraße 1, 69117 Heidelberg, Germany
[7]Department of Biology, Institute of Biochemistry, ETH Zürich, 8093 Zürich, Switzerland
[8]Stanford Genome Technology Center, Stanford University, Palo Alto, CA 94304, USA
[9]Department of Genetics, Stanford University School of Medicine, Stanford, CA 94305, USA
[10]Lead contact
*Correspondence: hannes.herrmann@biologie.uni-kl.de
https://doi.org/10.1016/j.celrep.2021.108936

SUMMARY

Most mitochondrial proteins are synthesized as precursors in the cytosol and post-translationally transported into mitochondria. The mitochondrial surface protein Tom70 acts at the interface of the cytosol and mitochondria. *In vitro* import experiments identified Tom70 as targeting receptor, particularly for hydrophobic carriers. Using *in vivo* methods and high-content screens, we revisit the question of Tom70 function and considerably expand the set of Tom70-dependent mitochondrial proteins. We demonstrate that the crucial activity of Tom70 is its ability to recruit cytosolic chaperones to the outer membrane. Indeed, tethering an unrelated chaperone-binding domain onto the mitochondrial surface complements most of the defects caused by Tom70 deletion. Tom70-mediated chaperone recruitment reduces the proteotoxicity of mitochondrial precursor proteins, particularly of hydrophobic inner membrane proteins. Thus, our work suggests that the predominant function of Tom70 is to tether cytosolic chaperones to the outer mitochondrial membrane, rather than to serve as a mitochondrion-specifying targeting receptor.

INTRODUCTION

With a concentration of 30,000 to 50,000 ribosomes per μm^3, the eukaryotic cytosol is densely packed with molecular machines for protein synthesis that make up a considerable fraction of its total volume (Marini et al., 2020). Rapid and efficient protein folding in the cytosol is of pivotal importance for rapidly growing cells. Chaperones, particularly those of the Hsp70 and Hsp90 family, with the assistance of different co-chaperones and accessory factors, bind to nascent chains as soon as they emerge from the ribosome in order to facilitate their folding (Hartl et al., 2011; Kramer et al., 2019; Sontag et al., 2017) or hold them in a translocation-competent state for transport across membranes of organelles (Deshaies et al., 1988; Jores et al., 2018; Hoseini et al., 2016; Young et al., 2003).

Mitochondria are essential organelles of eukaryotic cells. They synthesize a handful of very hydrophobic polypeptides on mitochondrial ribosomes in the matrix. All other 900 (yeast) to 1,500 (humans) mitochondrial proteins are encoded by nuclear genes and synthesized in the cytosol (Vögtle et al., 2017; Morgenstern et al., 2017; Calvo et al., 2016). With the exception of a small number of inner membrane proteins (Williams et al., 2014; Tsuboi et al., 2020), the import of mitochondrial proteins occurs post-translationally, meaning that they are first synthesized in the cytosol and subsequently translocated into mitochondria; however, the spatiotemporal details of these processes are largely elusive (Jan et al., 2014; Gold et al., 2017).

Mitochondrial protein biogenesis strictly depends on the cytosolic chaperone capacity (Becker et al., 1996; Terada et al., 1996; Hoseini et al., 2016; Ben-Menachem et al., 2018; Deshaies et al., 1988; Döring et al., 2017; Pfanner et al., 1987; Stein et al., 2019). Presumably as a consequence of their strong tendency to sequester chaperones, precursor proteins accumulating in the cytosol induce a sudden growth arrest, trigger the heat shock response to increase components of the chaperone and proteasome system, and activate specific factors on the mitochondrial surface that clean off translocation intermediates (Mårtensson et al., 2019; Wrobel et al., 2015; Weidberg and Amon, 2018;

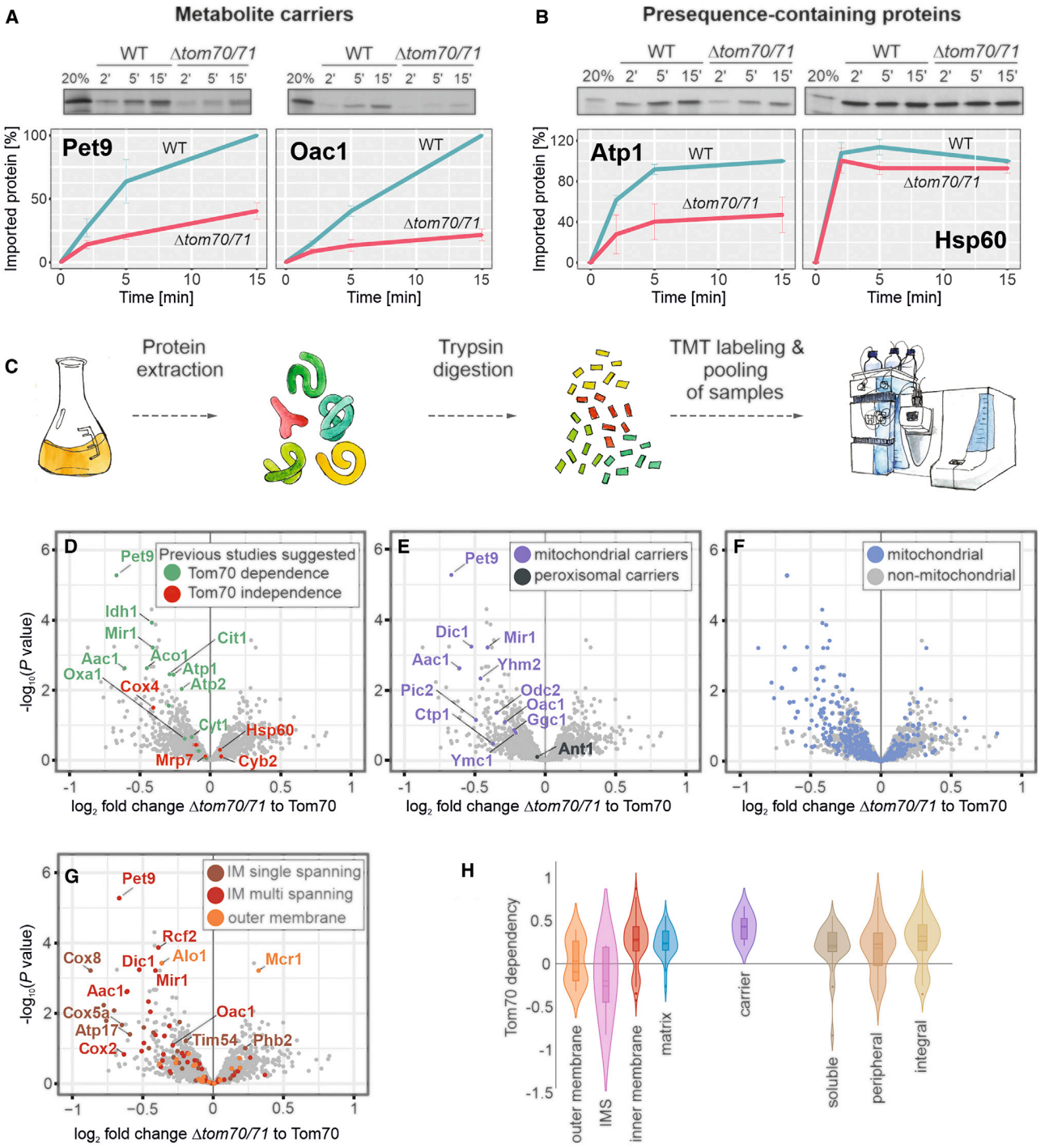

Figure 1. Identification of Tom70/71 clients

(A and B) Radiolabeled Atp1, Hsp60, Pet9, and Oac1 were incubated with isolated wild-type and *Δtom70/71* mitochondria for the times indicated at 25°C. Non-imported protein was removed by treatment with proteinase K, and samples were analyzed by SDS-PAGE and autoradiography. Graphs show mean values and standard deviations from three independent experiments.

(C) The proteomes of different mutants were compared using quantitative proteomics and multiplexing (see also Figure S1A).

(D–G) The proteomes of *Δtom70/71* cells carrying either empty or Tom70-expressing plasmids (three biological replicates each) were measured by mass spectrometry. Shown are the mean values of the ratios obtained from *Δtom70/71* (30°C) to Tom70-expressing cells (30°C) plotted against their statistical

(legend continued on next page)

Boos et al., 2019, 2020; Wang and Chen, 2015; Shakya et al., 2020).

Most mitochondrial proteins are synthesized with an N-terminal presequence that serves as a matrix-targeting signal (MTS) (Vögtle et al., 2009; von Heijne, 1986). Presequences are recognized by Tom20 and Tom22, two receptor proteins that are part of the translocase of the outer membrane (TOM) complex (Rimmer et al., 2011; Shiota et al., 2015; Araiso et al., 2019) before they lead the way into the matrix, across protein-conducting channels of the TOM complex and the presequence translocase (or TIM23 complex) in the inner membrane (Chacinska et al., 2009). Internal MTS-like (iMTS-L) sequences are frequently found in matrix proteins; although not sufficient as import signals, these patterns can strongly improve the import competence of precursors (Backes et al., 2018).

Many mitochondrial proteins, however, lack presequences and embark on other import routes into mitochondria. This is the case for all proteins of the outer membrane and most components of the intermembrane space (IMS) that use several distinct pathways (Drwesh and Rapaport, 2020; Wiedemann and Pfanner, 2017; Finger and Riemer, 2020; Edwards et al., 2020; Doan et al., 2020). In addition, many mitochondrial inner membrane proteins, in particular the members of the metabolite carrier family (carriers for short), lack presequences and are imported by a distinct "carrier pathway" (Horten et al., 2020; Rehling et al., 2004). From studies using the ATP/ADP carrier (i.e., Pet9 in yeast) as a model protein, it was proposed that the carrier pathway differs from the import route of matrix-destined proteins already on the surface of mitochondria, where carriers bind the "carrier receptor" Tom70 that would insert them into the universal protein-conducting channel of the TOM complex. In the IMS, a soluble chaperone complex consisting of small Tim proteins further transfers the carriers to a specific translocase of the inner membrane, the TIM22 complex, for membrane insertion. Although the mitochondrial steps of the carrier pathways were dissected in detail by powerful *in vitro* assays (Pfanner and Neupert, 1987; Ryan et al., 1999; Hasson et al., 2010), the early, i.e., cytosolic, steps remain unclear.

This lack of understanding is particularly obvious for the role of Tom70 (and its paralog Tom71), although this outer membrane protein was one of the first import components discovered (Söllner et al., 1990; Steger et al., 1990; Hines et al., 1990). In contrast to all other TOM subunits, Tom70 is presumably no stoichiometric component of the TOM complex but rather associates with the outer membrane translocase in a dynamic and transient fashion.

Tom70 offers dedicated binding sites for the recruitment of cytosolic Hsp70 and Hsp90 chaperones by their unique C-terminal EEVD tails (Young et al., 2003) and was found to interact with co-chaperones (Opaliński et al., 2018). It also directly binds mitochondrial precursor proteins (Papic et al., 2011; Brix et al., 1999, 2000; Iwata and Nakai, 1998; Melin et al., 2015) and prevents their aggregation (Yamamoto et al., 2009). However, the specific contribution of each of these properties in the context of mitochondrial protein import is not clear, particularly, because these functions of Tom70 cannot be reliably assessed with the *in vitro* import assays that were used in most studies.

In this study, we used a number of complementary *in vivo* approaches to elucidate the specific role of Tom70. Our assays demonstrate that Tom70 is not a specific receptor for carriers. Rather, Tom70 supports the biogenesis of some carriers (in particular, of Pet9) but also that of many other mitochondrial proteins. Many Tom70 clients contain hydrophobic transmembrane segments or other aggregation-prone regions. Most of these proteins are also sensitive to heat, which is in line with the temperature sensitivity of Tom70-deficient cells. Interestingly, the loss of Tom70 can be largely complemented in strains carrying an unrelated EEVD-binding protein on the mitochondrial surface. Thus, the predominant and crucial function of Tom70 is not that of a classical import receptor. Instead, Tom70 serves as co-chaperone on the mitochondrial surface to suppress the toxic effects of mitochondrial precursor proteins.

RESULTS

Tom70 is required for the biogenesis of many mitochondrial proteins

On the basis of *in vitro* experiments with a very small number of substrates, Tom70 was proposed to serve as a mitochondrial import receptor for precursors that are made without presequences (Papic et al., 2011; Becker et al., 2011; Brix et al., 1999; Steger et al., 1990), in particular of carriers such as Pet9 or Oac1 (Figure 1A). Tom70 also supports the *in vitro* import process of some presequence-containing proteins, such as Atp1, but not that of others, such as Hsp60 (Figure 1B). Hence, to date, there is no clear understanding of the substrate range of Tom70. To elucidate the *in vivo* substrate spectrum of Tom70, we hypothesized that proteins that are not properly imported into mitochondria will be degraded by cytosolic quality control and hence that we can use their steady-state cellular abundance as a proxy for their capacity to be properly targeted to mitochondria. Therefore, we measured, using quantitative mass spectrometry, the levels of all mitochondrial proteins in *Δtom70/71* mutants lacking the genes for Tom70 and its barely expressed paralog Tom71 (Schlossmann et al., 1996; Figures 1C, S1A, and S1B; Tables S1 and S2). Cells were grown on galactose at 30°C, at which a loss of Tom70 does not result in reduced growth rates, to avoid secondary-growth-dependent effects (Figure S1C). Cells were harvested at exponential growth phase from which proteins were extracted and digested with trypsin. Peptides were labeled using a tandem mass tag (TMT) protocol and multiplexed to quantify proteins in combined sample runs (samples from additional mutants, described later, were also pooled).

This experiment reliably confirmed previous reports about the Tom70-dependent or -independent nature of individual proteins (Figure 1D). The majority of mitochondrial carrier proteins, but

significances (p values). The points in the top left corner show the highest Tom70 dependence. The data point for Tom70 is shown in Figure S1B. Different groups of proteins are indicated in the same dataset. IM, inner membrane.
(H) The relative depletion of proteins in the Δ*tom70/71* to Tom70 comparison (log_2 fold changes [FCs]) were taken as proxy for the Tom70 dependence of proteins. Shown are the distributions of these Tom70 dependence values for different groups of mitochondrial proteins (Morgenstern et al., 2017).

not the peroxisomal carrier Ant1, were reduced in the *Δtom70/71* mutant, albeit to different degrees (Figure 1E). In particular, Pet9 was confirmed as a Tom70/71-dependent mitochondrial protein, which is in line with the results from *in vitro* import assays. Interestingly, however, many other mitochondrial proteins were diminished in *Δtom70/71* samples that were not previously reported to be dependent on Tom70 (Figure 1F). This observation points toward a much more general function of Tom70/71 in mitochondrial biogenesis. In particular, membrane proteins were found to be affected (Figure 1G). Many mitochondrial proteins belonging to all types of sub-mitochondrial compartments were consistently, but not strongly, reduced in the Δ*tom70/71* samples, and no proteins were depleted by more than 40%, explaining the efficient growth of the mutant even on respiratory media.

Taking protein levels in these strains as a proxy for their Tom70 dependence, we found that many inner membrane proteins, including carriers, as well as many proteins of the matrix use this outer membrane receptor (Figure 1H). Proteins of the outer membrane, on the other hand, showed a heterogeneous Tom70 dependence, and most IMS proteins did not show alterations in abundance in Tom70/71 mutants, which is consistent with previous studies (Lutz et al., 2003; Araiso et al., 2019; Gornicka et al., 2014). Many soluble proteins were affected in the Tom70 mutants, arguing against a role of Tom70 as a specific receptor for membrane proteins.

Mitochondrial proteins strongly differ in their dependence on Tom70

As a second, independent strategy to measure the Tom70 dependence of mitochondrial proteins under *in vivo* conditions, we selected a set of 113 MTS-independent mitochondrial proteins N-terminally fused with superfolder green fluorescent protein (sfGFP) and visualized them on the background of Tom70/71 mutants. Specifically, we picked the strains from the N-terminal SWAp-Tag (N-SWAT) library (Weill et al., 2018) in which each of these proteins is tagged with N-terminal sfGFP under the control of a *NOP1* promoter (Figure 2A; see STAR Methods for details). We used fluorescence intensity as a proxy for protein abundance and, in addition, to determine whether the proteins localize correctly to mitochondria. Using automated approaches, we introduced the tagged strains into genetic backgrounds that lack either Tom70 (Δ*tom70*), its paralog Tom71 (Δ*tom71*), or both (Δ*tom70/71*). High-content microscopy screening of these mutants showed three patterns (Figures 2B–2D and S2). The mitochondrial accumulation of some proteins, such as the ATP/ADP carrier Pet9, was considerably reduced in the absence of Tom70 and also affected to a certain degree in *Δtom71* single mutants (Figure 2B). The degree of Pet9 reduction in this microscopy screen was very similar to that of the proteomics measurements, and both approaches showed that in the absence of Tom70/71, about one-half of the normal Pet9 levels accumulated in mitochondria.

Some proteins, such as the phosphate carrier Pic2, were Tom71 independent but required Tom70 for efficient accumulation in mitochondria (Figure 2C). A third group, including the dicarboxylate carrier Odc2, was only mildly affected in all mutants, even in the *Δtom70/71* double deletion (Figure 2D). These results showed that Tom71 supports the biogenesis of some proteins but is not essential for any of them. But also, the relevance of Tom70 was surprisingly variable, and even many carrier proteins efficiently accumulated in mitochondria in *Δtom70/71* mutants (Figures 2D and 2E).

By using two orthogonal approaches, we consistently found that, *in vivo*, carriers strongly vary in their Tom70 dependence (Figures S3A and S3B). The results of the image-based screen with GFP-tagged carriers thereby correlated well with the proteomic data (Figure S3C). Carriers are not per se more affected in *Δtom70/71* mutants than other mitochondrial membrane proteins. These results challenge the long-standing notion that Tom70/71 is a specialized carrier receptor. Rather, Tom70 and (to a much lesser degree) Tom71 support mitochondrial biogenesis of many proteins. However, the individual dependence of mitochondrial proteins on these receptors varies considerably.

Tom70/71 supports biogenesis of aggregation-prone mitochondrial proteins

We mined our dataset of Tom70-dependent proteins for features that could determine whether a protein needs the assistance of Tom70 for its biogenesis. As expected, we found Tom70-dependent proteins to be enriched with iMTS-Ls, internal stretches that structurally mimic presequences (Figure 3A). They were reported before to be efficient binding sites for Tom70 (Backes et al., 2018). In addition, we found significantly higher aggregation propensities for Tom70-dependent proteins (Figure 3A). The large, hydrophobic carriers are predicted to be particularly aggregation prone, which might explain why many carriers depend more on Tom70; there is more heterogeneity for other inner membrane or matrix proteins (Figure 3B). The notion that Tom70 might be required for the correct biogenesis of proteins that are prone to misfolding and potentially aggregate is in line with the temperature-sensitive phenotype of the Δ*tom70/71* mutant (Figure 3C).

If Tom70 indeed predominantly supports the biogenesis of demanding, aggregation-prone proteins, one would expect that deletion of this stabilizing factor has similar effects on its clients as conditions that promote the general misfolding of proteins. To test this hypothesis, we compared the effect of the absence of Tom70 with the effect of a higher temperature. We grew cells on galactose at 30°C and 37°C and compared the temperature-dependent changes in proteome composition with those caused by deletion of *TOM70/71* (Figures 3D and 3E). We observed that many chaperones were found at higher levels in 37°C-grown cells but were hardly influenced by the absence or presence of Tom70 (Figure 3E, marked in red), showing that Δ*tom70/71* cells do not suffer from generally perturbed protein homeostasis. Interestingly, levels of many mitochondrial proteins were reduced by high temperatures as well as by the loss of Tom70, and the effects in these conditions are remarkably similar (Figure 3E). This is most impressive for Pet9 that was strongly reduced under both conditions, again indicating its aggregation-prone nature.

Hence, these results suggest that its tendency to misfold or even aggregate determines whether a mitochondrial protein requires Tom70 for its biogenesis. Thus, *in vivo*, the predominant role of Tom70 may be not so much that of a receptor that confers directed or specific targeting of its cargo to the surface of

CellPress
OPEN ACCESS

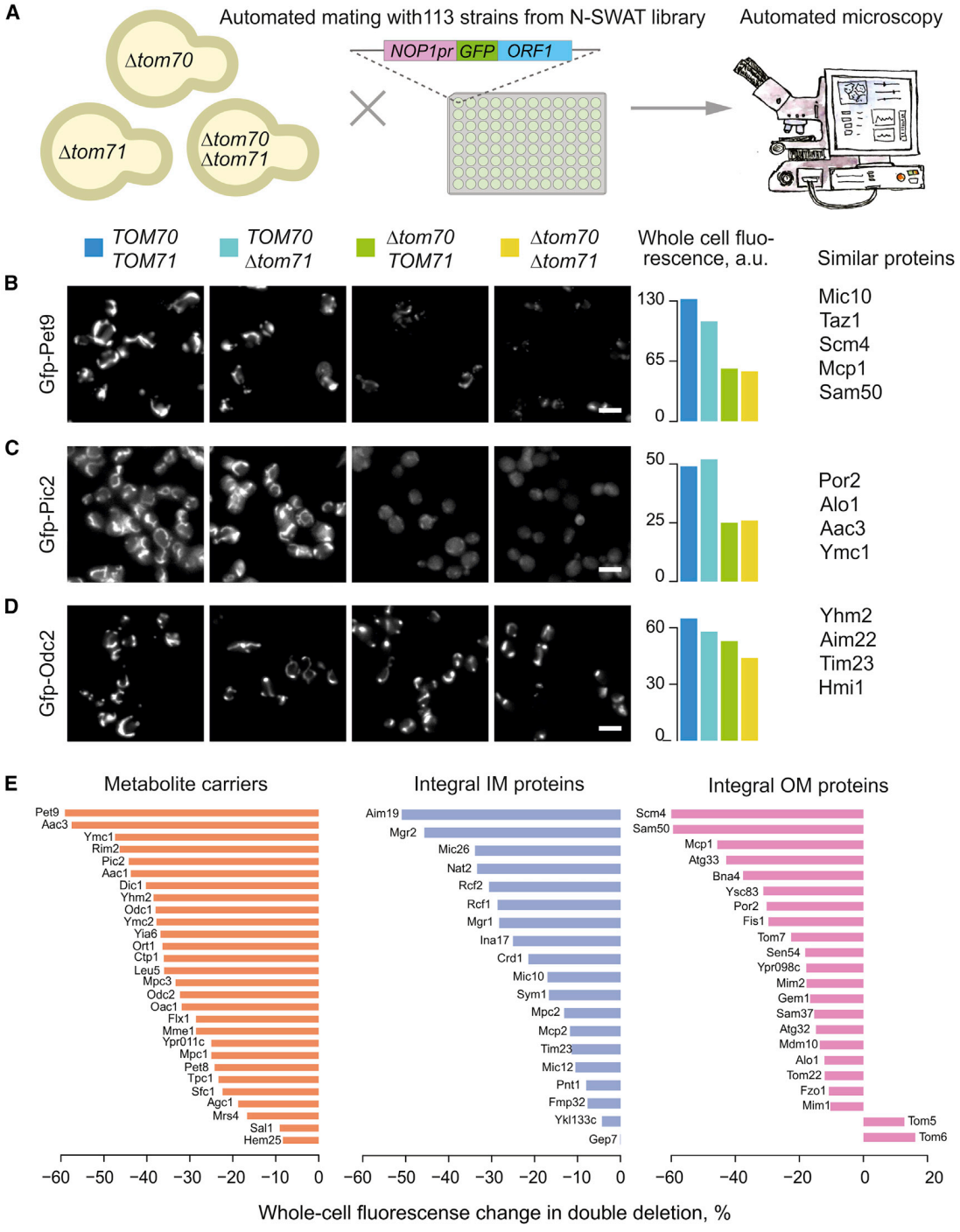

Figure 2. Mitochondrial proteins strongly differ in their Tom70 dependence

(A) Scheme of the systematic visual screen of GFP-tagged mitochondrial proteins.

(B–D) The mitochondrial localization of 113 N-terminally GFP-tagged mitochondrial proteins (all lacking an MTS) were visualized. Proteins shown in (B) showed a strongly reduced mitochondrial localization in the absence of Tom70 and moderately reduced levels if Tom71 was deleted. Thus, these proteins depend to some degree on both receptors. Proteins shown in (C) were unaffected if Tom71 was deleted but still required Tom70. For proteins shown in (D), Tom70 and Tom71 were hardly, if at all, relevant.

(E) The whole-cell GFP signal change in Δ*tom70*Δ*tom71* compared with wild-type cells measured for different mitochondrial protein classes. See Table S3 for details. Scale bars, 10 μm. OM, outer membrane.

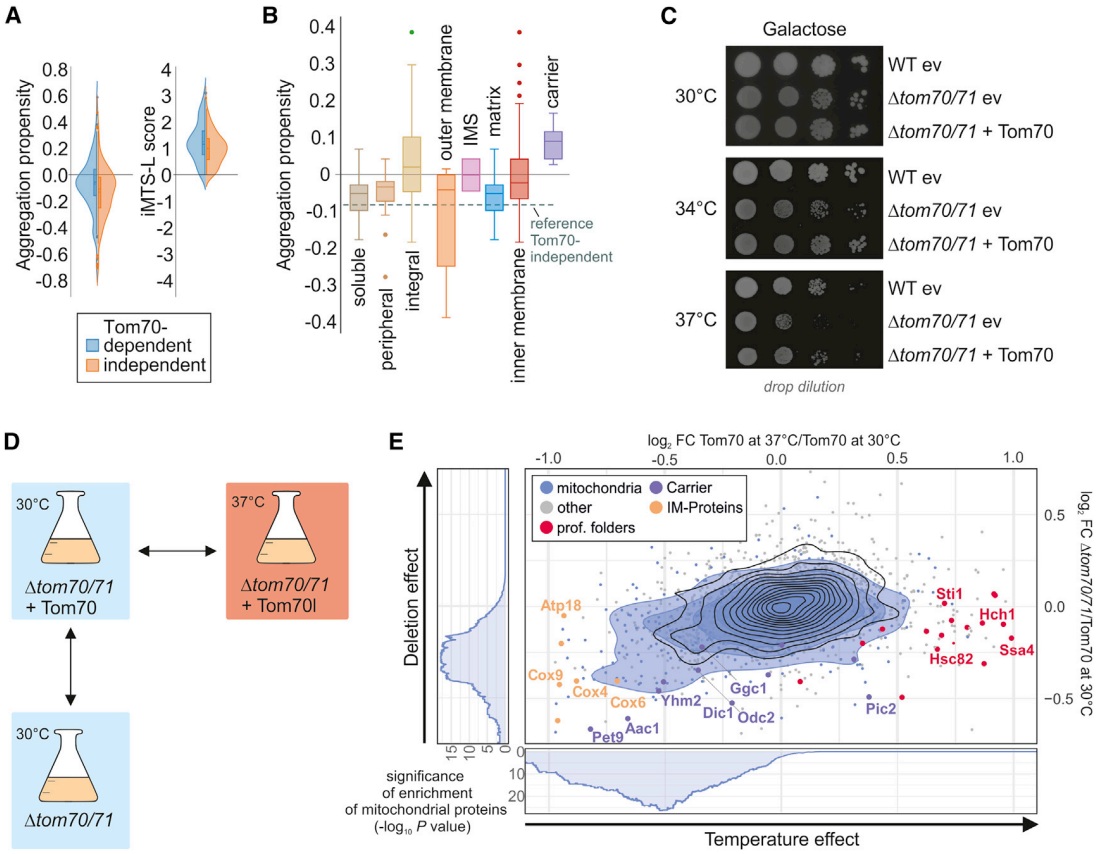

Figure 3. Tom70/71 supports biogenesis of aggregation-prone mitochondrial proteins

(A) The aggregation propensities (Conchillo-Solé et al., 2007) and the presence of iMTS-L sequences in proteins (Boos et al., 2018) were calculated. Plotted are the distributions of these values for Tom70-dependent (log_2 FC, <−0.2) and -independent (log2 FC, >0.2) proteins.

(B) Aggregation propensities were calculated for different groups of mitochondrial proteins. The dotted line shows the mean value of Tom70-independent proteins as a reference.

(C) The indicated strains were precultured in galactose-containing medium at 30°C and spotted on galactose medium, following 3 days of incubation at 30°C, 34°C, or 37°C. WT, wild-type; ev, empty vector.

(D and E) The influence of temperature (log_2 FC of Tom70 37°C as compared to Tom70 30°C) and the absence of Tom70 (log_2 FC of Δ*tom70/71* as compared to Tom70 at 30°C) were analyzed. Blue circles show the isobaric distribution of mitochondrial proteins, whereas black ones show the distribution of the entire proteome. Enrichment of mitochondrial proteins among proteins with a log_2 FC below a certain threshold was calculated, and significance of this enrichment was plotted (side panels).

mitochondria. Rather, Tom70 safeguards proteins that are intrinsically prone to acquire non-productive, presumably import-incompetent or even toxic conformations. This function seems particularly relevant at elevated temperatures when proteostasis is in any way challenged.

Tom70 can be replaced by a chaperone-tether on the mitochondrial surface

How does Tom70 support the biogenesis of proteins that are prone to misfolding and aggregation? The large size and the multi-domain structure of Tom70/71 indicate that it is not just a simple binder for precursor proteins, as is the case for the much smaller Tom20. Tom70 is tethered to the outer membrane by an N-terminal transmembrane domain and exposes three soluble domains to the cytosol, called Clamp, Core, and C-tail domains (Figure 4A; Young et al., 2003; Chan et al., 2006; Brix et al., 2000). For simplicity, we refer to them here as C1, C2, and C3. All three domains are formed by tetratricopeptide repeats (TPRs). C2 and C3 were reported to bind internal targeting signals of precursor proteins, such as Pic2 (Brix et al., 2000) (C2) or Adh3 (Chan et al., 2006) and rat alcohol dehydrogenase (Melin et al., 2015) (C3). In contrast, C1 forms a binding groove to recruit the C-terminal EEVD tetrapeptides of Hsp70 and Hsp90 chaperones (Young et al., 2003; Li et al., 2009). We reasoned that it might be this chaperone-binding activity that contributes to the function of Tom70 as a stabilizer of aggregation-prone proteins. Expression of a mutant version of Tom70 that contains only the C1 domain proved to be impossible because it was unstable *in vivo* and never accumulated to detectable levels (Figure S4A). However, TPR domains are found in many cellular proteins where they serve as specific binding modules for different groups of ligands (Perez-Riba and Itzhaki, 2019).

CellPress
OPEN ACCESS

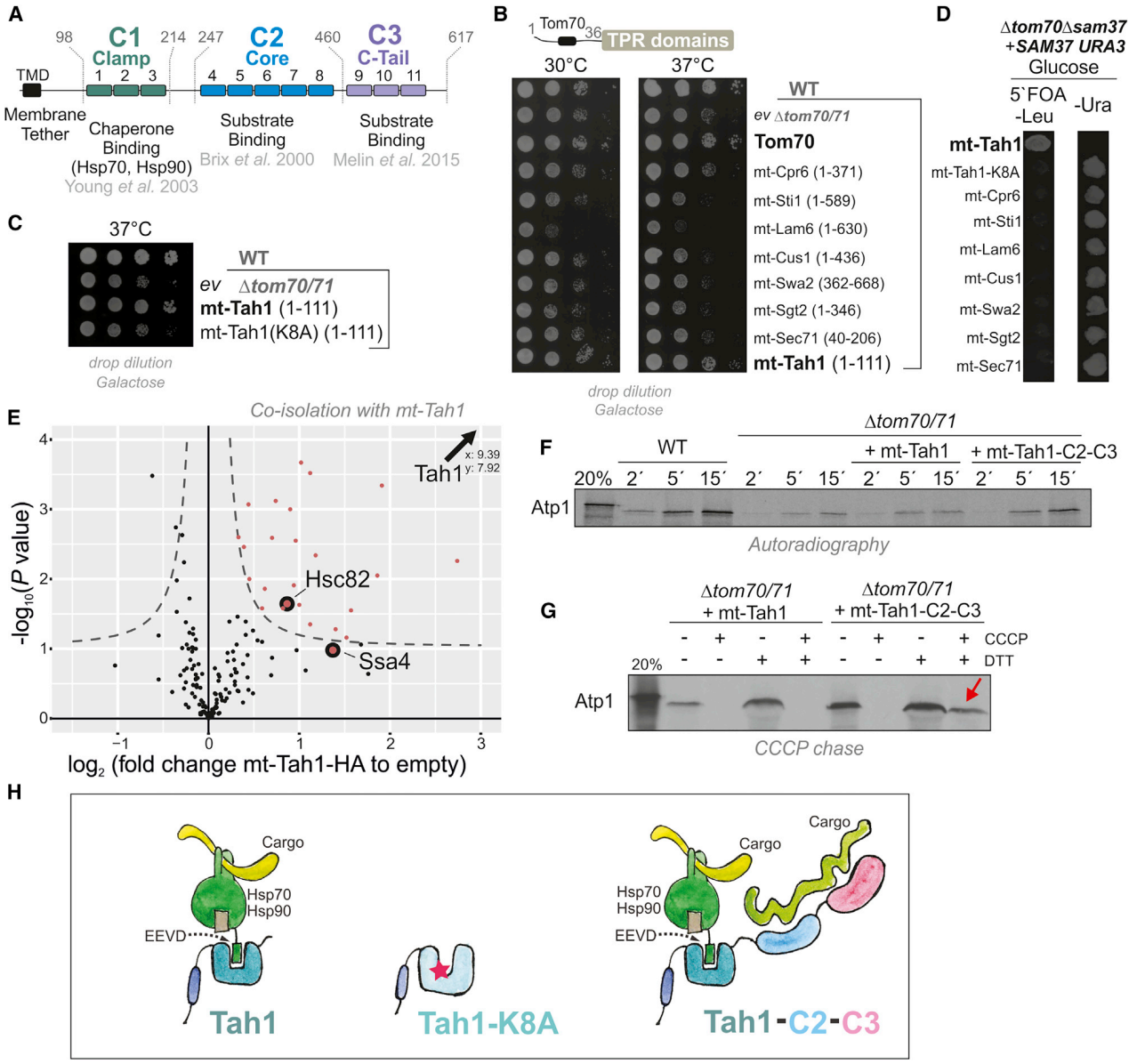

Figure 4. Tom70 can be replaced by a chaperone tether on the mitochondrial surface

(A) Schematic representation of the different domains of Tom70 formed by 11 TPR domains.

(B and C) The indicated sequences of yeast TPR proteins were fused to the membrane anchor of Tom70 and expressed in the *Δtom70/71* mutant.

(D) A *Δsam37 Δtom70* double mutant carrying *SAM37* on a *URA3*-containing plasmid was transformed with plasmids for the expression of the indicated fusion proteins. Upon addition of 5-fluoroorotic acid (5′FOA), only cells that lost the *URA3*-containing *SAM37* plasmid could grow.

(E) Cells of the *Δtom70/71* mutant carrying the mt-Tah1 expression or an empty plasmid were grown in galactose medium to mid-log phase. Cells were washed, gently lysed with Triton X-100, and incubated with Sepharose beads carrying HA-specific antibodies (to pull out mt-Tah1). Samples from four independent replicates for each strain were analyzed by mass spectrometry. The full dataset can be found in Table S4.

(F) Radiolabeled Atp1 was incubated with mitochondria isolated from the indicated mutants. Non-imported Atp1 was removed by adding proteinase K after the times indicated. Mt-Tah1-C2-C3 is a fusion protein in which the C2 and C3 domains of Tom70 were fused to mt-Tah1.

(G) Radiolabeled Atp1 was incubated with mitochondria after the membrane potential was depleted by treatment with carbonyl cyanide *m*-chlorophenyl hydrazone (CCCP). When indicated, CCCP was quenched by dithiothreitol (DTT) to restore the membrane potential. The presence of the C2-C3 domains was essential to keep Atp1 bound to the mitochondria (indicated by the red arrow).

(H) Model of the chaperone binding property of the C1 domain of Tom70/71 and of mt-Tah1. The C2 and C3 domains facilitate direct substrate binding that is particularly relevant under the conditions of the *in vitro* import reaction.

Alignments of the first three TPR domains of Tom70 show sequence similarity to other TPR proteins of yeast (Figures S4B), which inspired us to test whether any of these other TPR domains can functionally replace Tom70. To this end, we fused six TPR domains to the transmembrane domain of Tom70 and expressed these sequences in the *Δtom70/71* mutant (Figure S4C). Tethering the protein Tah1 to the outer membrane (mt-Tah1) suppressed the temperature-sensitive growth of the mutant, whereas the other TPR domains had no or even negative effects (Figures 4B and S4D).

Intriguingly, Tah1, just like Tom70, is an Hsp70/90-binding protein, although it functions in a completely different context as follows: Tah1 is a subunit of the cytosolic Rvb1-Rvb2-Tah1-Pih1 (R2TP) assembly complex that facilitates the biogenesis of RNA polymerases and other RNA-binding complexes (Back et al., 2013; Jiménez et al., 2012; Boulon et al., 2010). Its 111 residues form 1 globular domain comprising 2 TPR stretches and a capping helix that specifically bind the EEVD-tail of cytosolic Hsp90 (Millson et al., 2008). A point mutation in mt-Tah1 (K8A) that destroys its Hsp90-binding ability (Jiménez et al., 2012) was unable to suppress the phenotype of the *Δtom70/71* mutant (Figure 4C). mt-Tah1, but not mt-Tah1(K8A), was even able to rescue the synthetic lethal Δ*tom70* Δ*sam37* double mutant, demonstrating that mt-Tah1 can specifically replace Tom70 and not only indirectly buffers the adverse effects of its absence (Figures 4D, S4E, and S4F).

Next, we purified the mt-Tah1 protein from whole-cell extracts by using its hemagglutinin (HA) tag and identified bound proteins by quantitative mass spectrometry (Figure 4E). A number of interaction partners of mt-Tah1 were identified, including the cytosolic chaperones Hsp82/Hsc82 (the yeast representatives of Hsp90) and the cytosolic Hsp70 Ssa4 (Table S4).

In contrast to the *in vivo* situation, in *in vitro* import experiments, mt-Tah1 was not able to replace Tom70 in its ability to facilitate the import of Tom70-dependent substrate proteins such as Atp1 (Figure 4F). Only when mt-Tah1 was extended with the C2 and C3 domains of Tom70, it was able to support the import of radiolabeled Atp1. This was particularly apparent in "CCCP chase experiments" (Haucke et al., 1995; Backes et al., 2018) in which Atp1 was initially bound to de-energized mitochondria and subsequently chased across the outer membrane upon restoration of the membrane potential (Figure 4G). In that setup, Tom70 is crucial to hold Atp1 on the mitochondrial surface, a function that obviously is not carried out by mt-Tah1. These results confirm that mt-Tah1 rescues the Δ*tom70/71* mutant by replacing it as a chaperone-recruitment factor on the outer membrane (Young et al., 2003), and not by direct binding to precursor proteins (Figure 4H). In summary, we conclude that the ability of Tom70 to bind substrates directly is largely dispensable under physiological *in vivo* conditions.

Chaperone binding by Tom70 is important for different cellular activities

If indeed it is the co-chaperone activity of Tom70 that is essential for cellular and mitochondrial function, we would expect this to be evident from the cellular effects of its absence. To map such global effects, we set out to identify synthetic lethal or sick genetic interactions in Δ*tom70* mutants. We carried out a genome-wide genetic interaction screen (Baryshnikova et al., 2010; Tong and Boone, 2007) by crossing a *Δtom70* query strain with the systematic yeast knockout library in which all non-essential genes were individually deleted. We measured the colony size of the resulting double mutants as a proxy for their fitness. The genes whose deletions led to considerable fitness reduction or death in the *Δtom70* but not wild-type *TOM70* background were regarded as synthetic sick or lethal genetic interactors of Tom70. We identified many genetic interactors, of which most are components relevant for mitochondrial biogenesis (Figure 5A; Table S5), such as Sam37, Tom71, Tom7, Tim8, Tim13, Pam17, Mip1, or Afg3. In addition, we found components relevant for peroxisome biogenesis (Pex17 and Pex18), for lipid metabolism (Loa1, Elo1, Elo2, Crd1, and Psd1), the ERMES complex (Mdm10, Mdm34, and Gem1), and cytosolic proteostasis (Pfd1 and Hch1). The fitness of cells lacking any of these components dropped considerably in the absence of Tom70.

The observation that Tom70 showed genetic interactions with these seemingly different functional groups of proteins could either point to several distinct functions of Tom70 or, alternatively, to the relevance of its chaperone-binding activity for multiple cellular activities. To study these genetic interactions further, despite the lethality of many double mutants, we used an improved, plasmid-based CRISPR interference (CRISPRi) system to specifically knock down transcription (Figure 5B). We expressed catalytically inactive Cas9 coupled to a potent transcriptional repressor (dCas9-Mxi1) together with a *TOM70*-specific guide RNA under the control of a tetracycline-inducible promoter (Smith et al., 2016). The concentrations of anhydrotetracycline (ATc) necessary to induce expression did not affect the fitness of yeast cells (Figure S4G). Within a few hours of induction, the levels of *TOM70* mRNA and of the Tom70 protein dropped to about 10% (Figures 5C and 5D). Combining CRISPRi perturbations with several deletion backgrounds allowed us to verify genetic interaction partners of Tom70, including the genes encoding Tim8, Tim13, Sam37, Loa1, Elo2, and Hch1 (Figure 5E). Expression of mt-Tah1 in these strains partially rescued the synthetic defects of mitochondrial protein import mutants (Tim8, Tim13, and Sam37) but not those in lipid metabolism (Elo2 and Loa1). Interestingly, mutants lacking Elo2 or Loa1 could however be suppressed by expression of a mt-Tah1-C2-C3 fusion protein (Figure S4H), suggesting that the genetic interaction of Tom70 with other proteins can either be mediated by the C1 domain (with genes of the import components Tim8, Tim13, and Sam37) or by the C2-C3 domains for genes relevant for lipid biosynthesis (Figure S4I). Thus, the chaperone-recruiting function of Tom70 is of relevance especially in the context of protein biogenesis, and it might be dispensable for other roles.

Chaperone binding by Tom70 is crucial for the biogenesis of small inner membrane proteins

Artificial chaperone recruitment to the outer mitochondrial membrane through mt-Tah1 relieves the temperature sensitivity of Δ*tom70/71* and its synthetic defects with mitochondrial biogenesis components. To analyze the mechanistic basis of this unexpected observation, we tested how mt-Tah1 influences the proteomic changes that we observed in the Δ*tom70/71* mutant.

A

Name	Function
LOA1	lipid biosynthesis
THR1	amino acid biosynthesis
ELO2	lipid biosynthesis
WHI3	RNA binding
SHY1	mitochondrial import and assembly
APM3	vesicular transport
RMD9	mitochondrial respiration
YNL198C	unknown
FYV6	unknown
BNI1	cytoskeleton
RRG9	mitochondrial respiration
THR4	amino acid biosynthesis
VPS65	unknown
PHO23	transcription and chromatin
GEP3	mitochondrial translation
SAM37	mitochondrial import and assembly
MDM34	ERMES component

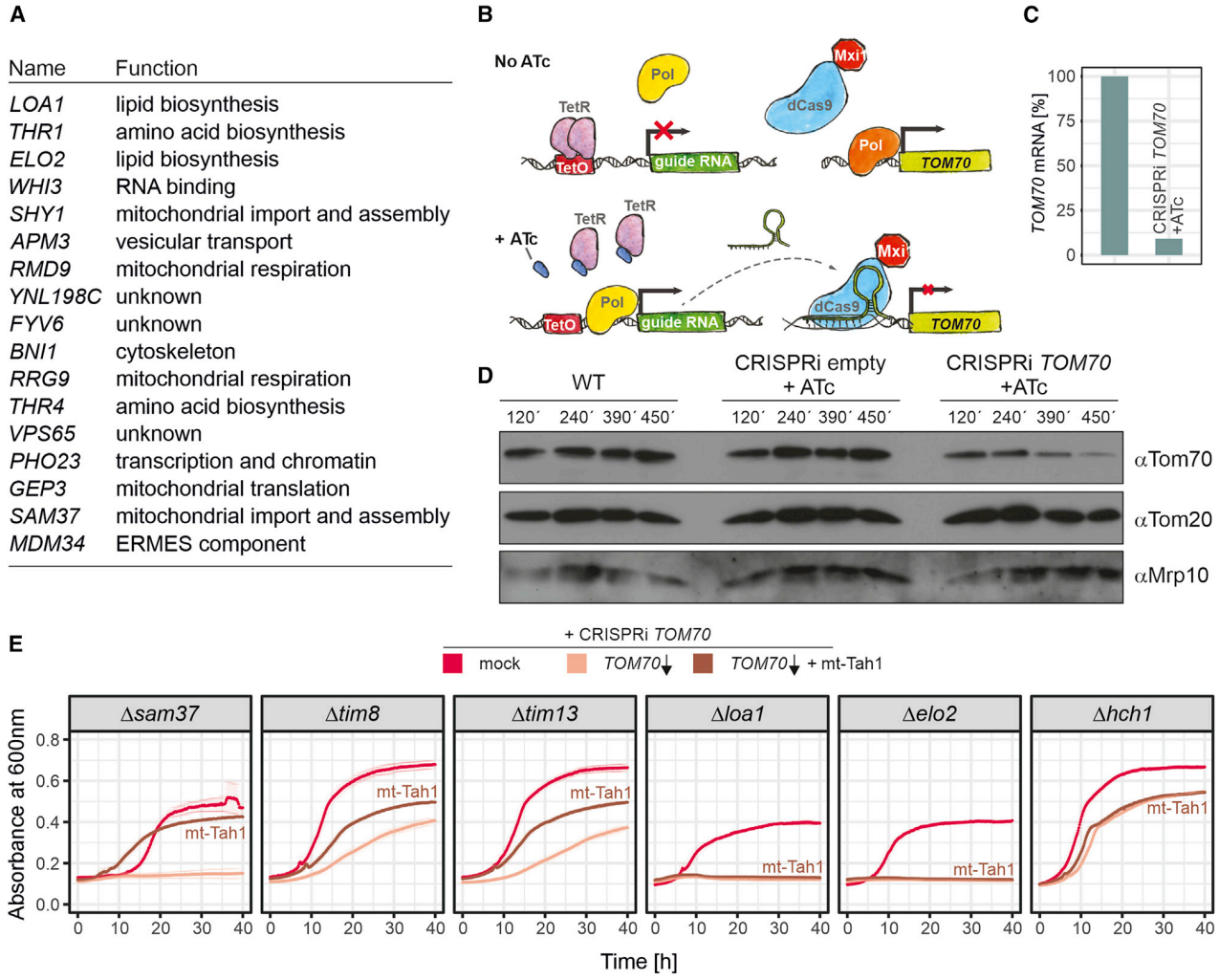

Figure 5. Chaperone binding by Tom70 is important for different cellular activities

(A) The *Δtom70* allele was introduced into a systematic yeast deletion library by automated genetic manipulations. Colony sizes were measured, and the 100 most-affected deletion mutants (Table S5) were analyzed (see STAR Methods for details).

(B) Schematic illustration of the CRISPRi strategy used to knock down *TOM70*.

(C) *TOM70* transcript levels were measured by qPCR 6.5 h after addition of anhydrotetracyclin (ATc). Shown are mean values of three replicates.

(D) Tom70 levels were analyzed by western blotting of the indicated strains at different time points after addition of ATc.

(E) Growth curves of the following strains: indicated single deletions without addition of ATc (mock); *TOM70* is knocked down through the addition of 960 ng/μl ATc (*TOM70* ↓); and *TOM70* is knocked down through the addition of 960 ng/μl ATc, but mt-Tah1 rescues the synthetic growth defect of some mutants (*TOM70* ↓ + mt-Tah1). Shown are mean values and standard deviations from three replicates.

Western blots of isolated mitochondria showed that the expression of mt-Tah1, but not that of mt-Tah1(K8A), restores the levels of Tom70-dependent proteins, such as Ugo1, Oxa1, and Pet9 (Figures 6A, 6B, and S4J). Which other proteins rely on the chaperone-binding activity of Tom70? To address this question systematically, we compared the cellular proteomes of Δ*tom70/71* with the same strains expressing Tom70, mt-Tah1, or mt-Tah1(K8A). Indeed, many proteins that were depleted from Δ*tom70/71* cells were rescued by expression of mt-Tah1, but not mt-Tah1(K8A) (Figures 6C and 6D). Thereby, mt-Tah1 particularly supported the accumulation of many small proteins of the inner membrane, including many single-spanning subunits of the complexes of the respiratory chain. The levels of these small proteins were reduced in *Δtom70/71* cells but restored if Tom70 or mt-Tah1 were expressed (Figures 6C–6F, protein names labeled in brown).

Chaperone binding by Tom70 prevents mitoprotein-induced toxicity

The inner membrane contains many proteins of less than 18 kDa, of which most are single-spanning non-catalytic subunits of respiratory chain complexes (Morgenstern et al., 2017). These small proteins lack iMTS-L sequences and thus predictable internal binding sites for the C2/C3 domains of Tom70, whereas iMTS-L

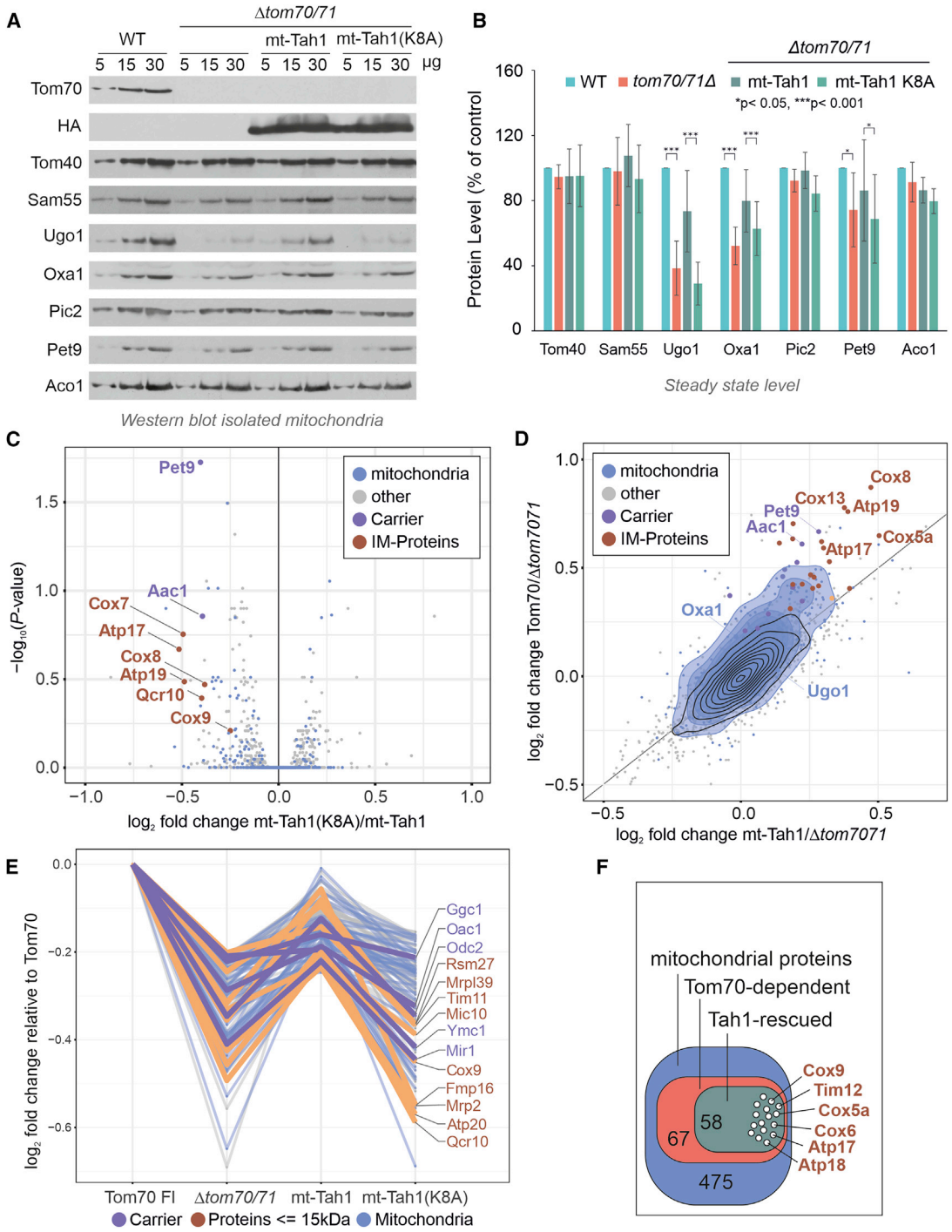

Figure 6. Chaperone binding by Tom70 is crucial for the biogenesis of small inner membrane proteins

(A and B) Protein levels in mitochondria isolated from either wild-type cells or the indicated *Δtom70/71* mutants were analyzed by western blotting. Six data points from three biological repeats were analyzed for each protein. The error bars refer to standard deviations. The p values were generated from the two-tailed paired t test.

(C) The volcano plot shows the comparison of the proteomes of *Δtom70/71* cells that express the mt-Tah1(K8A) to those with mt-Tah1. The positions of several small inner membrane proteins (brown) and of carriers (purple), which are considerably stabilized by mt-Tah1 but not by mt-Tah1(K8A), are indicated.

(D) The effects by which Tom70 and mt-Tah1 influence the cellular proteomes are plotted against each other.

(E) Relative log_2 FCs of Tom70-dependent mitochondrial proteins that are rescued by either mt-Tah1 or its variant.

(F) Graphical overview of the number of Tom70-dependent proteins that are rescued by expression of mt-Tah1 near to Tom70 full-length levels.

CellPress
OPEN ACCESS

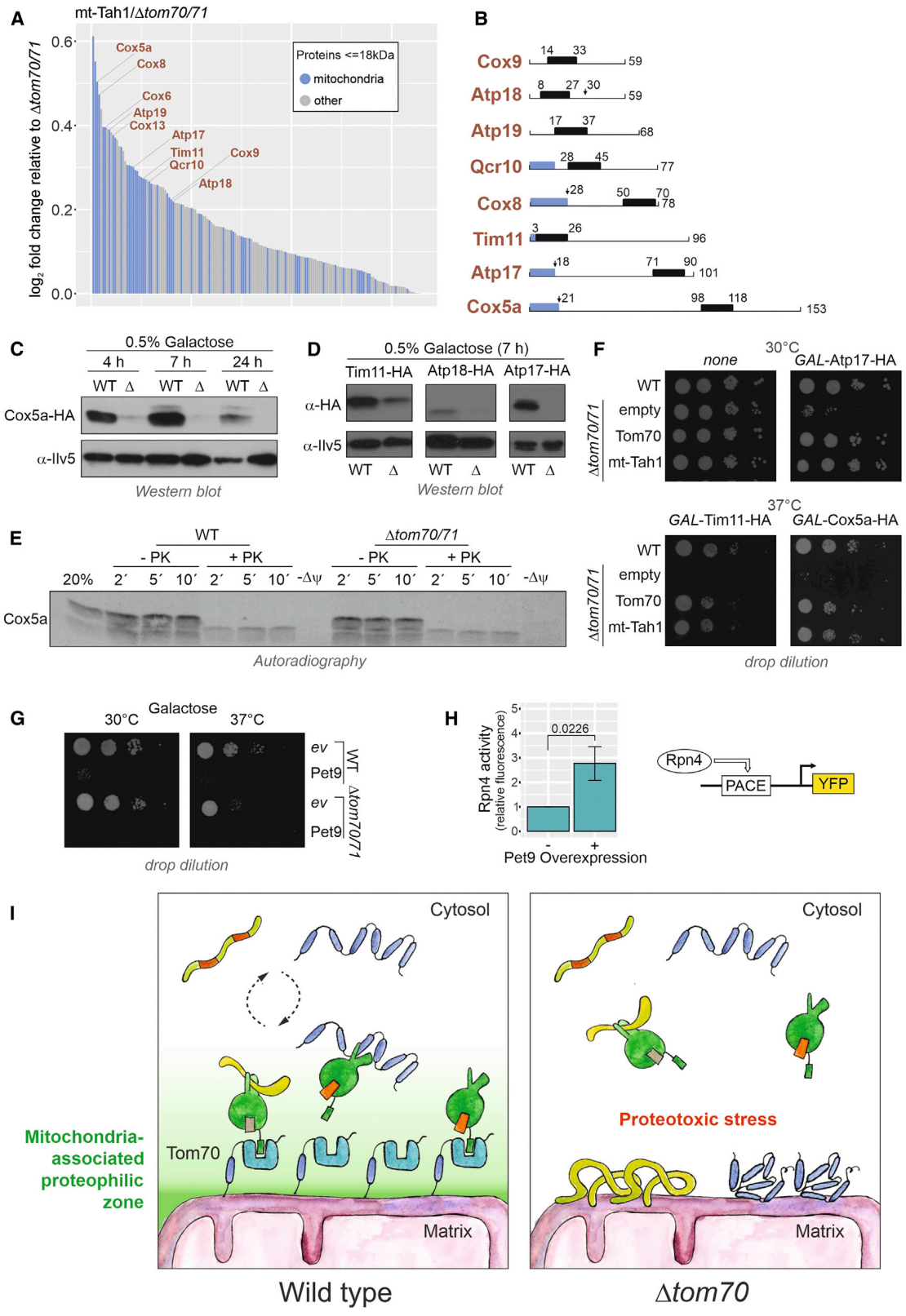

(legend on next page)

sequences are ubiquitously found in carriers and other Tom70 clients (Figure S5A).

The presence of mt-Tah1 restored the levels of many small inner membrane proteins (Figure 7A). Only some of these proteins carry N-terminal presequences, but others do not (Figure 7B), and their import process was not studied in the past. We therefore chose some of these Tom70-dependent small inner membrane proteins (Cox5a, Tim11, Atp17, and Atp18) as model proteins for further follow-up.

When expressed *in vivo* from a strong *GAL1* promoter, Cox5a accumulated in cells only in the presence of Tom70/71 but not in a deletion mutant (Figure 7C). The same strong Tom70/71 dependence was observed when Tim11, Atp18, or Atp17 were expressed from *GAL1* promoters (Figure 7D).

Cox5a was *in vitro* imported into wild-type and *Δtom70/71* mitochondria with similar, rather low efficiency (Figure 7E). Even if the import was carried out at 37°C, the *in vitro* import of Cox5a did not depend on Tom70 (Figure S5D). This result indicates that the striking Tom70 dependence *in vivo* is not recapitulated in the *in vitro* import assay. Aggregation-prone Tom70 substrates could be toxic in the absence of Tom70/71, impeding their intracellular accumulation. Indeed, we observed a high toxicity of overexpressed Cox5a, Atp17, Tim11, and Pet9 (Figures 7F, 7G, and S5C) and moderate toxicity of Atp18 (Figure S5D) in the *Δtom70/71* mutant, whereas wild-type cells were less sensitive. Regardless of whether Tom70 was present or absent, the overexpressed Cox5a co-isolated with mitochondria upon fractionation experiments (Figure S5E), and high temperature reduced the levels of cellular Cox5a to amounts similar to those found in *Δtom70/71* cells (Figure S5F).

Why is the overexpression of Pet9 and many small inner membrane proteins so toxic? The overexpression of Pet9 strongly induced an Rpn4-driven reporter indicative for problems in cytosolic proteostasis (Figure 7H). An Rpn4-mediated gene induction was observed as a characteristic element of the mitoprotein-induced stress response in yeast (Boos et al., 2019) but is also triggered by other cytosolic proteotoxic stress conditions.

In summary, we conclude that many small inner membrane proteins as well as carrier proteins have the potential to be toxic to cells. Tom70/71 suppresses this toxicity and facilitates the accumulation of these proteins in mitochondria. This property of Tom70/71 depends on its chaperone-binding ability (and hence can be replaced by mt-Tah1). Thus, the primary function of Tom70/71 is that of a co-chaperone on the mitochondrial surface that is crucial to protect the cytosolic compartment against proteotoxicity arising from mitochondrial precursors.

DISCUSSION

Traditionally, the problem of mitochondrial protein biogenesis is seen from the perspective of the organelle. From this direction, Tom70 was identified as "the carrier receptor," owing to its ability to bind precursor proteins on the mitochondrial surface (by its C2 and C3 domains) and to promote the transfer of these proteins into the protein-conducting channel of the TOM complex. This function of Tom70 is well reflected in the results obtained from *in vitro* import experiments, in which Tom70 clearly supports the import of specific mitochondrial proteins, in particular of the ATP/ADP carrier Pet9 but also of other mitochondrial proteins (Papic et al., 2011; Becker et al., 2011; Söllner et al., 1990; Brix et al., 2000; Ryan et al., 1999; Yamamoto et al., 2009; Backes et al., 2018; Wiedemann et al., 2001). In this study, we used different approaches to elucidate the relevance of Tom70 in the physiological *in vivo* context. These approaches included the microscopic screens of collections of GFP-tagged proteins, quantitative mass-spectrometry-based proteomics of whole-cell extracts, and the dominant-negative growth effects caused by excess precursor proteins. These three approaches clearly confirmed the particular relevance of Tom70/71 for Pet9 biogenesis. Nevertheless, even though the cellular levels of many mitochondrial proteins, and, in particular, those of some carriers, were clearly reduced in the absence of Tom70/71, this depletion was never severe. Even for Pet9, the levels in *Δtom70/71* cells were about 40% (GFP signal intensity) to 60% (proteomics) of those in wild-type cells, and all other carriers were affected even less. Despite these rather moderate effects, *Δtom70/71* cells are unable to grow under respiration conditions at elevated temperatures. The data presented here point at a crucial function of Tom70 to protect the cytosol against proteotoxic stress conditions for which mitochondrial precursors are presumably responsible. The rather abundant hydrophobic and aggregation-prone Pet9 protein is particularly problematic here. Previous studies already identified Pet9 and its human homolog ANT as proteins with high cytotoxic potential (Wang and Chen, 2015; Coyne and Chen, 2018; Liu et al., 2019; Hoshino et al., 2019; Wang et al., 2008). Mutations that even further increased their aggregation propensity are the cause of autosomal dominant progressive external ophthalmoplegia 2 in humans (Kaukonen

Figure 7. Chaperone binding by Tom70 prevents mitoprotein-induced toxicity

(A) Proteins that are enriched by the expression of mt-Tah1 compared with Δ*tom70/71* are shown. Only proteins with masses smaller than 18 kDa and positive enrichment factors were considered. Mitochondrial proteins are indicated in blue.

(B) Schematic representations of small inner membrane proteins for which information about their overall structure and targeting information exists. Blue regions show presequences, and black boxes indicate transmembrane domains.

(C and D) Cox5a-HA, Tim11-HA, Atp17-HA, and Atp18-HA were expressed under *GAL1* control from multi-copy plasmids in wild-type and Δ*tom70/71* cells. The times indicate how long cells were shifted to 0.5% galactose-containing medium.

(E) Radiolabeled Cox5a was incubated with isolated mitochondria for the times indicated at 30°C. The membrane potential ($\Delta\psi$) was depleted in control samples by addition of CCCP. Mitochondria were reisolated and incubated with or without proteinase K.

(F and G) The indicated strains were transformed with plasmids to express Atp17-HA, Tim11-HA, Cox5a-HA, and Pet9-HA under the control of the *GAL1* promoter. All cultures were grown on lactate medium to mid-log phase, induced with 0.5% galactose for 4.5 h, and dropped onto galactose plates.

(H) Rpn4-driven gene expression was measured using a yellow fluorescent protein (YFP) reporter system (Boos et al., 2019).

(I) Tom70 supports the biogenesis of aggregation-prone mitochondrial membrane proteins by recruiting cytosolic chaperones to the mitochondrial surface, thereby generating a "mitochondria-associated proteophilic zone."

et al., 2000) and trigger mitochondrial precursor over-accumulation stress (mPOS) in yeast (Wang and Chen, 2015).

The accumulation of mitochondrial precursor proteins in the cytosol was found to arrest cell growth (Wrobel et al., 2015; Boos et al., 2019; Labbadia et al., 2017; Melber and Haynes, 2018), presumably due to their ability to sequester cytosolic chaperones. Obviously, mitochondrial biogenesis is a considerable challenge for eukaryotic cells (Labbadia et al., 2017; Bar-Ziv et al., 2020), and our observations indicate that Tom70 serves as a component to reduce these mitoprotein-induced stress conditions. In the context of the early stages of precursor targeting to mitochondria, Tom70 apparently serves as the interface between the cytosolic chaperone system and the mitochondrial import machinery (Papić et al., 2013; Hansen et al., 2018; Opaliński et al., 2018; Boos et al., 2020; Eliyahu et al., 2012).

How does Tom70 exhibit its cytoprotective activity? In this study, we observe that the artificial tethering of the chaperone-binding TPR protein Tah1 to the mitochondrial surface can almost fully replace Tom70/71 in its properties to promote cell growth at increased temperature to stabilize the mitochondrial proteome and provide resistance against overexpressed inner membrane proteins. This observation is astonishing as the function of endogenous Tah1 is completely unrelated to mitochondrial biogenesis. The profound suppression of the *Δtom70/71* mutant by mt-Tah1 indicates that the physiologically relevant function of Tom70 is that of a chaperone-binding factor and that, *in vivo*, its direct substrate-binding properties and, hence, its receptor functions are of minor relevance. This is in line with the observation that an R171A mutation in the C1 domain completely wipes out Tom70 function *in vivo* (Young et al., 2003). This mutation is analogous to the K8A mutant in mt-Tah1 and prevents binding of the EEVD peptide. This again supports our conclusion that, *in vivo*, the chaperone-binding activity is of predominant relevance for the functionality of Tom70.

It appears likely that the recruitment of chaperones to the mitochondrial surface establishes a functionally important "mitochondria-associated proteophilic zone" at the organelle-cytosol interphase that facilitates protein biogenesis and suppresses the potential toxicity of precursor proteins (Figure 7I). The specific conditions of the *in vitro* import assay in which precursors and mitochondria are incubated in a relatively large volume of buffer might have overestimated the relevance of the high-affinity binding sites provided by the C2 and C3 domains of Tom70 for the import of hydrophobic mitochondrial precursor proteins such as carrier proteins.

The comparison of the proteome of the *Δtom70/71* mutant with that of cells that express mt-Tah1 (chaperone-binding) or Tom70 (chaperone and substrate binding) showed that many proteins require the chaperone-binding activity of Tom70, especially those that are intrinsically aggregation prone. A particularly interesting group of proteins are small (6–18 kDa) inner membrane proteins. Overexpression of these proteins in the absence of Tom70 or mt-Tah1 is highly toxic and prevents cell growth. Apparently, chaperones play a crucial role in facilitating the productive translocation of these proteins to mitochondria. *In vitro*, Tom70 was either not required for these proteins (as for Cox5a) or these proteins could not be imported from reticulocyte lysates (not shown), which points toward a requirement of additional factors—potentially chaperones—that are not accurately reflected in the *in vitro* assay. Finally, we observed that the levels of some Tom70-dependent proteins were not rescued by mt-Tah1. They were inner membrane proteins with bipartite targeting signals such as Sco1 or Dld1. Potentially, these proteins require the direct binding to Tom70, and hence, mt-Tah1 does not support their biogenesis. Further studies will be required to study the mechanistic reactions of the Tom70 modules and of cytosolic chaperones in the translocation reactions of these protein classes in more detail.

Ribosomes synthesizing Pet9 and other inner membrane proteins were found to be enriched on the surface of mitochondria, potentially to avoid the accumulation of hydrophobic precursors in the cytosol (Jan et al., 2014; Williams et al., 2014). Interestingly, on the contrary, ribosomes for small proteins (less than 180 residues) were strongly depleted from the mitochondrial surface, including those synthesizing Cox5a and other small inner membrane proteins, for which Tom70 was found in this study to be highly relevant (Figure S5G). The profound post-translational mode of their targeting might explain why the chaperone-assisted targeting by Tom70 (or mt-Tah1) is of such high importance for small inner membrane proteins.

The cytosol contains many TPR proteins that are structurally similar to Tom70 and Tah1 (Perez-Riba and Itzhaki, 2019; Zeytuni and Zarivach, 2012). Examples are co-chaperones such as Sti1 that, like Tah1 or the C1 domain of Tom70, binds cytosolic chaperones (Hoseini et al., 2016; Schmid et al., 2012). However, TPR proteins apparently are generally used for the translocation of proteins across cellular membranes. Examples include Sec71 and Sec72 for secretory proteins, Sgt2 for tail-anchored proteins, Pex5 for peroxisomal proteins, or Toc64 for plastid proteins (Chartron et al., 2011; Tripathi et al., 2017; Graham et al., 2019; Schwenkert et al., 2018; Harano et al., 2001). It appears likely that early sorting intermediates in general pose a considerable threat for cytosolic proteostasis, which is countered by multiple TPR proteins on organellar membranes. It will be exciting to study the specific roles of this group of proteins more comparatively, not only in respect to their relevance for protein targeting to their respective home organelle but also for cellular proteostasis and fitness in general.

STAR★METHODS

Detailed methods are provided in the online version of this paper and include the following:

- KEY RESOURCES TABLE
- RESOURCE AVAILABILITY
  - Lead contact
  - Materials availability
  - Data and code availability
- EXPERIMENTAL MODEL AND SUBJECT DETAILS
  - Yeast strains, plasmids and growth conditions
- METHOD DETAILS
  - CRISPRi system construction
  - Growth assays and viability tests
  - High-throughput screening of the GFP collection
  - TOM70 genetic interaction screen

- Overexpression assay
- Fractionation assay
- Heat-shock assay
- Sample preparation and mass spectrometric identification of proteins
- Analysis of mass spectrometry data
- Calculation of aggregation propensity
- Miscellaneous

- QUANTIFICATION AND STATISTICAL ANALYSIS

SUPPLEMENTAL INFORMATION

Supplemental information can be found online at https://doi.org/10.1016/j.celrep.2021.108936.

ACKNOWLEDGMENTS

We thank Vera Nehr and Sabine Knaus for technical assistance. We thank Mikhail Savitski, Per Haberkant, and Frank Stein for help with setting up the mass spectrometry workflow. We thank Carina Groh and Carsten Balzer for the help with data analysis and Amir Fadel for help with the microscopy screens. Additionally, we thank Anna Mariam Schlagowski for providing the *GAL1*-Pet9 overexpression plasmid, Janina Laborenz for the Tom70-TMD plasmid, and Klaus Pfanner and Ophry Pines for antibodies. This study was supported by funding from the Deutsche Forschungsgemeinschaft (DIP MitoBalance to J.M.H., D.R., and M.S. and HE2803/10-1 to J.M.H.), the Joachim Herz Stiftung (to F.B.), and the Forschungsinitiative Rheinland-Pfalz BioComp (to J.M.H. and F.B.). Y.S.B. is supported by an EMBO postdoctoral fellowship. M.S. is an incumbent of the Dr. Gilbert Omenn and Martha Darling Professorial Chair in Molecular Genetics.

AUTHOR CONTRIBUTIONS

S.B., Y.S.B., and T.F. designed, cloned, and verified the constructs and strains; J.M.H. conceived the project; S.B., L.K., F.B., M.R., and Z.S. carried out the mass-spectrometry-based proteomics; S.B., F.B., M.R., and T.M. performed the bioinformatical analysis of the mass spectrometry data; S.B., T.F., S.L., and J.Z. carried out the biochemical experiments to test the relevance of Tom70 for mitochondrial protein biogenesis; Y.S.B., C.B., and M.S. designed and performed genetic screens to identify Tom70-dependent proteins; C.J., J.D.S., and L.M.S. developed the CRISPR interference strategy and provided the tools that were used by S.B. and S.L.; S.B., D.R., M.S., F.B., and J.M.H. analyzed the data; J.M.H., S.B., and F.B. wrote the manuscript with the help and input of all authors.

DECLARATION OF INTERESTS

The authors declare no competing interests.

Received: October 2, 2020
Revised: December 22, 2020
Accepted: March 11, 2021
Published: April 6, 2021

REFERENCES

Altmann, K., Dürr, M., and Westermann, B. (2007). *Saccharomyces cerevisiae* as a model organism to study mitochondrial biology. In Mitochondria. Practical Protocols, D. Leister and J.M. Herrmann, eds. (Humana Press).

Araiso, Y., Tsutsumi, A., Qiu, J., Imai, K., Shiota, T., Song, J., Lindau, C., Wenz, L.S., Sakaue, H., Yunoki, K., et al. (2019). Structure of the mitochondrial import gate reveals distinct preprotein paths. Nature *575*, 395–401.

Back, R., Dominguez, C., Rothé, B., Bobo, C., Beaufils, C., Moréra, S., Meyer, P., Charpentier, B., Branlant, C., Allain, F.H., and Manival, X. (2013). High-resolution structural analysis shows how Tah1 tethers Hsp90 to the R2TP complex. Structure *21*, 1834–1847.

Backes, S., and Herrmann, J.M. (2017). Protein Translocation into the Intermembrane Space and Matrix of Mitochondria: Mechanisms and Driving Forces. Front. Mol. Biosci. *4*, 83.

Backes, S., Hess, S., Boos, F., Woellhaf, M.W., Gödel, S., Jung, M., Mühlhaus, T., and Herrmann, J.M. (2018). Tom70 enhances mitochondrial preprotein import efficiency by binding to internal targeting sequences. J. Cell Biol. *217*, 1369–1382.

Bar-Ziv, R., Bolas, T., and Dillin, A. (2020). Systemic effects of mitochondrial stress. EMBO Rep. *21*, e50094.

Baryshnikova, A., Costanzo, M., Kim, Y., Ding, H., Koh, J., Toufighi, K., Youn, J.Y., Ou, J., San Luis, B.J., Bandyopadhyay, S., et al. (2010). Quantitative analysis of fitness and genetic interactions in yeast on a genome scale. Nat. Methods *7*, 1017–1024.

Becker, J., Walter, W., Yan, W., and Craig, E.A. (1996). Functional interaction of cytosolic hsp70 and a DnaJ-related protein, Ydj1p, in protein translocation in vivo. Mol. Cell. Biol. *16*, 4378–4386.

Becker, T., Wenz, L.S., Krüger, V., Lehmann, W., Müller, J.M., Goroncy, L., Zufall, N., Lithgow, T., Guiard, B., Chacinska, A., et al. (2011). The mitochondrial import protein Mim1 promotes biogenesis of multispanning outer membrane proteins. J. Cell Biol. *194*, 387–395.

Ben-Menachem, R., Wang, K., Marcu, O., Yu, Z., Lim, T.K., Lin, Q., Schueler-Furman, O., and Pines, O. (2018). Yeast aconitase mitochondrial import is modulated by interactions of its C and N terminal domains and Ssa1/2 (Hsp70). Sci. Rep. *8*, 5903.

Benjamini, Y., and Hochberg, Y. (1995). Controlling the False Discovery Rate: A Practical and Powerful Approach to Multiple Testing. J. R. Stat. Soc. B *57*, 289–300.

Boos, F., Mühlhaus, T., and Herrmann, J.M. (2018). Detection of Internal Matrix Targeting Signal-like Sequences (iMTS-Ls) in Mitochondrial Precursor Proteins Using the TargetP Prediction Tool. Biol.-protocol *8*, e2474.

Boos, F., Krämer, L., Groh, C., Jung, F., Haberkant, P., Stein, F., Wollweber, F., Gackstatter, A., Zöller, E., van der Laan, M., et al. (2019). Mitochondrial protein-induced stress triggers a global adaptive transcriptional programme. Nat. Cell Biol. *21*, 442–451.

Boos, F., Labbadia, J., and Herrmann, J.M. (2020). How the Mitoprotein-Induced Stress Response Safeguards the Cytosol: A Unified View. Trends Cell Biol. *30*, 241–254.

Boulon, S., Pradet-Balade, B., Verheggen, C., Molle, D., Boireau, S., Georgieva, M., Azzag, K., Robert, M.C., Ahmad, Y., Neel, H., et al. (2010). HSP90 and its R2TP/Prefoldin-like cochaperone are involved in the cytoplasmic assembly of RNA polymerase II. Mol. Cell *39*, 912–924.

Breker, M., Gymrek, M., and Schuldiner, M. (2013). A novel single-cell screening platform reveals proteome plasticity during yeast stress responses. J. Cell Biol. *200*, 839–850.

Brix, J., Rüdiger, S., Bukau, B., Schneider-Mergener, J., and Pfanner, N. (1999). Distribution of binding sequences for the mitochondrial import receptors Tom20, Tom22, and Tom70 in a presequence-carrying preprotein and a non-cleavable preprotein. J. Biol. Chem. *274*, 16522–16530.

Brix, J., Ziegler, G.A., Dietmeier, K., Schneider-Mergener, J., Schulz, G.E., and Pfanner, N. (2000). The mitochondrial import receptor Tom70: identification of a 25 kDa core domain with a specific binding site for preproteins. J. Mol. Biol. *303*, 479–488.

Calvo, S.E., Clauser, K.R., and Mootha, V.K. (2016). MitoCarta2.0: an updated inventory of mammalian mitochondrial proteins. Nucleic Acids Res. *44* (*D1*), D1251–D1257.

Chacinska, A., Koehler, C.M., Milenkovic, D., Lithgow, T., and Pfanner, N. (2009). Importing mitochondrial proteins: machineries and mechanisms. Cell *138*, 628–644.

Chan, N.C., Likić, V.A., Waller, R.F., Mulhern, T.D., and Lithgow, T. (2006). The C-terminal TPR domain of Tom70 defines a family of mitochondrial protein import receptors found only in animals and fungi. J. Mol. Biol. *358*, 1010–1022.

Chartron, J.W., Gonzalez, G.M., and Clemons, W.M., Jr. (2011). A structural model of the Sgt2 protein and its interactions with chaperones and the Get4/Get5 complex. J. Biol. Chem. *286*, 34325–34334.

Chen, B., Gilbert, L.A., Cimini, B.A., Schnitzbauer, J., Zhang, W., Li, G.W., Park, J., Blackburn, E.H., Weissman, J.S., Qi, L.S., and Huang, B. (2013). Dynamic imaging of genomic loci in living human cells by an optimized CRISPR/Cas system. Cell *155*, 1479–1491.

Cohen, Y., and Schuldiner, M. (2011). Advanced methods for high-throughput microscopy screening of genetically modified yeast libraries. Methods Mol. Biol. *781*, 127–159.

Conchillo-Solé, O., de Groot, N.S., Avilés, F.X., Vendrell, J., Daura, X., and Ventura, S. (2007). AGGRESCAN: a server for the prediction and evaluation of "hot spots" of aggregation in polypeptides. BMC Bioinformatics *8*, 65.

Cox, J., and Mann, M. (2008). MaxQuant enables high peptide identification rates, individualized p.p.b.-range mass accuracies and proteome-wide protein quantification. Nat. Biotechnol. *26*, 1367–1372.

Cox, J., Neuhauser, N., Michalski, A., Scheltema, R.A., Olsen, J.V., and Mann, M. (2011). Andromeda: a peptide search engine integrated into the MaxQuant environment. J. Proteome Res. *10*, 1794–1805.

Coyne, L.P., and Chen, X.J. (2018). mPOS is a novel mitochondrial trigger of cell death - implications for neurodegeneration. FEBS Lett. *592*, 759–775.

Deshaies, R.J., Koch, B.D., Werner-Washburne, M., Craig, E.A., and Schekman, R. (1988). A subfamily of stress proteins facilitates translocation of secretory and mitochondrial precursor polypeptides. Nature *332*, 800–805.

Doan, K.N., Grevel, A., Mårtensson, C.U., Ellenrieder, L., Thornton, N., Wenz, L.S., Opaliński, Ł., Guiard, B., Pfanner, N., and Becker, T. (2020). The Mitochondrial Import Complex MIM Functions as Main Translocase for α-Helical Outer Membrane Proteins. Cell Rep. *31*, 107567.

Döring, K., Ahmed, N., Riemer, T., Suresh, H.G., Vainshtein, Y., Habich, M., Riemer, J., Mayer, M.P., O'Brien, E.P., Kramer, G., and Bukau, B. (2017). Profiling Ssb-Nascent Chain Interactions Reveals Principles of Hsp70-Assisted Folding. Cell *170*, 298–311.e20.

Drwesh, L., and Rapaport, D. (2020). Biogenesis pathways of α-helical mitochondrial outer membrane proteins. Biol. Chem. *401*, 677–686.

Edwards, R., Gerlich, S., and Tokatlidis, K. (2020). The biogenesis of mitochondrial intermembrane space proteins. Biol. Chem. *401*, 737–747.

Eliyahu, E., Lesnik, C., and Arava, Y. (2012). The protein chaperone Ssa1 affects mRNA localization to the mitochondria. FEBS Lett. *586*, 64–69.

Finger, Y., and Riemer, J. (2020). Protein import by the mitochondrial disulfide relay in higher eukaryotes. Biol. Chem. *401*, 749–763.

Giaever, G., Chu, A.M., Ni, L., Connelly, C., Riles, L., Véronneau, S., Dow, S., Lucau-Danila, A., Anderson, K., André, B., et al. (2002). Functional profiling of the Saccharomyces cerevisiae genome. Nature *418*, 387–391.

Gietz, R.D., and Woods, R.A. (2006). Yeast Transformation by the LiAc/SS Carrier DNA/PEG Method. In Yeast Protocol, W. Xiao, ed. (Humana Press).

Gietz, D., St Jean, A., Woods, R.A., and Schiestl, R.H. (1992). Improved method for high efficiency transformation of intact yeast cells. Nucleic Acids Res. *20*, 1425.

Gold, V.A., Chroscicki, P., Bragoszewski, P., and Chacinska, A. (2017). Visualization of cytosolic ribosomes on the surface of mitochondria by electron cryo-tomography. EMBO Rep. *18*, 1786–1800.

Gornicka, A., Bragoszewski, P., Chroscicki, P., Wenz, L.S., Schulz, C., Rehling, P., and Chacinska, A. (2014). A discrete pathway for the transfer of intermembrane space proteins across the outer membrane of mitochondria. Mol. Biol. Cell *25*, 3999–4009.

Graham, J.B., Canniff, N.P., and Hebert, D.N. (2019). TPR-containing proteins control protein organization and homeostasis for the endoplasmic reticulum. Crit. Rev. Biochem. Mol. Biol. *54*, 103–118.

Hansen, K.G., Aviram, N., Laborenz, J., Bibi, C., Meyer, M., Spang, A., Schuldiner, M., and Herrmann, J.M. (2018). An ER surface retrieval pathway safeguards the import of mitochondrial membrane proteins in yeast. Science *361*, 1118–1122.

Harano, T., Nose, S., Uezu, R., Shimizu, N., and Fujiki, Y. (2001). Hsp70 regulates the interaction between the peroxisome targeting signal type 1 (PTS1)-receptor Pex5p and PTS1. Biochem. J. *357*, 157–165.

Hartl, F.U., Bracher, A., and Hayer-Hartl, M. (2011). Molecular chaperones in protein folding and proteostasis. Nature *475*, 324–332.

Hasson, S.A., Damoiseaux, R., Glavin, J.D., Dabir, D.V., Walker, S.S., and Koehler, C.M. (2010). Substrate specificity of the TIM22 mitochondrial import pathway revealed with small molecule inhibitor of protein translocation. Proc. Natl. Acad. Sci. USA *107*, 9578–9583.

Haucke, V., Lithgow, T., Rospert, S., Hahne, K., and Schatz, G. (1995). The yeast mitochondrial protein import receptor Mas20p binds precursor proteins through electrostatic interaction with the positively charged presequence. J. Biol. Chem. *270*, 5565–5570.

Hines, V., Brandt, A., Griffiths, G., Horstmann, H., Brütsch, H., and Schatz, G. (1990). Protein import into yeast mitochondria is accelerated by the outer membrane protein MAS70. EMBO J. *9*, 3191–3200.

Horten, P., Colina-Tenorio, L., and Rampelt, H. (2020). Biogenesis of Mitochondrial Metabolite Carriers. Biomolecules *10*, 1008.

Hoseini, H., Pandey, S., Jores, T., Schmitt, A., Franz-Wachtel, M., Macek, B., Buchner, J., Dimmer, K.S., and Rapaport, D. (2016). The cytosolic cochaperone Sti1 is relevant for mitochondrial biogenesis and morphology. FEBS J. *283*, 3338–3352.

Hoshino, A., Wang, W.J., Wada, S., McDermott-Roe, C., Evans, C.S., Gosis, B., Morley, M.P., Rathi, K.S., Li, J., Li, K., et al. (2019). The ADP/ATP translocase drives mitophagy independent of nucleotide exchange. Nature *575*, 375–379.

Huber, W., von Heydebreck, A., Sültmann, H., Poustka, A., and Vingron, M. (2002). Variance stabilization applied to microarray data calibration and to the quantification of differential expression. Bioinformatics *18* (*Suppl 1*), S96–S104.

Hughes, C.S., Foehr, S., Garfield, D.A., Furlong, E.E., Steinmetz, L.M., and Krijgsveld, J. (2014). Ultrasensitive proteome analysis using paramagnetic bead technology. Mol. Syst. Biol. *10*, 757.

Hughes, C.S., Moggridge, S., Müller, T., Sorensen, P.H., Morin, G.B., and Krijgsveld, J. (2019). Single-pot, solid-phase-enhanced sample preparation for proteomics experiments. Nat. Protoc. *14*, 68–85.

Iwata, K., and Nakai, M. (1998). Interaction between mitochondrial precursor proteins and cytosolic soluble domains of mitochondrial import receptors, Tom20 and Tom70, measured by surface plasmon resonance. Biochem. Biophys. Res. Commun. *253*, 648–652.

Jan, C.H., Williams, C.C., and Weissman, J.S. (2014). Principles of ER cotranslational translocation revealed by proximity-specific ribosome profiling. Science *346*, 1257521.

Janke, C., Magiera, M.M., Rathfelder, N., Taxis, C., Reber, S., Maekawa, H., Moreno-Borchart, A., Doenges, G., Schwob, E., Schiebel, E., and Knop, M. (2004). A versatile toolbox for PCR-based tagging of yeast genes: new fluorescent proteins, more markers and promoter substitution cassettes. Yeast *21*, 947–962.

Jiménez, B., Ugwu, F., Zhao, R., Ortí, L., Makhnevych, T., Pineda-Lucena, A., and Houry, W.A. (2012). Structure of minimal tetratricopeptide repeat domain protein Tah1 reveals mechanism of its interaction with Pih1 and Hsp90. J. Biol. Chem. *287*, 5698–5709.

Jores, T., Lawatscheck, J., Beke, V., Franz-Wachtel, M., Yunoki, K., Fitzgerald, J.C., Macek, B., Endo, T., Kalbacher, H., Buchner, J., and Rapaport, D. (2018). Cytosolic Hsp70 and Hsp40 chaperones enable the biogenesis of mitochondrial β-barrel proteins. J. Cell Biol. *217*, 3091–3108.

Kaukonen, J., Juselius, J.K., Tiranti, V., Kyttälä, A., Zeviani, M., Comi, G.P., Keränen, S., Peltonen, L., and Suomalainen, A. (2000). Role of adenine nucleotide translocator 1 in mtDNA maintenance. Science *289*, 782–785.

Kramer, G., Shiber, A., and Bukau, B. (2019). Mechanisms of Cotranslational Maturation of Newly Synthesized Proteins. Annu. Rev. Biochem. *88*, 337–364.

Labbadia, J., Brielmann, R.M., Neto, M.F., Lin, Y.F., Haynes, C.M., and Morimoto, R.I. (2017). Mitochondrial Stress Restores the Heat Shock Response and Prevents Proteostasis Collapse during Aging. Cell Rep. *21*, 1481–1494.

Li, J., Qian, X., Hu, J., and Sha, B. (2009). Molecular chaperone Hsp70/Hsp90 prepares the mitochondrial outer membrane translocon receptor Tom71 for preprotein loading. J. Biol. Chem. *284*, 23852–23859.

Liu, Y., Wang, X., Coyne, L.P., Yang, Y., Qi, Y., Middleton, F.A., and Chen, X.J. (2019). Mitochondrial carrier protein overloading and misfolding induce aggresomes and proteostatic adaptations in the cytosol. Mol. Biol. Cell *30*, 1272–1284.

Lutz, T., Neupert, W., and Herrmann, J.M. (2003). Import of small Tim proteins into the mitochondrial intermembrane space. EMBO J. *22*, 4400–4408.

Marini, G., Nüske, E., Leng, W., Alberti, S., and Pigino, G. (2020). Reorganization of budding yeast cytoplasm upon energy depletion. Mol. Biol. Cell *31*, 1232–1245.

Mårtensson, C.U., Priesnitz, C., Song, J., Ellenrieder, L., Doan, K.N., Boos, F., Floerchinger, A., Zufall, N., Oeljeklaus, S., Warscheid, B., and Becker, T. (2019). Mitochondrial protein translocation-associated degradation. Nature *569*, 679–683.

Melber, A., and Haynes, C.M. (2018). UPR^{mt} regulation and output: a stress response mediated by mitochondrial-nuclear communication. Cell Res. *28*, 281–295.

Melin, J., Kilisch, M., Neumann, P., Lytovchenko, O., Gomkale, R., Schendzielorz, A., Schmidt, B., Liepold, T., Ficner, R., Jahn, O., et al. (2015). A presequence-binding groove in Tom70 supports import of Mdl1 into mitochondria. Biochim. Biophys. Acta *1853*, 1850–1859.

Millson, S.H., Vaughan, C.K., Zhai, C., Ali, M.M., Panaretou, B., Piper, P.W., Pearl, L.H., and Prodromou, C. (2008). Chaperone ligand-discrimination by the TPR-domain protein Tah1. Biochem. J. *413*, 261–268.

Morgenstern, M., Stiller, S.B., Lübbert, P., Peikert, C.D., Dannenmaier, S., Drepper, F., Weill, U., Höß, P., Feuerstein, R., Gebert, M., et al. (2017). Definition of a High-Confidence Mitochondrial Proteome at Quantitative Scale. Cell Rep. *19*, 2836–2852.

Opaliński, Ł., Song, J., Priesnitz, C., Wenz, L.S., Oeljeklaus, S., Warscheid, B., Pfanner, N., and Becker, T. (2018). Recruitment of Cytosolic J-Proteins by TOM Receptors Promotes Mitochondrial Protein Biogenesis. Cell Rep. *25*, 2036–2043.e5.

Papic, D., Krumpe, K., Dukanovic, J., Dimmer, K.S., and Rapaport, D. (2011). Multispan mitochondrial outer membrane protein Ugo1 follows a unique Mim1-dependent import pathway. J. Cell Biol. *194*, 397–405.

Papić, D., Elbaz-Alon, Y., Koerdt, S.N., Leopold, K., Worm, D., Jung, M., Schuldiner, M., and Rapaport, D. (2013). The role of Djp1 in import of the mitochondrial protein Mim1 demonstrates specificity between a cochaperone and its substrate protein. Mol. Cell. Biol. *33*, 4083–4094.

Peleh, V., Zannini, F., Backes, S., Rouhier, N., and Herrmann, J.M. (2017). Erv1 of Arabidopsis thaliana can directly oxidize mitochondrial intermembrane space proteins in the absence of redox-active Mia40. BMC Biol. *15*, 106.

Perez-Riba, A., and Itzhaki, L.S. (2019). The tetratricopeptide-repeat motif is a versatile platform that enables diverse modes of molecular recognition. Curr. Opin. Struct. Biol. *54*, 43–49.

Perez-Riverol, Y., Csordas, A., Bai, J., Bernal-Llinares, M., Hewapathirana, S., Kundu, D.J., Inuganti, A., Griss, J., Mayer, G., Eisenacher, M., et al. (2019). The PRIDE database and related tools and resources in 2019: improving support for quantification data. Nucleic Acids Res. *47*, D442–D450.

Pfanner, N., and Neupert, W. (1987). Distinct steps in the import of ADP/ATP carrier into mitochondria. J. Biol. Chem. *262*, 7528–7536.

Pfanner, N., Tropschug, M., and Neupert, W. (1987). Mitochondrial protein import: nucleoside triphosphates are involved in conferring import-competence to precursors. Cell *49*, 815–823.

Rappsilber, J., Mann, M., and Ishihama, Y. (2007). Protocol for micro-purification, enrichment, pre-fractionation and storage of peptides for proteomics using StageTips. Nat. Protoc. *2*, 1896–1906.

Rehling, P., Brandner, K., and Pfanner, N. (2004). Mitochondrial import and the twin-pore translocase. Nat. Rev. Mol. Cell Biol. *5*, 519–530.

Rimmer, K.A., Foo, J.H., Ng, A., Petrie, E.J., Shilling, P.J., Perry, A.J., Mertens, H.D., Lithgow, T., Mulhern, T.D., and Gooley, P.R. (2011). Recognition of mitochondrial targeting sequences by the import receptors Tom20 and Tom22. J. Mol. Biol. *405*, 804–818.

Ritchie, M.E., Phipson, B., Wu, D., Hu, Y., Law, C.W., Shi, W., and Smyth, G.K. (2015). limma powers differential expression analyses for RNA-sequencing and microarray studies. Nucleic Acids Res. *43*, e47.

Ryan, M.T., Müller, H., and Pfanner, N. (1999). Functional staging of ADP/ATP carrier translocation across the outer mitochondrial membrane. J. Biol. Chem. *274*, 20619–20627.

Saladi, S., Boos, F., Poglitsch, M., Meyer, H., Sommer, F., Mühlhaus, T., Schroda, M., Schuldiner, M., Madeo, F., and Herrmann, J.M. (2020). The NADH Dehydrogenase Nde1 Executes Cell Death after Integrating Signals from Metabolism and Proteostasis on the Mitochondrial Surface. Mol. Cell *77*, 189–202.e6.

Sanchez de Groot, N., Pallares, I., Vendrell, J., and Ventura, S. (2005). Prediction of "hot spots" of aggregation in disease-linked polypeptides. BMC Struct Biol *5*, 18.

Schlossmann, J., Lill, R., Neupert, W., and Court, D.A. (1996). Tom71, a novel homologue of the mitochondrial preprotein receptor Tom70. J. Biol. Chem. *271*, 17890–17895.

Schmid, A.B., Lagleder, S., Gräwert, M.A., Röhl, A., Hagn, F., Wandinger, S.K., Cox, M.B., Demmer, O., Richter, K., Groll, M., et al. (2012). The architecture of functional modules in the Hsp90 co-chaperone Sti1/Hop. EMBO J. *31*, 1506–1517.

Schwenkert, S., Dittmer, S., and Soll, J. (2018). Structural components involved in plastid protein import. Essays Biochem. *62*, 65–75.

Shakya, V.P.S., Barbeau, W.A., Xiao, T., Knutson, C.S., and Hughes, A.L. (2020). The nucleus is a quality control center for non-imported mitochondrial proteins. bioRxiv. https://doi.org/10.1101/2020.06.26.173781.

Shiota, T., Imai, K., Qiu, J., Hewitt, V.L., Tan, K., Shen, H.H., Sakiyama, N., Fukasawa, Y., Hayat, S., Kamiya, M., et al. (2015). Molecular architecture of the active mitochondrial protein gate. Science *349*, 1544–1548.

Smith, J.D., Suresh, S., Schlecht, U., Wu, M., Wagih, O., Peltz, G., Davis, R.W., Steinmetz, L.M., Parts, L., and St Onge, R.P. (2016). Quantitative CRISPR interference screens in yeast identify chemical-genetic interactions and new rules for guide RNA design. Genome Biol. *17*, 45.

Söllner, T., Pfaller, R., Griffiths, G., Pfanner, N., and Neupert, W. (1990). A mitochondrial import receptor for the ADP/ATP carrier. Cell *62*, 107–115.

Sontag, E.M., Samant, R.S., and Frydman, J. (2017). Mechanisms and Functions of Spatial Protein Quality Control. Annu. Rev. Biochem. *86*, 97–122.

Steger, H.F., Söllner, T., Kiebler, M., Dietmeier, K.A., Pfaller, R., Trülzsch, K.S., Tropschug, M., Neupert, W., and Pfanner, N. (1990). Import of ADP/ATP carrier into mitochondria: two receptors act in parallel. J. Cell Biol. *111*, 2353–2363.

Stein, K.C., Kriel, A., and Frydman, J. (2019). Nascent Polypeptide Domain Topology and Elongation Rate Direct the Cotranslational Hierarchy of Hsp70 and TRiC/CCT. Mol. Cell *75*, 1117–1130.e5.

Terada, K., Ueda, I., Ohtsuka, K., Oda, T., Ichiyama, A., and Mori, M. (1996). The requirement of heat shock cognate 70 protein for mitochondrial import varies among precursor proteins and depends on precursor length. Mol. Cell. Biol. *16*, 6103–6109.

Tong, A.H.Y., and Boone, C. (2007). High-Throughput Strain Construction and Systematic Synthetic Lethal Screening in Saccharomyces cerevisiae. Methods Microbiol. *36*, 369–386.

Tripathi, A., Mandon, E.C., Gilmore, R., and Rapoport, T.A. (2017). Two alternative binding mechanisms connect the protein translocation Sec71-Sec72 complex with heat shock proteins. J. Biol. Chem. *292*, 8007–8018.

Tsuboi, T., Viana, M.P., Xu, F., Yu, J., Chanchani, R., Arceo, X.G., Tutucci, E., Choi, J., Chen, Y.S., Singer, R.H., et al. (2020). Mitochondrial volume fraction and translation duration impact mitochondrial mRNA localization and protein synthesis. eLife *9*, e57814.

Tyanova, S., Temu, T., and Cox, J. (2016). The MaxQuant computational platform for mass spectrometry-based shotgun proteomics. Nat. Protoc. *11*, 2301–2319.

Vögtle, F.N., Wortelkamp, S., Zahedi, R.P., Becker, D., Leidhold, C., Gevaert, K., Kellermann, J., Voos, W., Sickmann, A., Pfanner, N., and Meisinger, C. (2009). Global analysis of the mitochondrial N-proteome identifies a processing peptidase critical for protein stability. Cell *139*, 428–439.

Vögtle, F.N., Burkhart, J.M., Gonczarowska-Jorge, H., Kücükköse, C., Taskin, A.A., Kopczynski, D., Ahrends, R., Mossmann, D., Sickmann, A., Zahedi, R.P., and Meisinger, C. (2017). Landscape of submitochondrial protein distribution. Nat. Commun. *8*, 290.

von Heijne, G. (1986). Mitochondrial targeting sequences may form amphiphilic helices. EMBO J. *5*, 1335–1342.

Wagih, O., Usaj, M., Baryshnikova, A., VanderSluis, B., Kuzmin, E., Costanzo, M., Myers, C.L., Andrews, B.J., Boone, C.M., and Parts, L. (2013). SGAtools: one-stop analysis and visualization of array-based genetic interaction screens. Nucleic Acids Res. *41*, W591–W596.

Wang, X., and Chen, X.J. (2015). A cytosolic network suppressing mitochondria-mediated proteostatic stress and cell death. Nature *524*, 481–484.

Wang, X., Salinas, K., Zuo, X., Kucejova, B., and Chen, X.J. (2008). Dominant membrane uncoupling by mutant adenine nucleotide translocase in mitochondrial diseases. Hum. Mol. Genet. *17*, 4036–4044.

Weidberg, H., and Amon, A. (2018). MitoCPR-A surveillance pathway that protects mitochondria in response to protein import stress. Science *360*, eaan4146.

Weill, U., Yofe, I., Sass, E., Stynen, B., Davidi, D., Natarajan, J., Ben-Menachem, R., Avihou, Z., Goldman, O., Harpaz, N., et al. (2018). Genome-wide SWAp-Tag yeast libraries for proteome exploration. Nat. Methods *15*, 617–622.

Werner, T., Sweetman, G., Savitski, M.F., Mathieson, T., Bantscheff, M., and Savitski, M.M. (2014). Ion coalescence of neutron encoded TMT 10-plex reporter ions. Anal. Chem. *86*, 3594–3601.

Wiedemann, N., and Pfanner, N. (2017). Mitochondrial Machineries for Protein Import and Assembly. Annu. Rev. Biochem. *86*, 685–714.

Wiedemann, N., Pfanner, N., and Ryan, M.T. (2001). The three modules of ADP/ATP carrier cooperate in receptor recruitment and translocation into mitochondria. EMBO J. *20*, 951–960.

Williams, C.C., Jan, C.H., and Weissman, J.S. (2014). Targeting and plasticity of mitochondrial proteins revealed by proximity-specific ribosome profiling. Science *346*, 748–751.

Woellhaf, M.W., Sommer, F., Schroda, M., and Herrmann, J.M. (2016). Proteomic profiling of the mitochondrial ribosome identifies Atp25 as a composite mitochondrial precursor protein. Mol. Biol. Cell *27*, 3031–3039.

Wrobel, L., Topf, U., Bragoszewski, P., Wiese, S., Sztolsztener, M.E., Oeljeklaus, S., Varabyova, A., Lirski, M., Chroscicki, P., Mroczek, S., et al. (2015). Mistargeted mitochondrial proteins activate a proteostatic response in the cytosol. Nature *524*, 485–488.

Yamamoto, H., Fukui, K., Takahashi, H., Kitamura, S., Shiota, T., Terao, K., Uchida, M., Esaki, M., Nishikawa, S., Yoshihisa, T., et al. (2009). Roles of Tom70 in import of presequence-containing mitochondrial proteins. J. Biol. Chem. *284*, 31635–31646.

Yofe, I., Weill, U., Meurer, M., Chuartzman, S., Zalckvar, E., Goldman, O., Ben-Dor, S., Schütze, C., Wiedemann, N., Knop, M., et al. (2016). One library to make them all: streamlining the creation of yeast libraries via a SWAp-Tag strategy. Nat. Methods *13*, 371–378.

Young, B.P., and Loewen, C.J. (2013). Balony: a software package for analysis of data generated by synthetic genetic array experiments. BMC Bioinformatics *14*, 354.

Young, J.C., Hoogenraad, N.J., and Hartl, F.U. (2003). Molecular chaperones Hsp90 and Hsp70 deliver preproteins to the mitochondrial import receptor Tom70. Cell *112*, 41–50.

Zeytuni, N., and Zarivach, R. (2012). Structural and functional discussion of the tetra-trico-peptide repeat, a protein interaction module. Structure *20*, 397–405.

STAR★METHODS

KEY RESOURCES TABLE

REAGENT or RESOURCE	SOURCE	IDENTIFIER
Antibodies		
anti-Ilv5	Johannes Herrmann lab	Peleh et al., 2017
anti-Sod1	Johannes Herrmann lab	Peleh et al., 2017
anti-Tom70	Nikolaus Pfanner lab	Söllner et al., 1990
anti-Tom20	Doron Rapaport lab	Papic et al., 2011
anti-Oxa1	Johannes Herrmann lab	Peleh et al., 2017
anti-Aco1	Ophry Pines Lab	Ben Menachem et al., 2018
anti-Fum1	Ophry Pines Lab	Ben Menachem et al., 2018
anti-Sam55	Doron Rapaport lab	Papic et al., 2011
anti-Mim1	Doron Rapaport lab	Papic et al., 2011
anti-AAC	Doron Rapaport lab	Papic et al., 2011
anti-Om14	Doron Rapaport lab	Papic et al., 2011
anti-Ugo1	Doron Rapaport lab	Papic et al., 2011
anti-Rabbit secondary antibody	BioRad	172-1019
anti-Mouse secondary antibody	BioRad	172-1011
anti-HA	Roche	12013819001
Chemicals, peptides, and recombinant proteins		
Sera-Mag Beads	Thermo Scientific	4515-2105-050250
Water, HPLC grade	Chromanorm	23595.294
0.2 M HEPES/NaOH pH 8.4	Sigma Aldrich	H3375
100% Ethanol, HPLC grade	VWR	153385E
Formic Acid, mass spectrometry grade	Sigma Aldrich	94318
Chloroacetamide	Sigma Aldrich	C0267
Trypsin	Sigma Aldrich	T6567
DMSO, HPLC grade	Sigma Aldrich	42780.AK
TMT10plex isobaric label reagent set	Thermo Scientific	90111
Acetonitrile	Honeywell	34967
Hydroxylamine	Sigma Aldrich	438227
Dithiothreitol	BioChemica	A1101,0025
Carbonyl cyanide 3-chlorophenylhydrazone	Sigma Aldrich	C2759-250MG
Anhydrotetracycline	Cayman chemical company	10009542
5′Fluorootic acid Monohydrate	US Biological	F5050
Critical commercial assays		
Quick Coupled Transcription/Translation kit	Promega	L2080
Turbo DNA free kit	Ambion	AM1907
qScript cDNA Synthesis Kit	Quanta Biosciences	95047
iQ SYBR Green Supermix	BioRad	1708886
Pierce BCA Protein Assay Kit	Thermo Scientific	23225
TMT10plex isobaric label reagent set	Thermo Scientific	90111
Deposited data		
Mass spectrometry proteomics data	This paper	ProteomeXchange PXD021173
IP mass spectrometry data	This paper	ProteomeXchange PXD023149

(*Continued on next page*)

Continued

REAGENT or RESOURCE	SOURCE	IDENTIFIER
Experimental models: Organisms/strains		
Yeast: YPH499 WT: *MATa ade2-101 his3-200 leu2-1 ura3-52 trp1-63 lys2-80*	Herrmann lab	Woellhaf et al., 2016
Yeast: YPH499 Δ*sam37: sam37*Δ::*HIS3* derivative of YPH499 WT	Doron Rapaport lab	N/A
Yeast: YPH499 Δ*sam37: sam37*Δ::*HIS3* (*SAM37 URA3*) derivative of YPH499 WT	Doron Rapaport lab	N/A
Yeast: YPH499 Δ*sam37*Δ*tom70* shuffle strain: *sam37*Δ::*HIS3 tom70*Δ::*NatNT2* (*SAM37 URA3*) derivative of YPH499 WT	This study	N/A
Yeast: BY4742 WT: *MATa his3*Δ1 *leu2*Δ0 *lys2*Δ0 *ura3*Δ0 [ρ^+]	Euroscarf	N/A
Yeast: BY4742 Δ*tim8: tim8*Δ:: *kanMX* derivative of BY4742 WT	Euroscarf	N/A
Yeast: BY4742 Δ*elo2: elo2*Δ:: *kanMX* derivative of BY4742 WT	Euroscarf	N/A
Yeast: BY4742 Δ*pex18: pex18*Δ:: *kanMX* derivative of BY4742 WT	Euroscarf	N/A
Yeast: BY4742 Δ*pex17: pex17*Δ:: *kanMX* derivative of BY4742 WT	Euroscarf	N/A
Yeast: BY4742 Δ *pfd1: pfd1*Δ:: *kanMX* derivative of BY4742 WT	Euroscarf	N/A
Yeast: BY4742 Δ *hch1: hch1*Δ:: *kanMX* derivative of BY4742 WT	Euroscarf	N/A
Yeast: BY4742 Δ*loa1: loa1*Δ:: *kanMX* derivative of BY4742 WT	Euroscarf	N/A
Yeast: BY4742 Δ*tim13: tim13*Δ:: *kanMX* derivative of BY4742 WT	Euroscarf	N/A
Yeast: BY4742 Δ*sam37: sam37*Δ:: *kanMX* derivative of BY4742 WT	Euroscarf	N/A
Yeast: W303 WT: *MATa ura3-1 ade2-1 his3-11 leu2-3,112 trp1Δ2*	Herrmann lab	Peleh et al., 2017
Yeast: W303 Δ*tom70/71: tom70Δ::KanMX4 tom71Δ::NatNT2* derivative of W303 WT	Doron Rapaport lab	Jores et al., 2018
Yeast: yMS721 WT: MATα *ura3Δ0 his3Δ1 leu2Δ0 his3Δ1 can1Δ::STE2pr-spHIS5; lyp1ΔSTE3pr-LEU2*; *met15Δ0*	Maya Schuldiner lab	Tong and Boone, 2007
Yeast: yMS721 Δ*tom70: tom70*Δ::*NAT2* derivative of yMS721 WT	This study	N/A
Yeast: yMS721 Δ*tom71: tom71*Δ::*kanMX* derivative of yMS721 WT	This study	N/A
Yeast: yMS721 Δ*tom70*Δ*tom71: tom70*Δ::*NAT2 tom71*Δ:: *kanMX* derivative of yMS721 WT	This study	N/A
Software and algorithms		
Coral Photopaint X7	Corel	N/A
BioFSharp	https://github.com/CSBiology/BioFSharp	1.2.0
Coral Draw X7	Corel	N/A
R 3.6.3	R Core Team	N/A
MaxQuant 1.6.10.43	N/A	Tyanova et al., 2016
Balony	Young and Loewen, 2013	N/A
iMTS-L profiles	http://iMLP.bio.uni-kl.de/	N/A
AIDA software	Elysia-raytest	N/A

RESOURCE AVAILABILITY

Lead contact

Further information and requests for resources and reagents should be directed to and will be fulfilled by the Lead Contact, Prof. Dr. Johannes M. Herrmann (hannes.herrmann@biologie.uni-kl.de).

Materials availability

All unique/stable reagents generated in this study are available from the Lead Contact without restriction.

Data and code availability

The mass spectrometry proteomics data (see also Tables S1 and S2) have been deposited to the ProteomeXchange Consortium via the PRIDE (Perez-Riverol et al., 2019) partner repository with the dataset identifier PXD021173.

reviewer13653@ebi.ac.uk

Mass spectrometry data of the immunoprecipitation experiments (see also Table S4) are available via ProteomeXchange with identifier PXD023149.

reviewer_pxd023149@ebi.ac.uk

EXPERIMENTAL MODEL AND SUBJECT DETAILS

Yeast strains, plasmids and growth conditions

The yeast strains used in this study are either based on BY4742, W303 or YPH499 background. All strains used in this study are described in detail in the key resources table.

All strains were either grown on YP (1% yeast extract and 2% peptone) medium containing 2% glucose or galactose (Altmann et al., 2007) or on minimal synthetic medium (S) containing 0.67% (w/v) yeast nitrogen base and 2% glucose, galactose or lactate as carbon source. To express proteins from the *GAL* promoter, cells were shifted to 0.5% galactose containing medium for 4.5 h.

The shuffle strain for *SAM37* was obtained by replacement of the *SAM37* genomic open reading frame with a *HIS3* cassette in a YPH499 WT. Afterward, a pRS426-TPI plasmid expressing *SAM37* was transformed, following the subsequent replacement of the *TOM70* genomic reading frame with a *NAT2* cassette.

In order to anchor the TPR-containing proteins to the mitochondrial outer membrane, a pYX142-TPI vector containing the N-terminal Tom70-anchor (residues 1-98) was used to insert the various constructs (for residues see Figure 4B). The Tah1 mutation in the MEEVD binding site was achieved by PCR-based site-directed mutagenesis (Quick-Change method, Stratagene) using suitable primer sequences with the desired mutation. For construction of the mt-Tah1-C2-C3 variant, the sequences corresponding to the protein sequence of C2 and C3 domains of Tom70 (residues 247-460 and 461-617) were cloned into the mt-Tah1-containing pYX142 vector.

Yeast transformation was carried out by the lithium acetate method (Gietz et al., 1992). Empty vectors were also transformed in parallel to serve as negative controls.

METHOD DETAILS

CRISPRi system construction

We employ an improved version of a previously generated single plasmid CRISPRi system (Smith et al., 2016) by making it compatible with Type IIS/Golden Gate Assembly, by employing an improved structural gRNA that reduces premature Polymerase III termination (Chen et al., 2013) and by addition of a KanMX resistance cassette. Briefly, we first generated the pKR297 plasmid, containing the RPR1(TetO) promoter, a BspQI-flanking gRNA cassette with an AscI site to remove uncut plasmid, the structural gRNA part and TetR. The pTef1-dCas9-Mxi1-tCyc1 fragment (from pRS416-dCas9-Mxi1: https://www.addgene.org/73796/) was then introduced to yield pKR359 (https://benchling.com/s/seq-gndJVnw6U1oisO0sL65k/edit), and KanMX was inserted to yield pKR366 (https://benchling.com/s/seq-Ymw9j7Wn3MM7g8N7Ny9K/edit).

To assemble the *TOM70* gRNA, two oligonucleotides were annealed in CutSmart buffer (NEB) to form a double-stranded sticky end fragment. pKR366 was digested with BspQI (NEB), gel-purified, and the fragment inserted matching with the BspQI sites using T4 ligase (NEB), according to the supplier's instructions.

Growth assays and viability tests

For spot analysis, the respective yeast strains were grown in liquid rich or synthetic media. Total yeast cells equivalent to 0.5/0.2 OD_{600} were harvested at exponential phase. The cells were washed in sterile water and subjected to ten-fold serial dilutions. Each dilution was spotted on rich or synthetic media followed by incubation at 30°C or 37°C. Pictures were taken after different days of the growth.

Growth curves were performed in a 96 well plate, using the automated ELx808 Absorbance Microplate Reader (BioTek®). The growth curves started at 0.1 OD_{600} and the OD_{600} was measured every 10 min for 72 h at 30°C. The mean of technical triplicates was calculated and plotted in R. For CRISPRi-mediated repression of *TOM70*, strains were incubated with 960 ng/ml Anhydrotetracycline for 6 h prior to growth curve analysis.

High-throughput screening of the GFP collection

To analyze the effect of *TOM70* and *TOM71* deletions on mitochondrial protein import we compiled a mini-library of 113 MTS-independent strains with mitochondrial GFP signal from the N-SWAT-library with NOP1 promotor and N-terminal sfGFP tag, but without a generic MTS inserted before the sfGFP (Yofe et al., 2016; Weill et al., 2018). This mini-library included many members of the metabolite carrier family, other inner membrane proteins, and outer membrane proteins (Table S3). We didn't include any MTS-dependent strains in the mini-library since in the N-SWAT library they all carry a very strong generic MTS inserted before sfGFP and thus considerably influencing the import pathway taken by the protein. We constructed *Δtom70*, *Δtom71*, and double mutant *Δtom70Δtom71* strains in the synthetic genetic array (SGA) compatible background (Tong and Boone, 2007) using standard yeast transformation techniques (Gietz and Woods, 2006; Janke et al., 2004) (See Key resources table). We mated these strains with the mitochondrial mini-library and selected for haploid cells harboring both the GFP tag and the required deletion using automated mating and selection approaches as described before (Tong and Boone, 2007; Cohen and Schuldiner, 2011). All mating and selection procedures were performed using RoToR high-density arrayer (Singer Instruments).

For imaging, the resulting haploid libraries with *TOM70*, *TOM71*, or double deletion were inoculated from agar plates into SD-URA liquid media (6.7 g l^{-1} yeast nitrogen base without amino acids, 20 g l^{-1} glucose, and optimized nutrient supplement without uracil supplemented with 200 μg ml^{-1} nourseothricin for *Δtom70*, 500 μg ml^{-1} geneticin for *Δtom71*, or both antibiotics for the *Δtom17Δtom71* double mutant in 384-well plates and grown overnight at 30°C with shaking. The donor mini-library was at the same time inoculated into SD-URA and grown in the same conditions. All liquid media operations and automated imaging were performed using a JANUS liquid handler (PelkinElmer) connected to an incubator (LiCONiC) and a microscope (Breker et al., 2013). The overnight cultures were diluted 20 times in SD-URA media without antibiotics. After 4 h of growth at 30°C the yeast cultures were transferred to Concanavalin A-coated (Sigma Aldrich) glass-bottom 384-well plates (Matrical Bioscience) and adhered for 20 minutes. Non-adhering cells were washed away with SD-URA-Riboflavin (same as regular SD-URA except yeast nitrogen base without riboflavin and without amino-acids is used to reduce media autofluorescence) that was also used as an imaging media. The plates were transferred to an automated ScanR miscroscopic system (Olympus) using a robotic swap arm (Hamilton). The cells were imaged in bright field and GFP (excitation filter 490/20 nm, emission filter 535/50 nm) channels with 60x air objective (NA 0.9) and the images were recorded on ORCA-ER charge-coupled device camera (Hammamatsu). The donor mini-library and the libraries crossed with *TOM70* and *TOM71* deletion strains were imaged on the same day.

For each strain the four images from the donor library, the library crossed with *Δtom70*, *Δtom71*, and *Δtom70Δtom71* were displayed side by side and GFP signal localization and intensity were visually assessed (Table S3).

For quantitive analysis, the cells' outlines were determined in bright field channel using a custom MATLAB script and median fluorescence intensity was calculated within these outlines. These values were averaged across all detected cells. The strain with the lowest mean cell intensity was taken as a cell background value and this value was subtracted from all other values to obtain background-corrected fluorescence intensities. The background fluorescence for each micrograph was also calculated using background subtraction procedure to assess illumination stability during the imaging process. The illumination was stable throughout the whole imaging period so we performed no additional corrections of the measured cell fluorescence intensities. Mean fluorescence for each strain of the donor mini-library was directly compared to the mean fluorescence of the same strain crossed to *TOM70* and *TOM71* deletions (Table S3).

For MitoTracker colocolazation experiments, yeast were adhered to Con A coated plates for 20 min and then stained with 50 nM MitoTracker CMTMRos in SD-URA without Riboflavin for 10 min. The staining solution was replaced with SD-URA without Riboflavin for imaging. The cells were imaged using VisiScope Confocal Cell explorer system consisting of Yokogawa spinning disk scanning unit attached to the Olympus IX83 microscope and equipped with PCO-Edge sCMOS detector controlled by VisView software. The imaging was performed with 60x oil objective. Representative areas of the micrographs were cropped and linearly adjusted for contrast using ImageJ.

TOM70 genetic interaction screen

To investigate genetic interactions of *TOM70* we crossed the *Δtom70* strain with the yeast full-genome knock-out collection (Giaever et al., 2002) and performed single and double mutant selection as described before (Tong and Boone, 2007). All mating and selection procedures were performed using RoToR high-density arrayer (Singer Instruments).

Briefly, after mating and sporulation all haploid MATα cells were selected on SD-LEU-LYS-ARG (6.7 g l^{-1} yeast nitrogen base without amino acids, 20 g l^{-1} glucose, complete set of supplements without leucine, lysine, and arginine) supplied with canavanine and thialysine. Then the haploids were plated on SD-LEU-LYS-ARG supplied with canavanine, thialysine, and geneticin (G418) to select all haploids that have the library knock-outs disregarding of the *TOM70* allele. From these plates the strains were simultaneously replicated either on the same media (SD-LEU-LYS-ARG + canavanine + thialysine + G418) to measure the library knock out colony size or on the media additionally supplied with nourseothricin (NAT) to select both for the library knock out and *Δtom70* allele and to measure the colony size of the double mutant. The plates were grown overnight and photographed the next day. Size of the colonies was determined and normalized for each plate using SGAtools (Wagih et al., 2013). For each library knock-out strain the colony size difference between single (library) mutant selection (SD-LEU-LYS-ARG + canavanine + thialysine + G418) and double mutant (library + *Δtom70*) selection media (SD-LEU-LYS-ARG + canavanine + thialysine + G418 + NAT) was calculated as a measure of genetic interaction with *TOM70* (Table S5).

Overexpression assay

Yeast cells were inoculated in non-inducing medium. At mid-log phase (OD 0.6 – 0.8), cells were shifted to inducing conditions (0.5% galactose). At the indicated time points, 2 OD_{600} were harvested by centrifugation (20,000 g, 3 min, RT) and whole cell lysates were prepared. Whole cell lysates were prepared for the indicated time points to investigate the degradation behavior.

Fractionation assay

Overnight cultures of respective strains were diluted and induced with 0.5% Galactose. After 4.5 hours cells of 10 OD600 were harvested by centrifugation (5,000 g, 10min, RT). After washing with dH2O the pellet was resuspended in 1 ml MP1 buffer (100 mM Tris, 10 mM DTT) and incubated for 30 min at 30°C. Cells were pelleted by centrifugation (5,000 g, 3 min, RT) and washed with 1 ml 1.2 M Sorbitol. Afterwards pellets were resuspended in 1 ml MP2 buffer (1.2 M Sorbitol, 20 mM KPi pH 7.4, Zymolyase) and incubated 30 min at 30 °C. From now on, any step was done at 4°C or on ice. Pelleted cells were resuspended in 1 ml Homogenisation buffer (10 mM Tris pH7.4, 1 mM EDTA, 0.6 M Sorbitol) and dounced in a cooled potter for 15 times. After centrifugation (5,000 g, 3 min, 4°C) the supernatant was taken and centrifuged again (5,000 g, 3 min, 4°C). The pellet (P1) was taken up in 100 µl Laemmli +DTT. To obtain the pellet (P2) the previous supernatant was centrifuged at 12,000 g for 5 min at 4°C and the pellet was taken up in 100 µl Laemmli +DTT. The supernatant was finally centrifuged at 30,000 g for 30min at 4°C. The pellet (P3) was resuspended in 100 µl Laemmli +DTT. The supernatant was transferred into a new tube and 200 µl 72% TCA was added. The samples were frozen at 20°C overnight. The next day the samples were thawed on ice and centrifuged at 30,000 g for 20 min at 4°C. The supernatant was discarded and the pellets were washed with ice-cold acetone. After centrifugation at 30,000 g for 20 min at 4°C the pellet (P4) was taken up in 100 µl Laemmli + DTT. To resuspend P1-P4, samples were incubated shaking for 30 min at 30°C. Per sample 25 µl were loaded on 16% SDS-Gel.

Overnight cultures of respective strains were diluted and induced with 0.5% galactose. After 4.5 hours cells of 10 OD_{600} were harvested by centrifugation (5,000 g, 10min, RT). After washing with dH_2O the pellet was resuspended in 1 mL MP1 buffer (100 mM Tris, 10 mM DTT) and incubated for 30 min at 30°C. Cells were pelleted by centrifugation (5,000 g, 3 min, RT) and washed with 1 mL 1.2 M Sorbitol. Afterward pellets were resuspended in 1 mL MP2 buffer (1.2 M Sorbitol, 20 mM KPi pH 7.4, Zymolyase) and incubated 30 min at 30°C. From now on, any step was done at 4°C or on ice. Pelleted cells were resuspended in 1 mL homogenization buffer (10 mM Tris pH7.4, 1 mM EDTA, 0.6 M Sorbitol) and dounced in a cooled potter 15 times. After centrifugation (5,000 g, 3 min, 4°C) the supernatant was taken and centrifuged again (5,000 g, 3 min, 4°C). The pellet (P1) was taken up in 100 µl Laemmli +DTT. To obtain the pellet (P2), the previous supernatant was centrifuged at 12,000 g for 5 min at 4°C and the pellet was taken up in 100 µl Laemmli +DTT. The supernatant was finally centrifuged at 30,000 g for 30min at 4°C. The pellet (P3) was resuspended in 100 µl Laemmli +DTT. The supernatant was transferred into a new tube and 200 µl 72% TCA was added. The samples were frozen at 20°C overnight. The next day the samples were thawed on ice and centrifuged at 30,000 g for 20 min at 4°C. The supernatant was discarded and the pellets were washed with ice-cold acetone. After centrifugation at 30,000 g for 20 min at 4°C the pellet (P4) was taken up in Laemmli + DTT. Samples were analyzed by SDS-Gel.

Heat-shock assay

Yeast cells were pre-grown in SD medium at 30°C. At mid-log phase (OD 0.6 – 0.8), 0.1 OD_{600} were exposed to a heat-shock at 50°C for the indicated time points. After each time point, 0.01 OD_{600} were equally plated on SD plates and incubated for two days at 30°C.

Sample preparation and mass spectrometric identification of proteins

For IP mass spectrometry, cells (Δ*tom70/71* + HA-tagged mt-Tah1 or Δ*tom70/71* + empty vector) were incubated in SGal-Leu medium and 20 OD of cells were harvested. Cell lysates were prepared in 1000 µl lysis buffer (10mM tris, 150mM NaCl, 0,5mM EDTA, 0.5% Triton, 1mM PMSF) using a FastPrep-24 5 G homogenizer (MP Biomedicals) with 3 cycles of 30 s, speed 6.0 m s–1, 120 s breaks, glass beads. Samples were centrifuged 10 min at 20.000 g. Cell lysates were used for an IP with protein-A-Sepharose beads (expedeon) and HA-serum. The tagged proteins were bound to the beads for 1 h at 4°C. After spinning the samples down the beads were washed 3x with 800 µl wash buffer I (150 mM NaCl, 50 mM Tris pH 7.5, 5% Glycerol, 0.05% Tx-100) and afterward 2x with 500 µl wash buffer II (150 mM NaCl, 50 mM Trish pH 7.5, 5% Glycerol). For elution and trypsin digestion 50 µl elution buffer I was added (2M Urea, 50 mM Tris pH 7.5, 1 mM DTT, 5 ng/µl Trypsin) and incubated for 1 h at RT. Afterward 1 µl Trypsin was added and incubated for 10 min at RT. 50 µl elution buffer II (2M Urea, 50 mM Tris pH 7.5, 5mM CAA) were added. Samples were incubated ON in the dark at RT. pH of samples was adjusted to pH < 2 with Tri-flouracetic acid. Desalting/reversed-Phase cleanup with 3xC18 stage tips. Samples were dried down in speed-vac and resolubilized in 9 µl buffer A (0.1 % formic acid in MS grad water) and 1 µl buffer A* (0.1 % formic acid, 0.1 % TFA in MS grad water).

For mass spectrometry sample preparation of whole cell lysates, strains were pregrown in S-medium containing 2% galactose at 30°C and either shifted to 37°C or kept at 30°C for 16 h.

50 OD_{600} of cells were harvested at each time point by centrifugation (17,000 g, 3 min, 2°C), washed with prechilled water, snap-frozen in liquid nitrogen and stored at −80°C. Cells lysates were prepared in lysis buffer (50 mM Tris pH 7.6, 5% (w/v) SDS) using a FastPrep-24 5G homogenizer (MP Biomedicals, Heidelberg, Germany) with 3 cycles of 30 s, speed 8.0 m/s, 120 s breaks, glass beads). Lysates were diluted to 2% (w/v) SDS and protein concentrations were determined using the Pierce BCA Protein Assay (Thermo Scientific, #23225). 20 µg of each lysate were subjected to an in-solution tryptic digest using a modified version of the Single-Pot Solid-Phase-enhanced

Sample Preparation (SP3) protocol (Hughes et al., 2014, 2019). Here, lysates were added to Sera-Mag Beads (Thermo Scientific, #4515-2105-050250, 6515-2105-050250) in 10 μl 15% formic acid and 30 μl of ethanol. Binding of proteins was achieved by shaking for 15 min at room temperature. SDS was removed by four subsequent washes with 200 μl of 70% ethanol. Proteins were digested with 0.4 μg of sequencing grade modified trypsin (Promega, #V5111) in 40 μl HEPES/NaOH, pH 8.4 in the presence of 1.25 mM TCEP and 5 mM chloroacetamide (Sigma-Aldrich, #C0267) overnight at room temperature. Beads were separated, washed with 10 μl of an aqueous solution of 2% DMSO and the combined eluates were dried down. In total three biological replicates were prepared (n = 3). Each replicate included samples of all 5 strains at 30°C or 37°C (in total 10 samples per replicate). Peptides were reconstituted in 10 μl of H_2O and reacted with 80 μg of TMT10plex (Thermo Scientific, #90111) (Werner et al., 2014) label reagent dissolved in 4 μl of acetonitrile for 1 h at room temperature. Excess TMT reagent was quenched by the addition of 4 μl of an aqueous solution of 5% hydroxylamine (Sigma, 438227). Peptides were mixed to achieve a 1:1 ratio across all TMT-channels. Mixed peptides were desalted on home-made StageTips containing Empore C_{18} disks (Rappsilber et al., 2007). The samples were then analyzed by LC-MS/MS on a Q Exactive HF instrument (Thermo Scientific) as previously described.

Briefly, peptides were separated using an Easy-nLC 1200 system (Thermo Scientific) coupled to a Q Exactive HF mass spectrometer via a Nanospray-Flex ion source. The analytical column (50 cm, 75 μm inner diameter (NewObjective) packed in-house with C18 resin ReproSilPur 120, 1.9 μm diameter Dr. Maisch) was operated at a constant flow rate of 250 nl/min. A 3 h gradient was used to elute peptides (Solvent A: aqueous 0.1% formic acid; Solvent B: 80 % acetonitrile, 0.1% formic acid). Peptides were analyzed in positive ion mode applying with a spray voltage of 2.3 kV and a capillary temperature of 250°C. MS spectra with a mass range of 375–1.400 m/z were acquired in profile mode using a resolution of 120.000 [maximum fill time of 80 ms or a maximum of 3e6 ions (automatic gain control, AGC)]. Fragmentation was triggered for the top 15 peaks with charge 2–8 on the MS scan (data-dependent acquisition) with a 30 s dynamic exclusion window (normalized collision energy was 32). Precursors were isolated with a 0.7 m/z window and MS/MS spectra were acquired in profile mode with a resolution of 60,000 (maximum fill time of 100 ms, AGC target of 2e5 ions, fixed first mass 100 m/z).

Analysis of mass spectrometry data

Peptide and protein identification and quantification was done using the MaxQuant software (version 1.6.10.43) (Cox and Mann, 2008; Cox et al., 2011; Tyanova et al., 2016) and a *Saccharomyces cerevisiae* proteome database obtained from Uniprot. 10plex TMT was chosen in Reporter ion MS2 quantification, up to 2 tryptic miss-cleavages were allowed, protein N-terminal acetylation and Met oxidation were specified as variable modifications and Cys carbamidomethylation as fixed modification. The "Requantify" and "Second Peptides" options were deactivated. False discovery rate was set at 1% for peptides, proteins and sites, minimal peptide length was 7 amino acids.

The output files of MaxQuant were processed using the R programming language. Only proteins that were quantified with at least two unique peptides were considered for the analysis. Moreover, only proteins that were identified in at least two out of three MS runs were kept. A total of 2920 proteins passed the quality control filters. Raw signal sums were cleaned for batch effects using limma (Ritchie et al., 2015) and further normalized using variance stabilization normalization (Huber et al., 2002). Proteins were tested for differential expression using the limma package for the indicated comparison of strains.

A reference list of yeast mitochondrial proteins was obtained from (Morgenstern et al., 2017). Gene set enrichment analysis was performed using Fisher's exact test. A Benjamini-Hochberg procedure was used to account for multiple testing, where this was performed (Benjamini and Hochberg, 1995).

Calculation of aggregation propensity

Aggregation propensity is determined from primary protein sequence using the "hot spot" approach according to Sanchez de Groot et al., 2005. A predictive model is based on the individual aggregation propensities of natural amino acids, which have already been experimentally validated in the literature and provide insights into the effect of disease-linked mutations in these polypeptides. Here, we used the average over a sliding window of 5, 7, 9 or 11 residues depending on total sequence length ($\leq$75, $\leq$ 175, $\leq$ 300, or > 300). The resulting value is assigned to the central residue in the window and then averaged to obtain the aggregation-propensity of the respective protein (Conchillo-Solé et al., 2007). For convenient application the algorithm was implemented using BioFSharp 1.2.0 (https://github.com/CSBiology/BioFSharp).

Miscellaneous

The following methods were performed according to already published methods: Import into isolated mitochondria (Backes and Herrmann, 2017), CCCP chase experiment (Backes and Herrmann, 2017), iMTS-L profile generation (Backes and Herrmann, 2017), isolation of mitochondria (Saladi et al., 2020), whole cell lysates (Saladi et al., 2020), RNA-isolation (Boos et al., 2019), quantitative real-time PCR assays (Boos et al., 2019), PACE-YFP reporter assay (Boos et al., 2019).

QUANTIFICATION AND STATISTICAL ANALYSIS

Unless otherwise indicated, experiments were performed in n = 3 independent biological replicates and mean values and standard deviations are presented in the figures. Significance of results was assessed using standard statistical tests as detailed in the respective

figure legends and descriptions in the STAR Methods section. In particular, statistical analysis of the mass spectrometry data was performed with the limma package within R.

Where multiple comparisons were analyzed, *P value*s were adjusted for multiple hypothesis testing with the Benjamini-Hochberg procedure.

Western blot analyses were independently replicated with similar results, and representative data are shown in the figures. Quantification was performed with Fiji/ImageJ and significance testing was performed with Student's *t*-Test.

Cell Reports, Volume *35*

Supplemental information

The chaperone-binding activity of the mitochondrial surface receptor Tom70 protects the cytosol against mitoprotein-induced stress

Sandra Backes, Yury S. Bykov, Tamara Flohr, Markus Räschle, Jialin Zhou, Svenja Lenhard, Lena Krämer, Timo Mühlhaus, Chen Bibi, Cosimo Jann, Justin D. Smith, Lars M. Steinmetz, Doron Rapaport, Zuzana Storchová, Maya Schuldiner, Felix Boos, and Johannes M. Herrmann

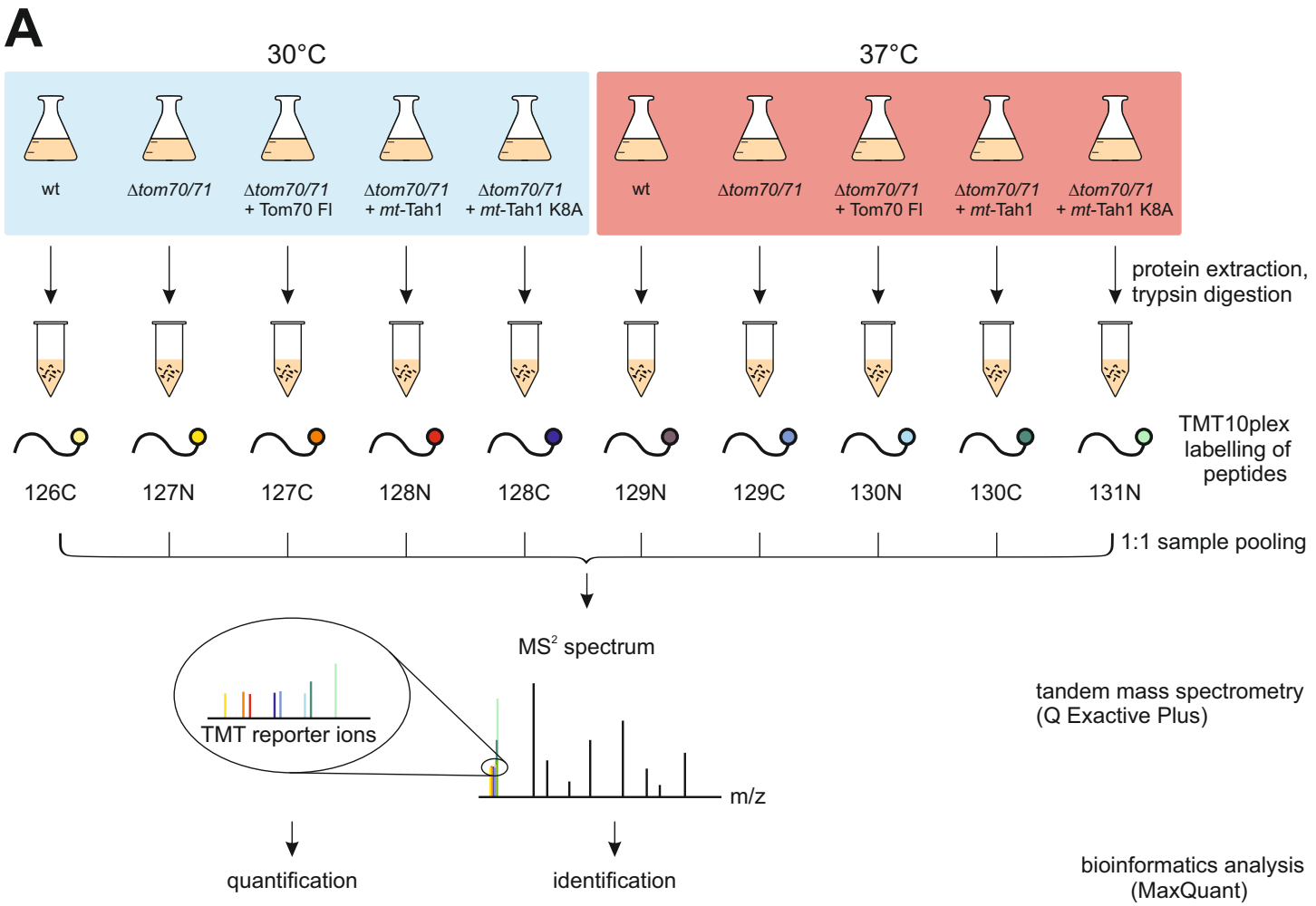
A
30°C
37°C
wt
Δtom70/71
Δtom70/71 + Tom70 FI
Δtom70/71 + mt-Tah1
Δtom70/71 + mt-Tah1 K8A
wt
Δtom70/71
Δtom70/71 + Tom70 FI
Δtom70/71 + mt-Tah1
Δtom70/71 + mt-Tah1 K8A
protein extraction, trypsin digestion
126C
127N
127C
128N
128C
129N
129C
130N
130C
131N
TMT10plex labelling of peptides
1:1 sample pooling
MS² spectrum
TMT reporter ions
m/z
tandem mass spectrometry (Q Exactive Plus)
quantification
identification
bioinformatics analysis (MaxQuant)

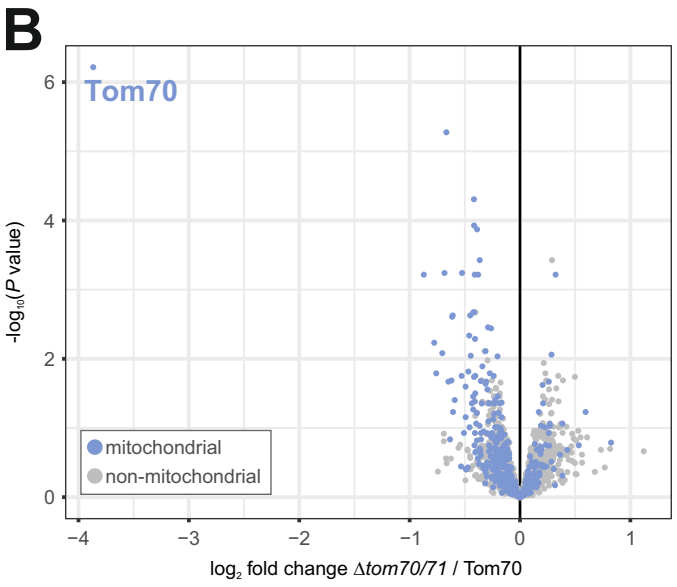
B
Tom70
mitochondrial
non-mitochondrial
-log10(P value)
log2 fold change Δtom70/71 / Tom70

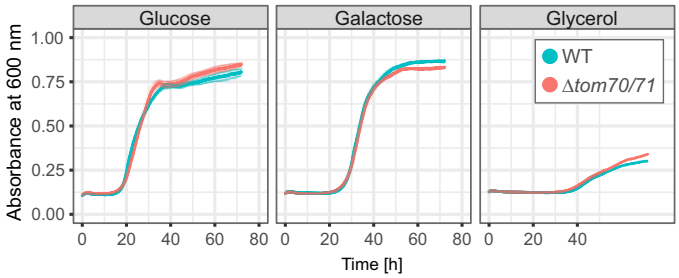
C
Glucose
Galactose
Glycerol
WT
Δtom70/71
Absorbance at 600 nm
Time [h]

Figure S1. Schematic workflow of the mass spectrometry analysis. A. Related to Figure 1. The indicated strains were cultured at 30°C or 37°C for 16 h. Proteins were extracted and digested with trypsin. The obtained peptides were labelled with TMT10plex and the 10 different samples were pooled in 1:1 ratio. The samples were subjected to mass spectrometry and subsequent bioinformatical analysis. The wild type was not further analyzed in this study. **B.** The proteomes of *Δtom70/71* cells carrying empty or Tom70-expressing plasmids (three replicates each) were measured by mass spectrometry. Shown are the mean values of the ratios obtained from *Δtom70/71* to Tom70-expressing cells and statistical significances (*P* values). The data point for Tom70 is indicated. **C.** WT and *Δtom70/71* mutant were grown under constant shaking at 30°C in either glucose-, galactose- or glycerol-containing medium. Shown are mean values and standard deviations of three technical replicates.

GFP
MitoTracker
Overlay
GFP
MitoTracker
Transmitted
GFP-PET9
GFP-SCM4
GFP-MIC10
GFP-HEM14
GFP-PIC2
GFP-AAC3
GFP-ODC2
GFP-YHM2
GFP-AIM22
TOM70 TOM71
Δtom70 Δtom71

Figure S2. Microscopy-based screen to identify Tom70-dependent mitochondrial proteins. Related to Figure 2. Yeast cells grown in glucose medium were adhered to Con A coated plates and stained with MitoTracker CMTMRos. The cells were imaged by fluorescence microscopy. GFP panels for the same GFP-tagged proteins have the same contrast setting for TOM70/71 and Δtom70/71 conditions. Scale bars = 10 μm.

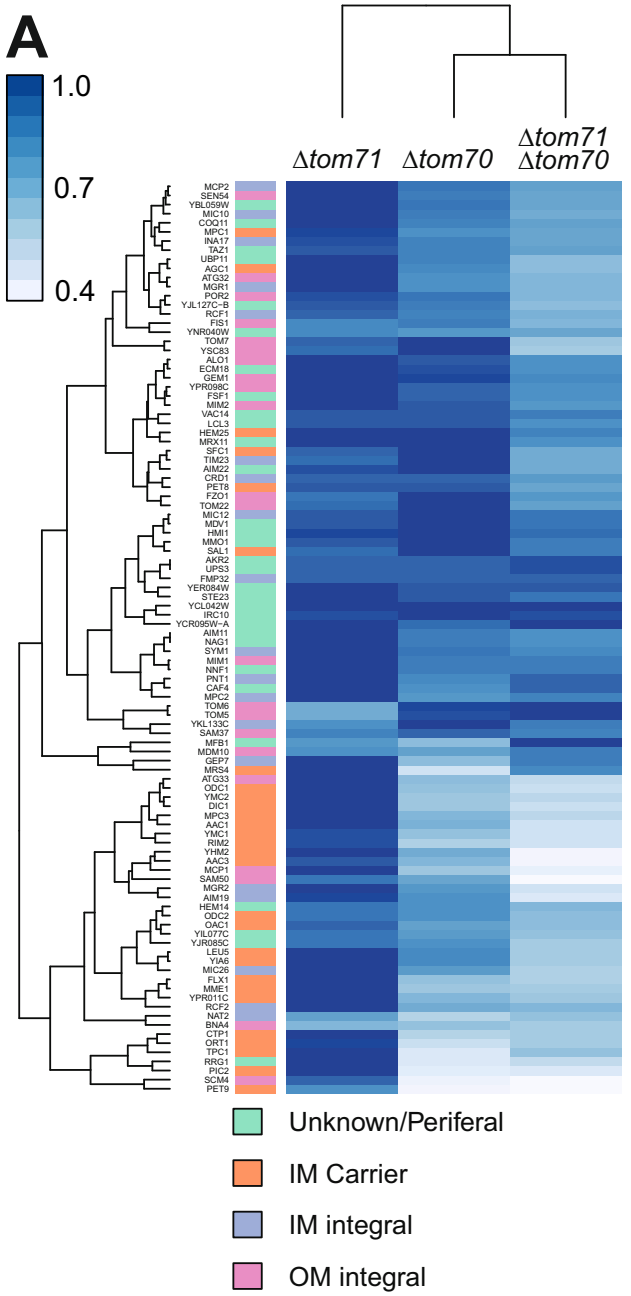
A
1.0
0.7
0.4
Δtom71
Δtom70
Δtom71
Δtom70
Unknown/Periferal
IM Carrier
IM integral
OM integral

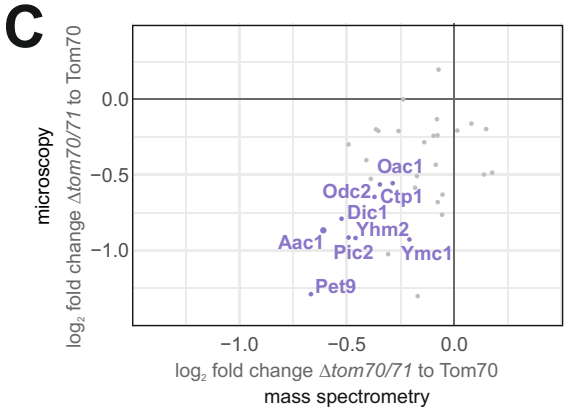
C
microscopy
log2 fold change Δtom70/71 to Tom70
0.0
−0.5
−1.0
Oac1
Odc2
Ctp1
Dic1
Yhm2
Aac1
Pic2
Ymc1
Pet9
−1.0
−0.5
0.0
log2 fold change Δtom70/71 to Tom70
mass spectrometry

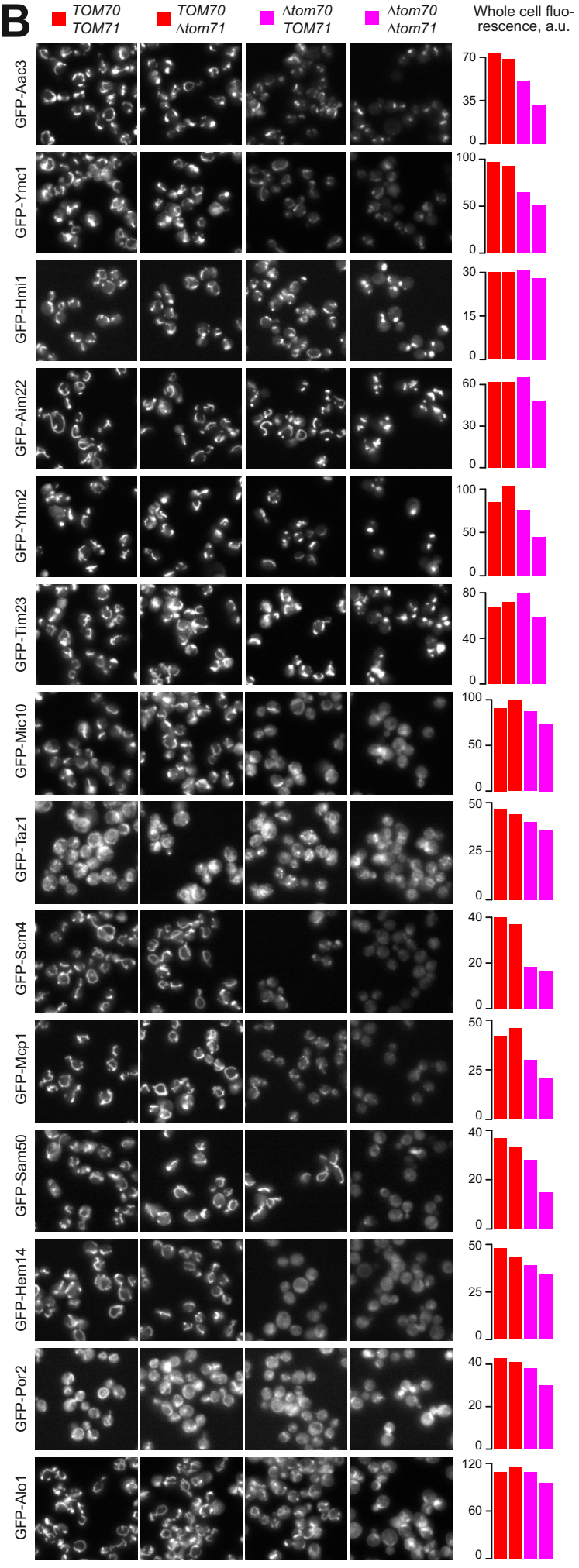
B
TOM70 TOM71
TOM70 Δtom71
Δtom70 TOM71
Δtom70 Δtom71
Whole cell fluorescence, a.u.
GFP-Aac3
GFP-Ymc1
GFP-Hmi1
GFP-Aim22
GFP-Yhm2
GFP-Tim23
GFP-Mic10
GFP-Taz1
GFP-Scm4
GFP-Mcp1
GFP-Sam50
GFP-Hem14
GFP-Por2
GFP-Alo1

Figure S3. Mitochondrial proteins strongly differ in their Tom70-dependence. Related to Figure 2. **A.** Hierarchical clustering of fluorescent signals of 113 N-terminally GFP tagged mitochondrial proteins in the indicated strains. **B.** The mitochondrial staining of 113 N-terminally GFP-tagged mitochondrial proteins was systematically quantified (>100 cells per strain). Tom70/71-dependence strongly differs among different mitochondrial proteins and members of the carrier family are not particularly Tom70-dependent. IM, inner membrane; OM, outer membrane. **C.** The relative $\log_2$ fold changes (Δ*tom70/71* to Tom70 full length) obtained from the mass spectrometry experiment and the GFP-screen were blotted against each other. Carrier proteins are labeled, pointing out the correlation between these two datasets.

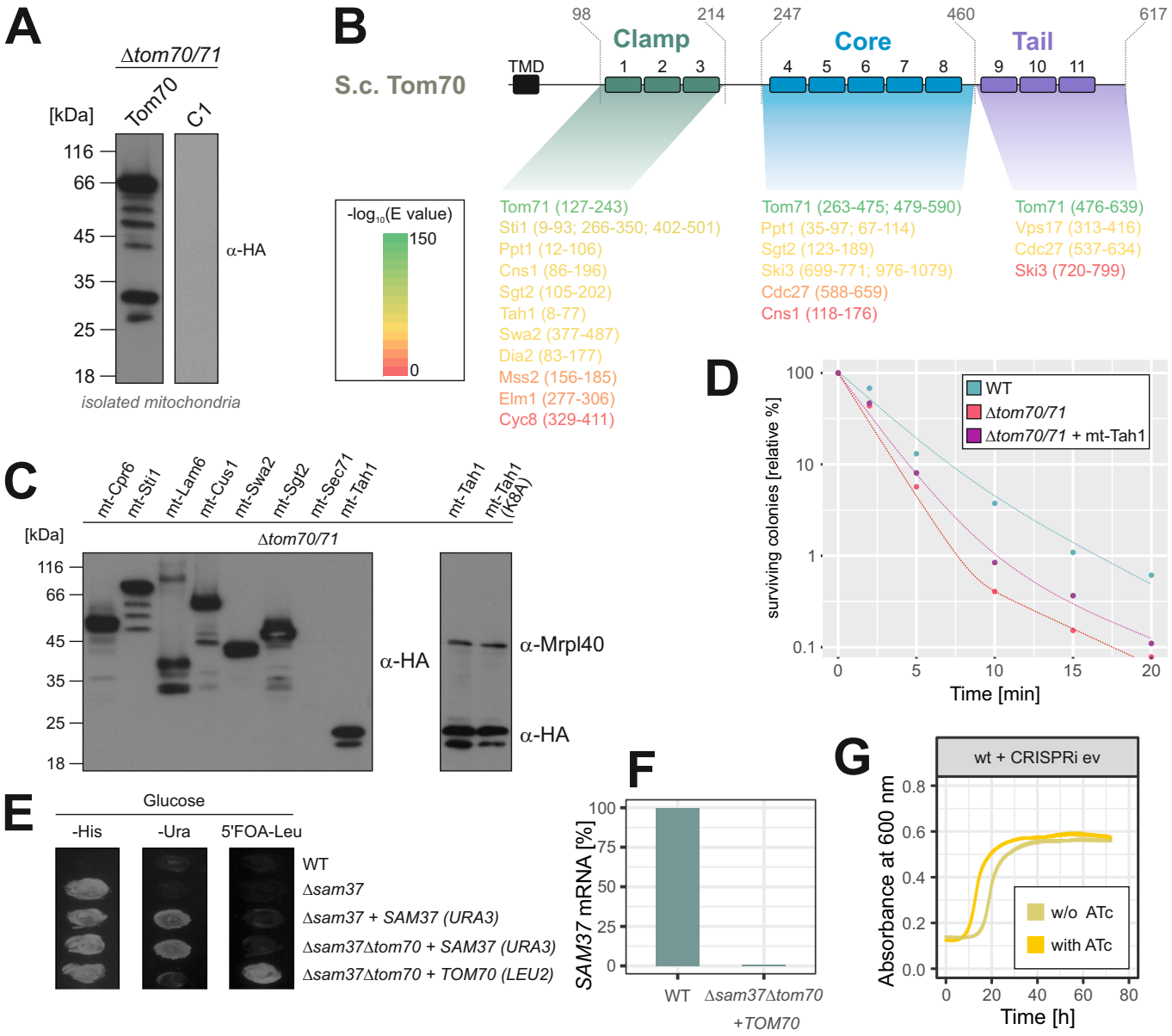
A
Δtom70/71
Tom70
C1
[kDa]
116
66
45
35
25
18
α-HA
isolated mitochondria
B
S.c. Tom70
98
214
247
460
617
Clamp
Core
Tail
TMD
1 2 3
4 5 6 7 8
9 10 11
-log10(E value)
150
0
Tom71 (127-243)
Sti1 (9-93; 266-350; 402-501)
Ppt1 (12-106)
Cns1 (86-196)
Sgt2 (105-202)
Tah1 (8-77)
Swa2 (377-487)
Dia2 (83-177)
Mss2 (156-185)
Elm1 (277-306)
Cyc8 (329-411)
Tom71 (263-475; 479-590)
Ppt1 (35-97; 67-114)
Sgt2 (123-189)
Ski3 (699-771; 976-1079)
Cdc27 (588-659)
Cns1 (118-176)
Tom71 (476-639)
Vps17 (313-416)
Cdc27 (537-634)
Ski3 (720-799)
C
mt-Cpr6
mt-Sti1
mt-Lam6
mt-Cus1
mt-Swa2
mt-Sgt2
mt-Sec71
mt-Tah1
mt-Tah1
mt-Tah1 (K8A)
[kDa]
Δtom70/71
116
66
45
35
25
18
α-HA
α-Mrpl40
α-HA
D
surviving colonies [relative %]
100
10
1
0.1
0
5
10
15
20
Time [min]
WT
Δtom70/71
Δtom70/71 + mt-Tah1
E
Glucose
-His
-Ura
5'FOA-Leu
WT
Δsam37
Δsam37 + SAM37 (URA3)
Δsam37Δtom70 + SAM37 (URA3)
Δsam37Δtom70 + TOM70 (LEU2)
F
SAM37 mRNA [%]
100
75
50
25
0
WT
Δsam37Δtom70 +TOM70
G
wt + CRISPRi ev
Absorbance at 600 nm
0.8
0.6
0.4
0.2
0.0
w/o ATc
with ATc
0
20
40
60
80
Time [h]
H
+ CRISPRi TOM70
mock
TOM70↓
TOM70↓ + mt-Tah1
TOM70↓ + mt-Tah1-C2-C3
Δloa1
Δelo2
Δtim8
Δtim13
Absorbance at 600 nm
mt-Tah1-C2-C3
mt-Tah1
Time [h]
I
Genetic interactions with Tom70
sam37
tim8
tim13
Protein Import
Hsp70
Hsp90
EEVD
C1
C2
C3
loa1
elo2
Lipid Metabolism
J
Tom70
Δtom70/71
mt-Tah1
mt-Tah1 K8A
relative logFC
100
75
50
25
0
Oxa1
Pet9
Ugo1

Figure S4. Mitochondria-bound Tah1 can functionally replace Tom70 *in vivo*. Related to Figure 4. **A.** Δ*tom70/71* cells were transformed with a *pYX142* plasmid containing either the Tom70 full length sequence or only the C1 part of Tom70. Mitochondria were isolated from these strains and analyzed by western blotting. **B.** The sequences of the indicated domains of Tom70 were used for BLAST searches against the yeast proteome. Sequences with similarity to these regions are indicated. **C.** Left: The sequences corresponding to the different TPR-proteins were cloned into a pYX142 vector with Tom70 transmembrane domain (TMD). The plasmids were transformed into the Δ*tom70/71* strain. Whole cell lysates were prepared and constructs detected with an HA antibody. Right: Expression levels of the mt-Tah1 and mt-Tah1(K8A) are shown. Mrpl40 serves as a loading control. **D.** Yeast cells of the indicated strains were exposed to 55°C for the times indicated. Aliquots were removed after different times and surviving cells were quantified by plating. **E.** The shuffle strain used in Fig. 4D and its origin are shown. The Δ*sam37::HIS3* deletion strain was transformed with a *SAM37(URA3)* plasmid. In this background, the *TOM70* open reading frame (ORF) was replaced with a *NatNT2* cassette, yielding the shuffle strain. After successful shuffling of the *SAM37(URA3)* plasmid with a *TOM70* (*LEU2*) plasmid, the strain is able to grow on 5' fluoroorotic acid (5´FOA) plates. **F.** Due to the lack of a Sam37 antibody, the successful loss of *SAM37* was verified via qPCR. **G.** The BY4742 wild type was transformed with a CRISPRi empty plasmid. The growth of the strain with or without addition of 960 ng/µl ATc for was monitored for 72 h. **H.** Cells were transformed with the indicated plasmids. Cells were grown under conditions at which Tom70 had been knocked down by CRISPRi. **I.** Two types of genetic interactions of Tom70 can be distinguished. **J.** Proteomics data of the indicated proteins were analyzed as described for Figure 6B.

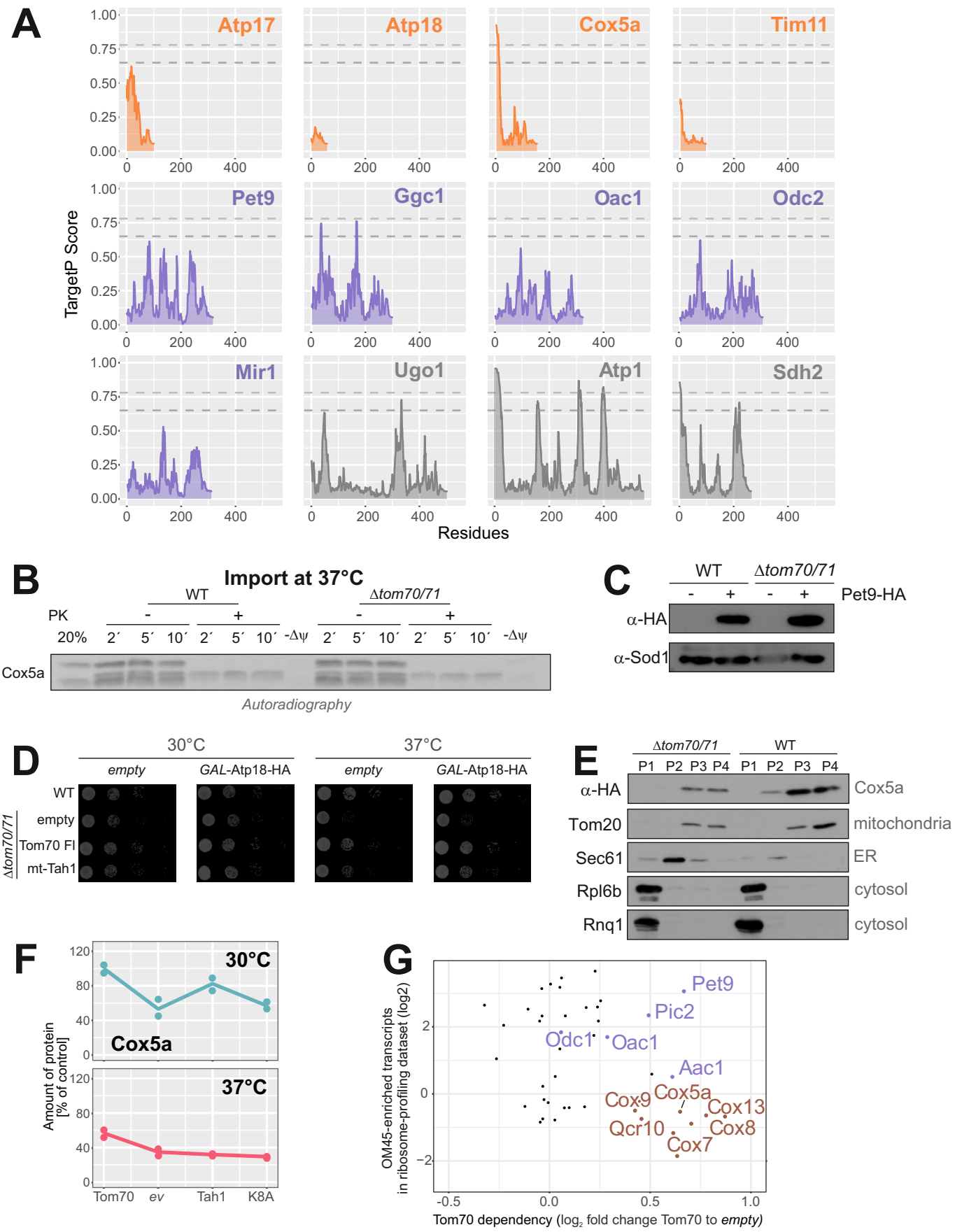
A
Atp17
Atp18
Cox5a
Tim11
Pet9
Ggc1
Oac1
Odc2
Mir1
Ugo1
Atp1
Sdh2
TargetP Score
Residues
B
Import at 37°C
WT
Δtom70/71
PK
20%
2´ 5´ 10´ 2´ 5´ 10´ -Δψ 2´ 5´ 10´ 2´ 5´ 10´ -Δψ
Cox5a
Autoradiography
C
WT
Δtom70/71
Pet9-HA
α-HA
α-Sod1
D
30°C
37°C
empty
GAL-Atp18-HA
WT
Δtom70/71
empty
Tom70 FI
mt-Tah1
E
Δtom70/71
WT
P1 P2 P3 P4 P1 P2 P3 P4
α-HA
Tom20
Sec61
Rpl6b
Rnq1
Cox5a
mitochondria
ER
cytosol
cytosol
F
30°C
Cox5a
37°C
Amount of protein [% of control]
Tom70
ev
Tah1
K8A
G
Pet9
Pic2
Odc1
Oac1
Aac1
Cox9
Cox5a
Cox13
Qcr10
Cox8
Cox7
OM45-enriched transcripts in ribosome-profiling dataset (log2)
Tom70 dependency (log2 fold change Tom70 to empty)

Figure S5. Overexpression of mitochondrial proteins can lead to proteotoxic effects. Related to Figure 7. **A.** Distribution of MTS and iMTS-L sequences in different mitochondrial proteins (Backes et al., 2019). **B.** Radiolabeled Cox5a was imported into isolated mitochondria at 37°C. See Fig. 7E for details. **C.** Western blot of wild type and Δ*tom70/71* cells transformed with empty (-) or *GAL1*-Pet9-HA (+) plasmids. Sod1 served as a loading control. **D.** The indicated strains were transformed with plasmids to express Atp18-HA under the control of *GAL1* promoter. All cultures were grown on lactate medium to mid-log phase, induced with 0.5% galactose for 4.5 h and dropped onto galactose plates. E. The Cox5a-expressing strains were grown for 4.5 h on galactose medium before cells were fractionated. Cytosolic proteins are present in the P1 fraction, ER proteins predominantly in P2 and mitochondrial proteins are found in low-speed pellets P3 and P4, which also contains the signal for Cox5a. **F.** Cox5a levels in the *Δtom70/71* cells expressing the indicated proteins were measured by mass spectrometry. **G**. The Tom70-dependence measured in our study by mass spectrometry was compared to the results of Williams et al. 2014 which revealed for each of these proteins whether they are synthesized in proximity to the mitochondrial outer membrane (high score) or on free ribosomes (low score). Carriers are shown in purple and small inner membrane proteins are shown in brown.

JCB Journal of Cell Biology

ARTICLE

The multi-factor modulated biogenesis of the mitochondrial multi-span protein Om14

Jialin Zhou[1], Martin Jung[2], Kai S. Dimmer[1], and Doron Rapaport[1]

The mitochondrial outer membrane (MOM) harbors proteins that traverse the membrane via several helical segments and are called multi-span proteins. To obtain new insights into the biogenesis of these proteins, we utilized yeast mitochondria and the multi-span protein Om14. Testing different truncation variants, we show that while only the full-length protein contains all the information that assures perfect targeting specificity, shorter variants are targeted to mitochondria with compromised fidelity. Employing a specific insertion assay and various deletion strains, we show that proteins exposed to the cytosol do not contribute significantly to the biogenesis process. We further demonstrate that Mim1 and Porin support optimal membrane integration of Om14 but none of them are absolutely required. Unfolding of newly synthesized Om14, its optimal hydrophobicity, and higher fluidity of the membrane enhanced the import capacity of Om14. Collectively, these findings suggest that MOM multi-span proteins follow different biogenesis pathways in which proteinaceous elements and membrane behavior contribute to a variable extent to the combined efficiency.

Introduction

Mitochondria are double-membrane organelles, which, according to the endosymbiotic hypothesis, descended from engulfed aerobic prokaryotes. As the main powerhouse of eukaryotic cells, mitochondria possess about 800 proteins in yeast and 1,500 in humans, of which 99% are encoded in the nucleus, synthesized by cytosolic ribosomes, and then directed to their specific mitochondrial sub-compartment (Neupert and Herrmann, 2007; Walther and Rapaport, 2009; Drwesh and Rapaport, 2020; Pfanner et al., 2019).

While the mitochondrial inner membrane sets a border between the intermembrane space and the matrix, the mitochondrial outer membrane (MOM) constitutes a barrier to separate the organelle from the rest of the cellular environment. Transmembrane proteins residing in the MOM play a critical role in many mitochondrial activities such as protein biogenesis, the formation of contact sites with other organelles, maintenance of mitochondrial morphology, as well as modulation of mitochondrial motility (Friedman et al., 2011; Hermann et al., 1998; Cohen et al., 2008; Sogo and Yaffe 1994). Dysfunction of these proteins may lead to failure in the aforementioned processes and even to severe human diseases such as neurodevelopmental disorders (Ghosh et al., 2019; Wei et al., 2020). Considering their importance, it is critical to understand the biogenesis of MOM proteins, including their targeting to the organelle, membrane integration, and final maturation into a stable and functional form.

In the past decades, some insights into targeting and integration of multi-span helical MOM proteins have been obtained (Becker et al., 2011; Sauerwald et al., 2015; Vögtle et al., 2015; Papić et al., 2011; Coonrod et al., 2007; Doan et al., 2020; Sinzel et al., 2017). The mitochondrial outer membrane receptor Tom70 has been found to support the targeting process by either directly recognizing the precursors of multi-span proteins or indirectly by serving as a docking site for chaperones that bind to and stabilize such newly synthesized proteins (Backes et al., 2021; Doan et al., 2020; Kreimendahl et al., 2020; Otera et al., 2007; Papić et al., 2011; Becker et al., 2011). In yeast, two additional MOM proteins, Mim1 and Mim2, are also involved in the biogenesis of multi-span proteins before and during their integration into the MOM (Becker et al., 2011; Papić et al., 2011; Dimmer et al., 2012). However, the exact role of Mim1/2 is yet to be elucidated as it was reported that newly synthesized Ugo1, a multi-span MOM protein, can be inserted in vitro into pure lipid vesicles in a process that was enhanced by elevated levels of phosphatidic acid within the lipid bilayers (Vögtle et al., 2015). Similarly unclear are the initial cytosolic steps in the biogenesis of such multi-span proteins as well as the targeting signals that assure their specific sorting to the organelle.

[1]Interfaculty Institute of Biochemistry, University of Tübingen, Tübingen, Germany; [2]Medical Biochemistry and Molecular Biology, Saarland University, Homburg, Germany.

Correspondence to Doron Rapaport: doron.rapaport@uni-tuebingen.de.

To shed light on these understudied processes, we decided to use the multi-span MOM protein Om14 as a model protein. Om14 is one of the most abundant MOM proteins and it contains three predicted α-helical transmembrane domains (TMDs), exposing the N-terminus toward the cytosol and the C-terminus toward the intermembrane space (Burri et al., 2006). The function of Om14 is not resolved yet. It was reported to form a complex with the MOM proteins VDAC (Porin in yeast) and Om45 and be involved in the import of metabolites (Lauffer et al., 2012). In addition, Om14 was suggested to function as a receptor for cytosolic ribosomes (Lesnik et al., 2014). Although it is still unclear whether the targeting of Om14 is promoted by the Tom70 receptor, an interaction of newly synthesized Om14 molecules and cytosolic chaperones such as Hsp70, Hsp90, and Hsp40 and cochaperones such as Ydj1 and Sis1 was reported (Jores et al., 2018). Similar to Ugo1, the biogenesis of Om14 has been suggested to be dependent on Mim1 (Becker et al., 2011). Additionally, the cardiolipin level in the mitochondria affects the biogenesis of Om14 (Sauerwald et al., 2015). Although some common factors such as Tom70 and the MIM complex seem to support the biogenesis of both Om14 and Ugo1, it is currently unclear what are the contributions of other features such as folding of the protein, its hydrophobicity, and the behavior of the lipid phase. It might well be that, similarly to the variety of pathways described for single-span proteins (Vitali et al., 2020), multi-span proteins follow rather individual routes.

To address these issues, we investigated cis and trans elements that might impact Om14 biogenesis. Our findings indicate that the targeting and membrane integration of Om14 involve cis elements such as hydrophobicity of the putative TMDs and an unfolded state as well as multiple trans factors, such as Tom70, Mim1, and Porin, together with the fluidity of the membrane. The comprehensive evaluation of the modulatory effects of all these factors provides a new concept for our understanding of the biogenesis of MOM proteins.

Results

Multiple targeting signals within Om14 collectively contribute to its mitochondrial location

As the initial step of our efforts to dissect the biogenesis pathway of Om14, we asked which parts of the molecule serve as a mitochondrial targeting signal. To address this question, we fused GFP to full-length OM14 or three segments including each one of the three putative TMDs of Om14 and its flanking regions (Fig. 1 A). To minimize interference from the GFP module, the fusion proteins were constructed according to a suggested topology model such that the GFP moiety does not have to cross the membrane (Burri et al., 2006). Next, we investigated whether one of the individual TMDs or a truncated protein containing two of them is sufficient for mitochondrial targeting. To this end, we examined the localization of these truncated variants by fluorescence microscopy (Fig. 1 B). As expected, the full-length Om14 showed a clear co-localization with mitochondrial-targeted RFP (Mito-RFP). While all the truncated constructs display clear mitochondrial signal, all three constructs with a single TMD displayed also some GFP stain in the cytosol (Fig. 1 B). This cytosolic signal can result, at least partially, from proteolytic cleavage of the OM14 portion and a cytosolic location of the remaining GFP moiety. We also observed a possible ER localization of the construct GFP–Om14(1-62) as indicated by the peri-nuclear fluorescent signal (Fig. 1 B, marked with an arrow).

To further study the intracellular location of the GFP-tagged fragments, we performed a subcellular fractionation procedure and analyzed the localization of the different constructs via immunodecoration with anti-GFP antibody (Fig. 1 C). In line with our fluorescence microscopic findings, the full-length Om14 was detected solely in the mitochondrial fraction, while all the truncated constructs were detected primarily in the mitochondrial fraction with a variable subpopulation mislocalized to the ER. In addition, a band slightly smaller than the intact GFP–Om14(1-62) construct, which is caused probably by cleavage of several amino acids at the C-terminus of this variant, was observed in the whole cell lysate and cytosol fractions but not in the mitochondrial one (Fig. 1 C). This indicates that amino acid residues at the C-terminus of this construct are important for mitochondrial targeting. In two cases (GFP–Om14(1-62) and GFP–Om14(96-134)), a clear band in the cytosolic fraction at the expected size of GFP alone could be detected (Fig. 1 C, asterisk). This observation supports our proposal that a major portion of the cytosolic GFP fluorescence signal might be related to degradation products.

The capacity of the single TMDs to associate with mitochondria was supported by in vitro import assays where radiolabeled constructs containing the single TMD were imported into isolated mitochondria (Fig. S1). Interestingly, this import was hardly dependent on the presence of Mim1, pointing to the possibility that a complete Om14 is required for optimal interaction with Mim1. The compromised organelle specificity in the targeting of the truncated constructs might be explained by the absence of a clear involvement of Mim1. Of note, a construct containing the first two TMDs (GFP–Om14(1-95)) was targeted to mitochondria to a higher extent as compared to the constructs harboring single TMDs (Fig. 1, B and C). We conclude that each one of the putative TMDs and its flanking region is sufficient for mitochondrial targeting, although with compromised specificity. An improved specificity is achieved with a protein fragment with two TMDs, but only the combination of all three segments in one protein assures the high mitochondrial specificity observed for native Om14.

Tom70 plays only a minor role in the biogenesis of Om14

Obtaining this insight on the mitochondrial targeting information, we next aimed to understand how these signals are recognized at the organelle surface. An obvious candidate to function as an import receptor for Om14 is Tom70, which was reported to contribute to the biogenesis of multi-span MOM proteins in both yeast and human cells (Papić et al., 2011; Becker et al., 2011; Otera et al., 2007). To investigate the involvement of Tom70 in the biogenesis of Om14, we first characterized the interaction interface between Tom70 and Om14 using a peptide scan blot assay. Peptides of 20 amino acid residues with a shift of 3 amino acids covering the whole sequence of Om14 were synthesized as spots on a cellulose membrane. This membrane was

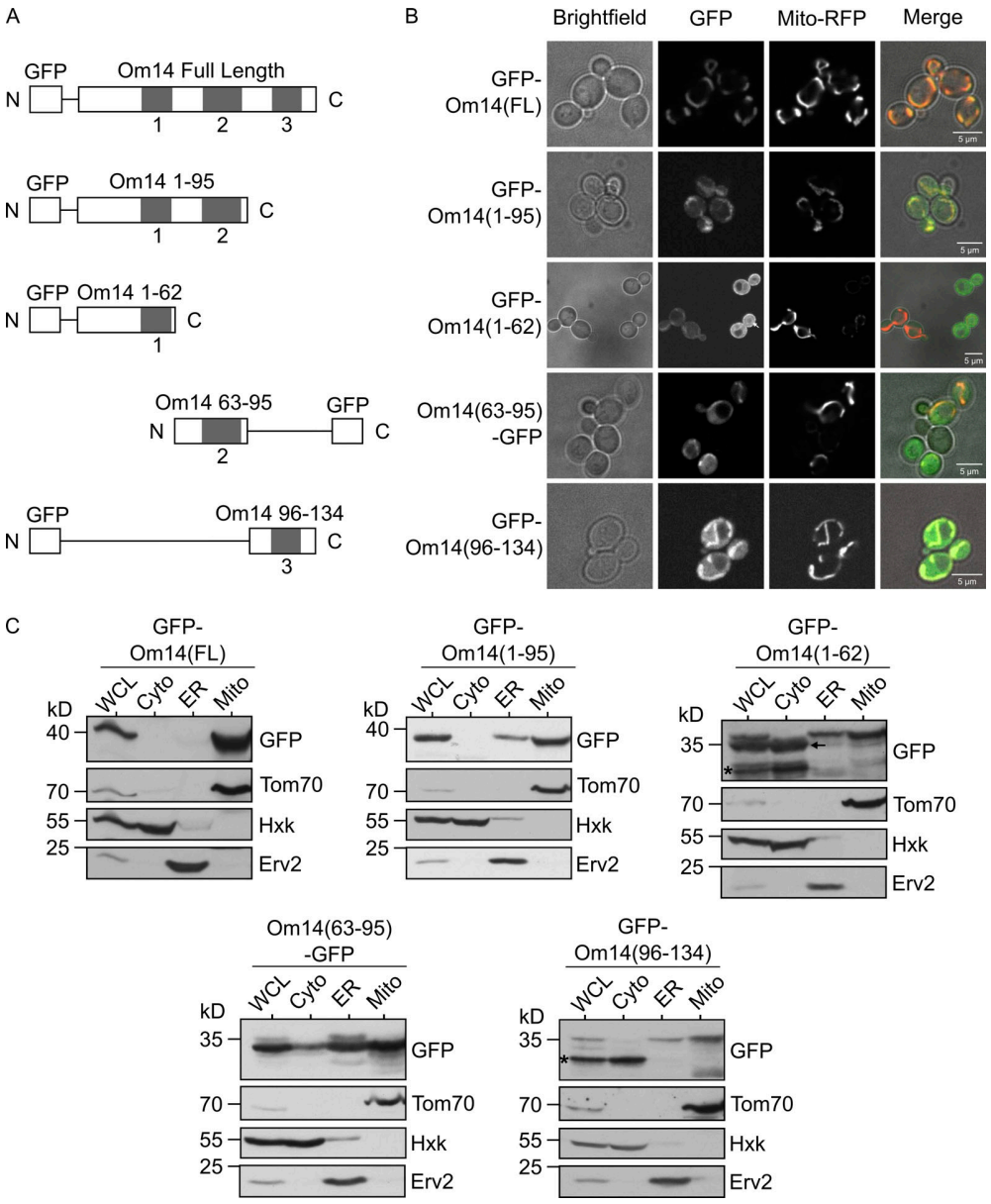

Figure 1. **Om14 harbors multiple mitochondrial targeting signals. (A)** Schematic representation of GFP fusion proteins of full-length Om14 and its truncated variants. **(B)** Localization of Om14 constructs as visualized by fluorescence microscopy. RFP targeted to mitochondria (Mito-RFP) was used as a marker for mitochondrial structures. **(C)** Cells expressing the various Om14 variants were subjected to sub-cellular fractionation. Fractions corresponding to whole cell lysate (WCL), cytosol (Cyto), microsomes (ER), and mitochondria (Mito) were analyzed by SDS–PAGE and immunodecoration with the indicated antibodies. Tom70, Hexokinase, and Erv2 were used as markers for mitochondria, cytosol, and microsomes, respectively. Asterisk marks the GFP moiety alone, whereas an arrow indicates a slightly processed form of GFP–Om14(1-62). Source data are available for this figure: SourceData F1.

incubated with GST-tagged cytosolic domain of Tom70 expressed recombinantly in *Escherichia coli* cells. We initially verified that GST alone does not bind in this assay (data not shown). Using GST-Tom70, we observed that the strongest interaction occurred to peptides representing the C-terminal region of Om14, whereas moderate binding was detected with peptides residing inside or close to the first two predicted TMDs of the protein (Fig. 2 A). These findings clearly indicate that Tom70 does not bind to only a single well-defined segment of Om14 and are in line with previously reported peptide scan of Tom70 and carrier substrate protein that also failed to detect a clear single Tom70-binding domain in this substrate (Brix et al., 1999).

To elaborate the physiological relevance of Tom70 for the biogenesis of Om14, we conducted an in vitro import assay in which newly synthesized radiolabeled Om14 was incubated with mitochondria isolated from either WT cells or from cells of a strain where *TOM70* and its paralog *TOM71* were deleted (*tom70/71Δ*). As a read-out for the correct membrane integration of Om14, we utilized the formation of a characteristic 13 kD fragment (F′) upon addition of external trypsin (Fig. S2 A; Burri

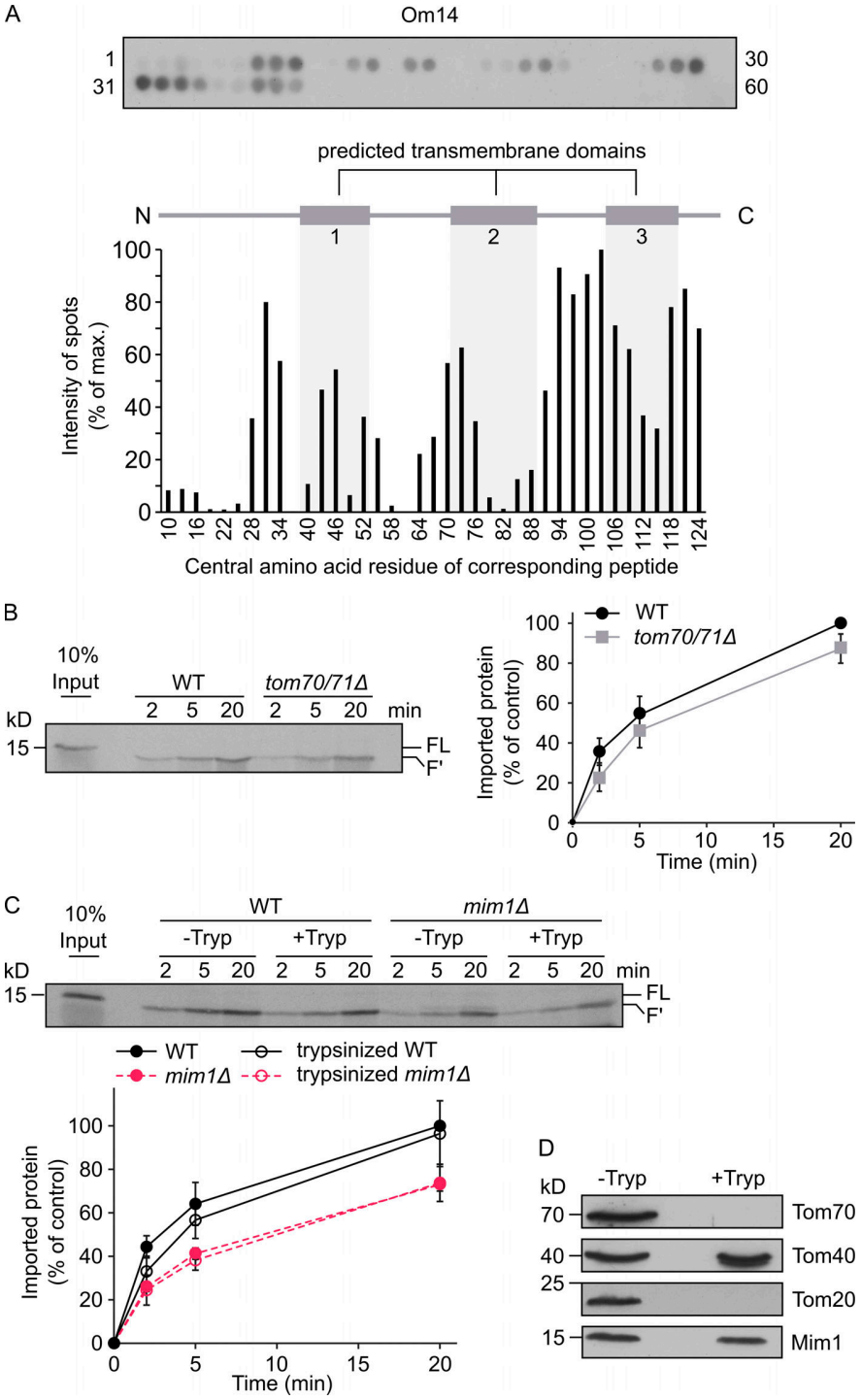

Figure 2. **Loss of Tom70 has a minor impact on the biogenesis of Om14. (A)** Nitrocellulose membrane containing 20-mer peptides covering the sequence of Om14 was incubated with the recombinant fusion protein GST-Tom70 (cytosolic domain). After incubation, the interaction was visualized by immunodecoration using an antibody against GST (top). The numbers flanking the panel reflect the serial numbers of the peptides. Bottom: The intensity of each dot was quantified and the average quantification of three independent experiments was plotted. The dot with the strongest intensity was set as 100%. The numbers on the x-axis reflect the central amino acid residue of each peptide. **(B)** Radiolabeled Om14 was imported into mitochondria isolated from either WT or *tom70/71Δ* cells. After import, samples were treated with trypsin and were further analyzed by SDS–PAGE and autoradiography. FL, full length input; F′, the trypsin-related proteolytic fragment of Om14. Right: The intensity of the trypsin-related fragment (F′) was quantified and the average intensity of three independent experiments is shown. The band representing import for 20 min into control organelles was set to 100%. Error bars represent ± SD. **(C)** Mitochondria isolated from either WT or *mim1Δ* cells were left intact (–Tryp) or were pre-treated with trypsin (+Tryp). Radiolabeled Om14 was then added to the isolated organelles for the indicated periods. After import, samples were again trypsinized and analyzed by SDS–PAGE and autoradiography. Bottom: Quantification of three independent experiments was performed as described in B. Error bars represent ± SD. **(D)** Mitochondria isolated from WT cells were either left intact or treated with trypsin. Both samples were analyzed by SDS–PAGE and immunodecoration using the indicated antibodies. Source data are available for this figure: SourceData F2.

et al., 2006). As is common for many mitochondrial precursor proteins, the overall efficiency of import into control organelles, in terms of imported fraction out of the added radiolabeled protein, was in the range of 2 to 15% (Fig. 2 B). We observed a reduction of ∼10 to 15% in the integration capacity of Om14 into organelles lacking both Tom70 and Tom71 (Fig. 2 B). We therefore conclude that while Tom70/71 contributes to the biogenesis of Om14, a large portion of newly synthesized Om14 molecules can be integrated into the MOM also in the absence of Tom70/71.

To study whether the involvement of Tom70 is evolutionarily conserved, we performed the same import assay using mitochondria isolated from human cells depleted of TOM70. Interestingly, although no homolog of Om14 was found in the human genome, Om14 was still able to be inserted into mammalian organelles in a correct topology (Fig. S2 B). Compared to yeast mitochondria, Om14 showed a slightly higher dependence on Tom70 in human mitochondria as reflected by a 30% import reduction upon knocking down TOM70 (Fig. S2 B). Thus, in

agreement with a previous report on the importance of TOM70 for the biogenesis of mammalian multi-span MOM proteins (Otera et al., 2007), Om14 can be integrated into mammalian MOM in a TOM70-dependent manner.

The rather minor import reduction of Om14 in the absence of Tom70/71 might suggest that other cytosol-exposed proteins such as Tom20 can take over the receptor function in the absence of Tom70/71. To abolish simultaneously the receptor function of Tom20 and Tom70, we pre-treated isolated mitochondria with trypsin before the import reaction. Although this treatment completely removed the cytosolic domains of both receptors (Fig. 2 D), we observed only a minor reduction in Om14 import into mitochondria treated in this way (Fig. 2 C). Hence, it appears that both Tom70 and Tom20, or any other MOM proteins exposed to the cytosol, play only a subordinate role in the biogenesis of Om14. These findings are in sharp contrast to the behavior of other types of mitochondrial precursor proteins. Tryptic removal of exposed receptors resulted in a dramatic decrease of 70–95% in the import efficiency of presequence-containing or β-barrel precursor proteins (Pfaller et al., 1989). Of note, Mim1 was not affected by the addition of trypsin (Fig. 2 D). Hence, we next wanted to investigate the involvement of Mim1 in the membrane integration of Om14. In line with a previous publication (Becker et al., 2011), the import of Om14 into *mim1Δ* mitochondria was significantly impaired (Fig. 2 D). However, even in the absence of Mim1, the removal of exposed proteins by pre-treatment with trypsin did not cause further reduction in the import capacity of these mitochondria (Fig. 2 D). Hence, it seems that the general import receptors Tom20 and Tom70/71 do not contribute to the remaining 60% import capacity in the absence of Mim1.

Next, we asked whether the cytosolic domain of Mim1 might function as a receptor for Om14 substrate molecules. To that end, we introduced into *mim1Δ* cells plasmid-encoded constructs representing either native Mim1 or a variant lacking the putative cytosol-exposed region and harboring only the central TMD of Mim1 (residues 35–75, Mim1-TMD). We previously demonstrated that over-expression of this variant can rescue the growth phenotype in the absence of native Mim1 (Popov-Čeleketić et al., 2008). Importantly, the presence of this truncated construct could rescue the steady-state levels of known MIM1 substrates, including Om14, to the same extent as native Mim1 (Fig. S3 A). Furthermore, organelles harboring this variant could facilitate the assembly of newly synthesized Om14 molecules as good as native Mim1 (Fig. S3 B). Collectively, these results demonstrate that Tom70, Tom20, or the cytosolic region of Mim1 do not play a decisive role in the biogenesis of Om14.

Hydrophobicity of the second TMD influences the membrane integration capacity of Om14

Whereas the membrane integration of Om14 is promoted by Mim1, we wondered whether we could identify cis-elements that affect this process. Thus, we had a closer look at the hydrophobicity of the three putative TMDs. Using the Wimley and White Hydrophobicity Scale (Wimley and White, 1996), we noticed that the first TMD of Om14 displays the lowest hydrophobicity (1.0), whereas the other two TMDs have a similar value of 1.5. To determine how the hydrophobicity of TMDs affects the biogenesis of Om14, we analyzed the membrane integration capacity of two constructs that exhibit either an increased hydrophobicity of the first TMD (Om14-3I) or a decreased hydrophobicity of the second TMD (Om14-4A; Figs. S4 A and 3 A, respectively). Om14-3I showed a similar topology and membrane integration capacity as the native protein (Fig. S4 B), suggesting that the hydrophobicity of the first TMD does not affect the overall biogenesis of the protein. In contrast, replacing four hydrophobic residues of TMD2 by alanine, as in Om14-4A, caused a dramatic reduction in both the steady-state levels and the integration capacity of the protein (Fig. 3, B and C). Notably, although Om14 contains three putative transmembrane segments, previous reports and our current experiments find a subpopulation of Om14 in the supernatant fraction (Fig. 3 B; Burri et al., 2006; Sauerwald et al., 2015). Approximately 70% of the OM14-4A molecules, as compared to ∼30% of the native protein, were found in the supernatant fraction. This altered membrane integration points to the possibility that the mutated variant is less stable and accordingly, the reduced steady-state levels might result from enhanced turn-over.

To address the question which stage of Om14-4A biogenesis was compromised and whether the obstruction was Mim1-dependent, we imported in vitro radiolabeled Om14-4A into organelles isolated from either control or *mim1Δ* cells. As revealed in Fig. 3 D, the in vitro import efficiency of Om14-4A was largely compromised compared to native Om14. The import of Om14-4A was further impaired in the absence of Mim1, suggesting that the loss of integration capacity was probably not triggered by a reduced interaction of the variant with Mim1. Taken together, these results support the assumption that reduced hydrophobicity of TMD2 of Om14 interferes with MIM complex–independent membrane integration steps.

Unfolding and elevated temperature strongly accelerate the import of Om14

Our results so far indicate that the complete length of the protein is required for optimal biogenesis of Om14. This led us to ask whether partial folding events are required to support the import of Om14. To address this point, we denatured in vitro translated Om14 using 6 M urea before the import reaction. Interestingly, this treatment enhanced fourfold the import capacity into control organelles (Fig. 4 A). Of note, such an increase was observed also upon import into mitochondria lacking Mim1 (Fig. 4 A), suggesting that the enhanced capacity upon unfolding is not related to a better interaction of the unfolded substrates with the MIM complex. These observations suggest that optimal biogenesis of Om14 is favored by its unfolding in the initial stages arguing against the requirement of a tertiary structural targeting signal.

Considering that many of the effects that we detected so far do not necessarily depend on a proteinaceous element, we wondered whether increasing the fluidity of the membrane by elevated temperature can also improve the biogenesis of Om14. To test this issue, we performed the in vitro import reaction while incubating the isolated organelles at either 25°C or 37°C. Importantly, we observed an increased import efficiency of

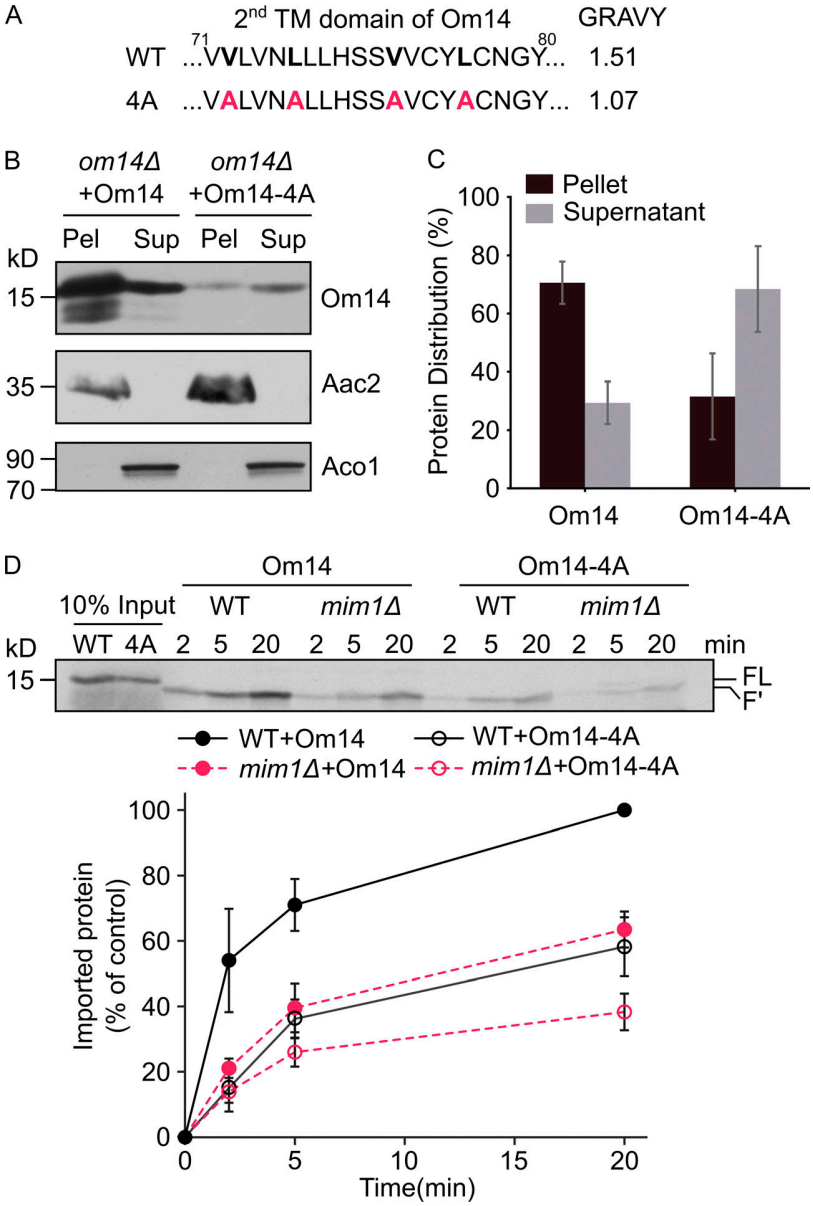

Figure 3. **Reduced hydrophobicity of TMD2 compromises the import capacity of Om14. (A)** Amino acid sequence of the putative second TMD of both native Om14 (WT) and a variant with reduced hydrophobicity due to the introduction of four Ala residues (4A). Mutated residues are shown in bold. **(B)** Mitochondria isolated from *om14Δ* yeast strains expressing either native Om14 or Om14-4A were subjected to alkaline extraction. Pellet (P) and supernatant (S) fractions were analyzed by SDS–PAGE and immunodecoration with antibodies against the indicated proteins. ATP–ADP carrier (Aac2) is embedded in the mitochondrial inner membrane, whereas aconitase (Aco1) is a matrix-soluble protein. **(C)** Quantification of at least three independent experiments as in B. The combined intensity of Om14 in the pellet and supernatant fractions from each strain was set to 100%. Error bars represent ± SD. **(D)** Radiolabeled versions of Om14 and its Om14-4A variant were imported into mitochondria isolated from either WT or *mim1Δ* cells. At the end of the import reactions, mitochondria were treated with trypsin and further analysis and quantification were as described in the legend to Fig. 2 B. Bottom: Quantification of three independent experiments is presented. The intensity of the band corresponding to the import of native Om14 into control organelles for 20 min was set to 100%. Error bars represent ± SD. Source data are available for this figure: SourceData F3.

Om14 after incubation at 37°C (Fig. 4 B). To test whether this behavior is shared by other proteins, we also imported in vitro other MOM proteins such as Ugo1 or Porin under the same conditions. As shown in Fig. 4, C and D, the elevated temperature increased the import efficiency of Ugo1, although only after 20 min. In contrast, the elevated temperature resulted in a reduced import of the β-barrel protein Porin. Taken together, although it seems that increased fluidity of the membrane supports enhanced membrane integration of Om14, we cannot exclude the possibility that the beneficial effect of the higher temperature is also partially due to enhanced unfolding of the Om14 substrate.

Porin and Om45 regulate different stages in the biogenesis of Om14

The aforementioned findings imply that mitochondria lacking Mim1, Tom20, and Tom70 can still maintain more than half of their capacity to import Om14. Hence, it seems that additional proteins might be involved in this process. As interaction partners of Om14, Porin and Om45 might be such mediators. It was previously reported that the steady-state level of Om14 was not notably affected in *om45Δ* mitochondria, whereas deletion of Porin resulted in a reduction in Om14 levels (Lauffer et al., 2012). To better understand the dependence of Om14 on Porin and Om45, we isolated mitochondria from WT and cells lacking either Porin or Om45 and separated peripheral protein from integral protein by alkaline extraction. We observed a drastic increase of Om14 in the supernatant fraction of *om45Δ* cells, whereas the absence of Porin did not affect the behavior of Om14 (Fig. 5, A and B). These findings indicate an altered membrane association of Om14 upon the loss of Om45. Furthermore, the absence of Om45 also caused a significant shift in the migration of Om14-containing oligomeric structures as observed by blue

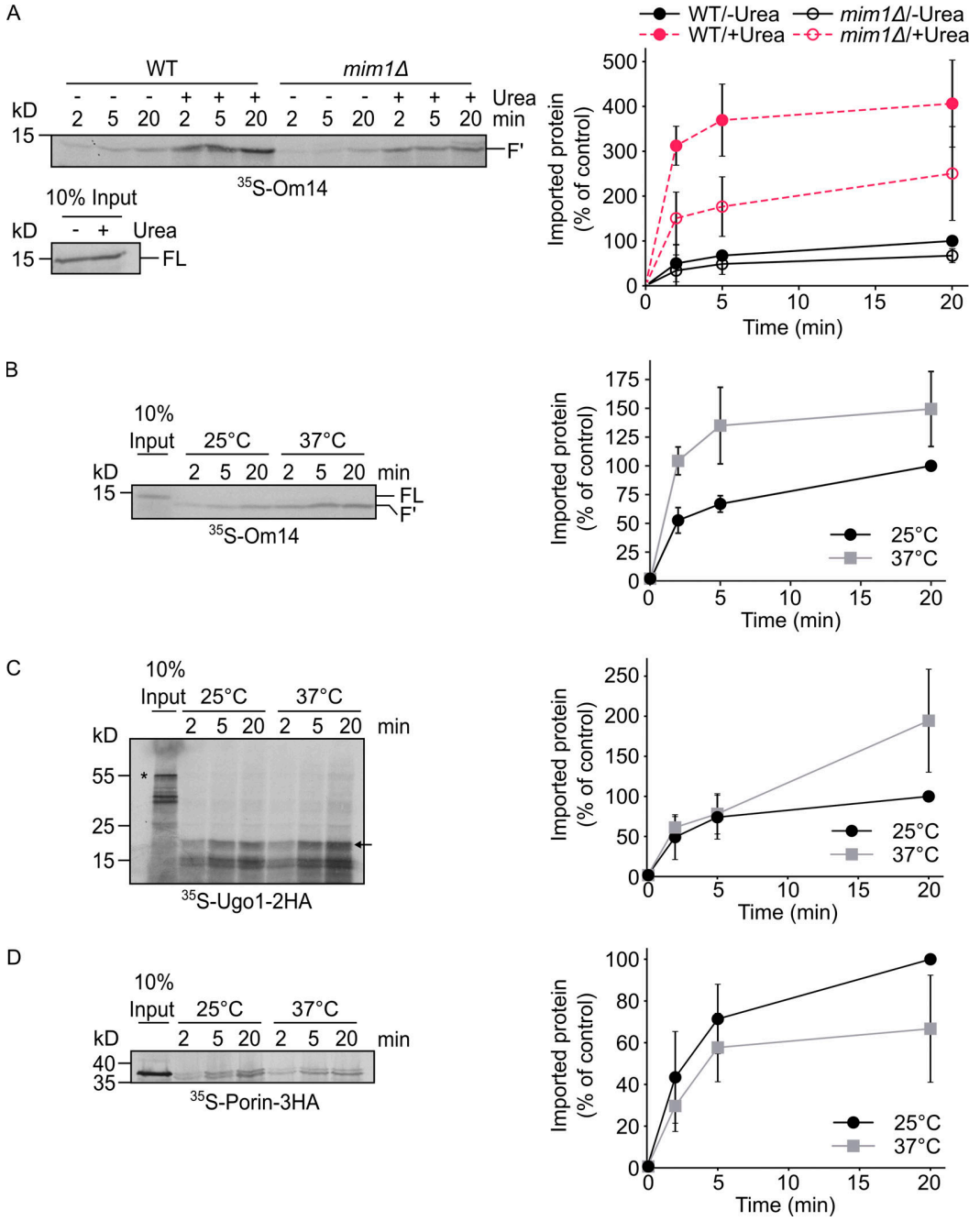

Figure 4. **Unfolding and elevated temperature facilitate the import of Om14. (A)** Radiolabeled Om14 was either denatured in 6 M urea or left untreated before its import into mitochondria isolated from either WT or *mim1Δ* strains. After the import, mitochondria were treated with trypsin, and further analysis and quantification were done as described in the legend to Fig. 2 B. Right: Quantification of three independent experiments is presented. The intensity of the band corresponding to the import of native Om14 into control organelles for 20 min was set to 100%. Error bars represent ± SD. **(B–D)** Radiolabeled Om14 (B), Ugo1-2HA (C), or Porin-3HA (D) were imported at either 25°C or 37°C into mitochondria isolated from WT cells. At the end of the import reactions, mitochondria were treated with either trypsin (B, C) or PK (D) and further analyzed by SDS–PAGE and autoradiography. Right: Quantification of the typical proteolytic fragments of Om14 (B) or Ugo1 (C) as well as the PK-protected correctly inserted Porin (D) of three independent experiments are shown. The intensity of the band corresponding to import for 20 min at 25°C was set to 100%. Error bars represent ± SD. Source data are available for this figure: SourceData F4.

native (BN)-PAGE (Fig. 5 C). As a further approach, we imported in vitro radiolabeled Om14 into mitochondria isolated from WT, *om45Δ*, or *por1Δ* strains and analyzed membrane integration of Om14 with the trypsinization assay. The import efficiency of Om14 dropped by ∼20% or 30% in mitochondria lacking either Om45 or Porin, respectively (Fig. 5 D). These findings indicated that both Porin and Om45 contribute to the membrane integration of Om14, whereas Om45 seems to play

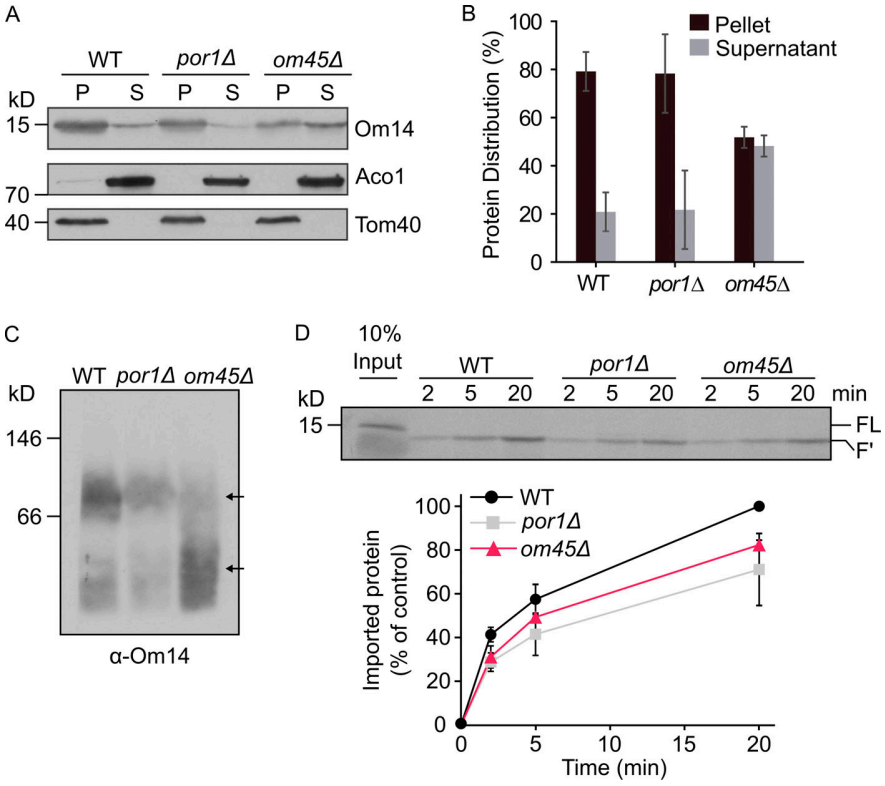

Figure 5. **Om45 regulates the stability of Om14 oligomeric structures. (A)** Mitochondria isolated from the indicated cells were subjected to alkaline extraction. Pellet (P) and supernatant (S) fractions were analyzed by SDS–PAGE and immunodecoration with the indicated antibodies. Aconitase (Aco1) serves as a marker for soluble matrix proteins, whereas Tom40 is embedded in the mitochondrial outer membrane. **(B)** Quantification of three independent experiments as in A. The combined intensity of Om14 in the pellet and supernatant fractions from each cell type was set to 100%. Error bars represent ± SD. **(C)** Mitochondria isolated from WT, *por1Δ*, or *om45Δ* cells were lysed using digitonin and analyzed by BN–PAGE. The blot was immunodecorated with an antibody against Om14. Arrows indicate the migration of oligomeric species of Om14. **(D)** Radiolabeled Om14 was imported into mitochondria isolated from WT, *por1Δ*, or *om45Δ* cells. At the end of the import reactions, mitochondria were treated with trypsin and analyzed by SDS–PAGE and autoradiography. Bottom: The intensity of the proteolytic fragment (F′) in three independent experiments was quantified as described in the legend to Fig. 1 B. The intensity of the band corresponding to import into control organelles for 20 min was set to 100%. Error bars represent ± SD. Source data are available for this figure: SourceData F5.

a more important role in the downstream stages of complex assembly.

Since a similar import reduction was observed in the absence of either Mim1 or Porin (compared Fig. 2 C to Fig. 5 D), we speculated that Mim1 and Porin might compensate for the loss of each other in mediating the early biogenesis of Om14. To test this possibility, we generated a *por1Δmim1Δ* double deletion mutant and analyzed the steady-state level of Om14 in these cells. We observed that the level of Om14 in the double deletion mutant was drastically reduced while the reduction fits the additive effect of the single deletions (Fig. 6, A and B). Importantly, the steady-state levels of other MIM substrates such as Tom70 and Tom20 were reduced upon the deletion of Mim1 but were not significantly further reduced upon the co-deletion of Porin (Fig. 6, A and B). This observation illustrates the specificity in the contribution of Porin to the biogenesis of Om14.

To further test whether the reduction in the steady-state levels of Om14 in *por1Δmim1Δ* cells resulted from downstream effects such as inefficient assembly or instability of integrated Om14, we imported in vitro radiolabeled Om14 into organelles isolated from *por1Δ*, *mim1Δ*, or *por1Δmim1Δ* cells. Compared to the impairment of import efficiency in the single *por1Δ* or *mim1Δ* deletions, no further reduction in the import capacity was detected upon the double deletion (Fig. 6 C). Finally, we tested whether the absence of both Mim1 and Porin would influence the membrane integration of Om14. To that goal, we monitored the portion of Om14 molecules in the supernatant fraction of alkaline extraction and found that, although the steady-state levels of Om14 were dramatically reduced, the extracted fraction was not increased in the double deletion strain (Fig. 6 D). These results suggest that Mim1 and Porin are separately involved in mediating the early biogenesis steps of Om14 but, in contrast to Om45, both proteins do not contribute to the stability of Om14 within the membrane.

Discussion

In the current study, we dissected the biogenesis pathways of the MOM multi-span protein Om14. Initially, we asked which segment(s) provide the mitochondrial targeting information within this protein. It is known that mitochondrial targeting of such proteins is not mediated by a canonical N-terminal presequence but rather by elements that are part of the mature form of the protein. However, the exact signals of such proteins were not resolved yet. We observed that truncated variants are targeted to mitochondria but in addition also to extra-mitochondrial locations. In this context, it is interesting that the removal of only several amino acid residues at the C-terminal flanking region of the first TMD was sufficient to compromise the mitochondrial targeting of this construct. Collectively, these results strongly support a model in which only the additive contribution of several local signals assure specific mitochondrial targeting. Currently, it is still unclear which factors decode this information.

A clear candidate for such a function was the import receptor Tom70, which appears to have a dual function: it can recognize internal mitochondrial signals (Brix et al., 1999; Papić et al., 2011), and it serves as a docking site for cytosolic (co)

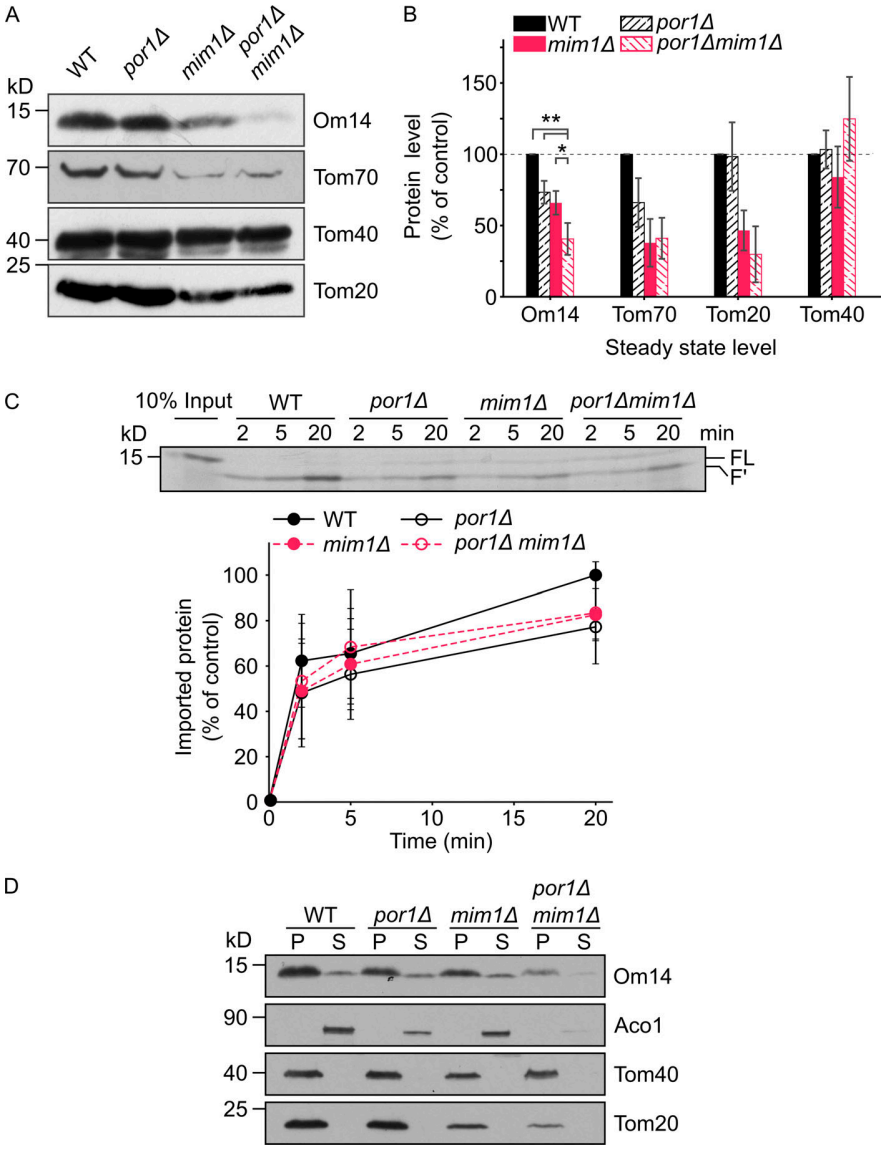

Figure 6. **Both Mim1 and Porin contribute to the biogenesis of Om14. (A)** Mitochondria isolated from WT, *por1Δ*, *mim1Δ*, or *por1Δmim1Δ* cells were analyzed by SDS–PAGE and immunodecoration with antibodies against the indicated proteins. **(B)** The steady-state levels of the proteins analyzed in A were quantified and the levels in the WT cells were set to 100%. Error bars represent ±SD. $n > 3$; *, $P \le 0.05$; **, $P \le 0.01$. **(C)** Radiolabeled Om14 was imported into mitochondria isolated from the cells described in A. At the end of the import reactions, mitochondria were treated with trypsin and the import reactions were further analyzed and quantified as described in the legend to Fig. 2 B. Bottom: Quantification of three independent experiments is presented. The intensity of the band corresponding to import into control organelles for 20 min was set to 100%. Error bars represent ± SD. **(D)** Mitochondria as in A were subjected to alkaline extraction. Pellet (P) and supernatant (S) fractions were analyzed by SDS–PAGE and immunodecoration using the indicated antibodies. Aconitase (Aco1) serves as a marker for soluble matrix proteins, whereas Tom40 and Tom20 are embedded in the mitochondrial outer membrane. Source data are available for this figure: SourceData F6.

chaperones on the mitochondrial surface (Young et al., 2003; Opaliński et al., 2018; Backes et al., 2021). Once Om14 is synthesized in the cytosol, co-chaperones of the Hsp40 family together with Hsp70 chaperones associate with it (Jores et al., 2018). Although the precise physiological relevance of this association was not studied yet, one can speculate that the (co) chaperones shield the hydrophobic segments and help to avoid misfolding and/or premature aggregation in the cytosol. The reported association of Om14 with cytosolic chaperones can explain, at least partially, the reported contribution of Tom70 for the biogenesis of such proteins (Becker et al., 2011; Papić et al., 2011).

Indeed, deletion of *TOM70* in yeast or knock-down of the protein in mammalian cells was found in the current study and was reported before to cause a reduction in the import of MOM multi-span proteins (Brix et al., 1999; Papić et al., 2011; Becker et al., 2011; Otera et al., 2007; Wan et al., 2016). However, the absence of Tom70 results often, including the current study, in only a moderate decrease in the import efficiency of these substrates. Such a variable dependency on Tom70 might be related to the different associations of substrates with cytosolic chaperones and/or to the capacity of the substrates to use alternative routes. In addition, in the case of Om14, which is a very abundant protein (Morgenstern et al., 2017), one can speculate that its minor dependence on Tom70 might be a mechanism to avoid a situation where a large portion of Tom70 molecules is busy processing Om14 while leaving a limited capacity for other substrates.

The mild effect of the absence of Tom70/71 suggests the existence of alternative pathways. Interestingly, Om14 showed a higher Tom70 dependence in human cells, maybe because it is not a natural substrate of these cells and thus is not an optimal substrate of alternative pathways. Considering that the current model proposes that Tom70 relays the substrate proteins toward the insertase, the MIM complex (Fig. 7, pathway I), alternative routes might include direct recognition of substrates by the MIM

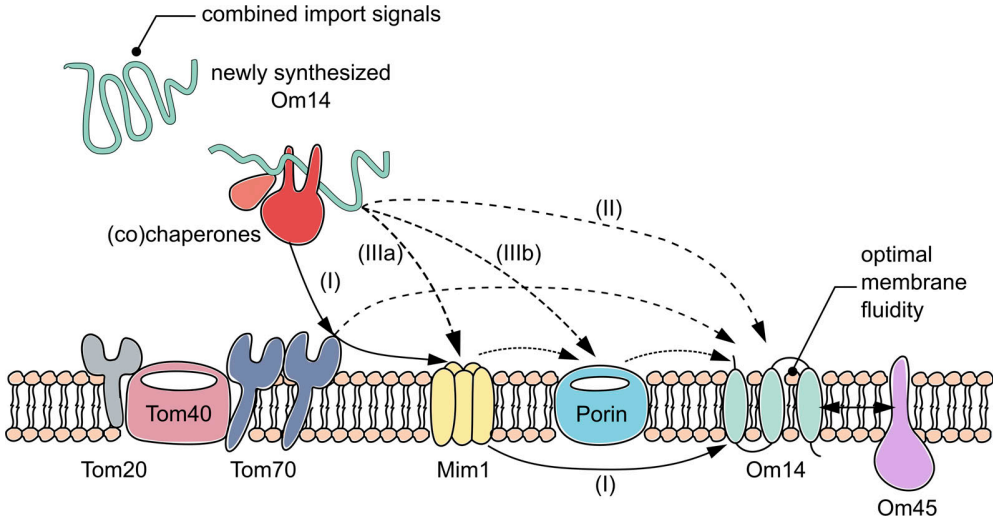

Figure 7. **Various potential routes for the biogenesis of Om14.** Newly synthesized molecules of Om14 can follow different pathways on their way to be integrated into the MOM. Pathway (I): The Om14 precursor is recognized by Tom70 and then relayed to the MIM insertase, which integrates it into the MOM; Pathway (II): The newly synthesized protein is integrated into the MOM in an unassisted process; Pathways (IIIa and IIIb): Om14 is not recognized by Tom70 but rather interacts directly with MIM (IIIa), Porin (IIIb), or both. All these options can be combined with an early association of Om14 with cytosolic (co)chaperones. See the Discussion section for more details.

complex (Fig. 7, pathway IIIa). However, our previous observation that the central TMD of Mim1, which lacks the putative cytosolic part of Mim1, can compensate for the growth phenotype in the absence of the native protein (Popov-Čeleketić et al., 2008) and our current observation that this domain supports normal levels of MIM substrates argue against a receptor-like function of Mim1.

A further additional option is a direct recognition of Om14 substrate by Porin (Fig. 7, pathway IIIb), as our findings indicate a clear contribution of Porin to the correct membrane integration of Om14. However, Porin exposes only short loops toward the cytosol, and therefore its function as a receptor is questionable. Hence, it seems that Porin promotes the correct membrane integration of Om14 but does not function as an initial receptor for the recognition of substrate molecules. This membrane-integration promoting function of Porin is yet another example of its multi-functionality in the biogenesis of other proteins. Recently, Porin was suggested to contribute to the assembly of the TOM complex by interacting with Tom22 (Sakaue et al., 2019) and to the import of carrier-like proteins to the mitochondrial inner membrane (Ellenrieder et al., 2019). The mechanism by which Porin can promote the membrane integration of Om14 should be the topic of future studies.

Importantly, even in the combined absence of both Mim1 and Porin, we observed that a substantial portion of the Om14 molecules could still be properly integrated both in vitro and in vivo into the MOM. Hence it seems that either a yet unknown protein mediates this integration in the absence of these two proteins, or as suggested before by Vögtle et al. (2015), such multi-span proteins can be assembled into the membrane in an unassisted manner (Fig. 7, pathway II). Our findings that unfolding of Om14 or maintaining the hydrophobicity of its second TMD are important for the membrane integration of the protein support such direct substrate–lipids crosstalk. Further support for the importance of the membrane behavior is the increased membrane integration of Om14 at elevated temperatures. As elevated temperature is known to enhance membrane fluidity (Kolodziej and Zammit, 1990), it is tempting to speculate that lowering the stiffness of the membrane increases the capacity of the hydrophobic segments of Om14 to integrate into the membrane. This suggestion is also in line with the previous observations of Vögtle et al. (2015) where the anionic phospholipid phosphatidic acid (PA), which is also known to induce curvature in membranes, supported membrane integration of the multi-span protein Ugo1. Further support for the increased dependency of Om14 integration on the membrane properties rather than on other proteinaceous factors is coming from the comparison to the reduced membrane integration of Porin at a higher temperature. The reduced import of this β-barrel protein reflects most likely its high dependency on the activity of multiple proteinaceous machineries such as the TOM and TOB/SAM complexes.

Regardless of the precise route for the membrane integration of Om14, it appears that once the protein is embedded in the membrane, its interaction partner Om45 mediates its final maturation. The absence of Om45 resulted in an enhanced fraction of Om14 molecules that can be extracted from the membrane as well as an alteration in the oligomeric structures of Om14. Since in addition to Om45, also the hydrophobicity of the second TMD of Om14 appears to be important for its stable membrane integration, it might be that the second TMD of Om14 interacts with the putative N-terminal TMD of Om45.

Collectively, our findings provide a novel insight into the diversity of parameters affecting the biogenesis of a multi-span mitochondrial outer membrane protein. They reveal that rather than a single determinative factor, the import of Om14 is

modulated by various membrane proteins and their structural properties. Considering the outcome of a previous study suggesting the existence of multiple pathways regulating the biogenesis of MOM single-span proteins (Vitali et al., 2020), it seems that all the helical MOM proteins are integrated into the membrane in a process that is affected by cis elements in the substrate protein itself, a combination of trans proteinaceous elements, and the behavior of the membrane.

Materials and methods

Yeast strains and growth conditions

The *Saccharomyces cerevisiae* strains used in this study are listed in Table S1. The *por1Δmim1Δ* strain was created by mating the single deletion strains and then performing tetrad dissection. Yeast cells were grown at 30°C on selective media containing 2% of either galactose or lactate.

Recombinant DNA techniques

Primers containing different restriction sites were designed to amplify by PCR segments encoding different regions of Om14. The plasmid pGEM4-Om14 was used as a template. The PCR products were subcloned into either the plasmid pGEM4 for in vitro protein translation or into the yeast expression vector pYX142-eGFP to study the in vivo behavior. The site-directed mutagenesis within Om14 was generated by using a pair of primers that contain a mutated sequence of Om14 using pGEM4–Om14 as a template. The PCR products were digested using DpnI before being transformed into *E. coli* cells for further selection. Full lists of all primers and plasmids used in this study are found in Tables S2 and S3, respectively.

Mitochondria isolation from yeast cells

Isolation of yeast mitochondria was performed by differential centrifugation following a previously published protocol (Daum et al., 1982). Yeast cells were grown in 2–4 liters of media at 30°C and were harvested at OD600 of 0.8–2.0 (3,000 x*g*, 5 min, RT). The cell pellets were washed with H_2O and resuspended in suspension buffer (100 mM Tris and 10 mM DTT). Suspensions were prepared by centrifugation after 10 min incubation (30°C) and cell pellets were washed with spheroblasting buffer (1.2 M sorbitol and 20 mM potassium phosphate, pH 7.2). Then, the cells were incubated with zymolyase-containing spheroblasting buffer (60 min, 120 rpm, 30°C). Spheroblasts were harvested (1,100 x*g*, 5 min, 2°C) and resuspended in homogenization buffer (0.6 M sorbitol, 1 mM EDTA, 1 mM PMSF, 0.2% [w/v] fatty acid-free BSA, and 10 mM Tris, pH 7.4). Spheroblasts were then opened by 12 times douncing on ice. The dounced solution was clarified (2,000 x*g*, 5 min, 2°C) and underwent a high-speed centrifugation (17,500 x*g*, 15 min, 2°C). Pellets were washed with SEM buffer (250 mM sucrose, 10 mM MOPS/KOH, and 1 mM EDTA, pH 7.2) and again centrifuged (17,500 x*g*, 15 min, 2°C). The pure mitochondrial pellets were resuspended in SEM buffer containing 2 mM PMSF and snap-frozen in liquid nitrogen before their storage at −80°C.

Mitochondria isolation from mammalian cells

The mammalian HeLa cell line, which was used in this study, was a gift from Dr. Vera Kozjak-Pavlovic, and doxycycline was used to induce knock-down of TOM70 as described previously (Kozjak-Pavlovic et al., 2007). For isolation of mammalian mitochondria, cells were washed once with PBS buffer and collected from the 150 mm tissue culture-treated dish using a spatula. The collected cells were transferred to a test tube and were centrifuged (300 x*g*, 5 min, 4°C). Afterwards, the cell pellet was resuspended in HMS buffer (0.22 M Mannitol, 0.02 M Hepes-KOH, pH 7.6, 1 mM EDTA, 0.07 M Sucrose, 0.1% BSA, and 1 mM PMSF). The cells were then lysed nine times through each of the three different needles used (20G, 23G, and 27G; Sterican). After homogenization, samples were centrifuged (900 x*g*, 5 min, 4°C) and the supernatant was centrifuged (9,000 x*g*, 15 min, 4°C). The pellet of the latter centrifugation step was washed with HMS buffer and re-isolated (10,000 x*g*, 15 min, 4°C). The pellet from the last centrifugation step represents the crude mitochondria and was used for further in vitro import experiments.

In vitro protein import into mitochondria

Proteins encoded in pGEM4 plasmid were transcribed in vitro by SP6 polymerase. The acquired mRNA was then translated in rabbit reticulocyte lysates (Promega) containing ^{35}S-labelled Met and Cys. After translation, ribosomes were removed (94,000 x*g*, 45 min, 4°C) and discarded. For an import reaction, mitochondria were diluted to a concentration of 1 µg/µl with F5 import buffer (250 mM sucrose, 0.25 mg/ml BSA, 80 mM KCl, 10 mM MOPS-KOH, 5 mM $MgCl_2$, 8 mM ATP, and 4 mM NADH, pH 7.2). In a standard import reaction, 10% (v/v) of translated protein was added to 50 µl of mitochondria solution and incubated at 25°C for 2, 5, or 20 min. In some experiments, mitochondria were incubated at 37°C in total for 20 min (before and during the import reaction). The import reactions were stopped by adding 400 µl of SEM-K^{80} buffer followed by a 10 min centrifugation (13,200 x*g*, 2°C). For further proteolytic assay, import reactions were treated for 25 min at 4°C with 50 µg/ml of either Proteinase K or Trypsin. The protease activity was terminated by incubation for 10 min at 4°C with either PMSF or trypsin inhibitor, respectively. Afterward, samples were centrifuged (18,000 x*g* 10 min, 2°C) and the supernatants were discarded. For SDS–PAGE, the pellets were dissolved in 2× sample buffer and then heated at 95°C for 10 min. Then, samples were loaded on either 12.5% or 15% SDS gels and blotted onto nitrocellulose membranes.

For analysis of import reactions with BN-PAGE, samples were dissolved in 1% (w/v) digitonin. After a clarifying spin (30,000 x*g*, 30 min, 2°C), the soluble supernatant was mixed with 10× BN loading dye. Samples were further analyzed by BN–PAGE and blotted onto polyvinylidene difluoride membranes. The imported proteins were visualized by autoradiography and AIDA image analyzer was used to quantify the intensity of protein bands.

Subcellular fractionation

Different cell fractions from yeast were separated using published subcellular fractionation protocol (Walther et al., 2009).

To obtain pure mitochondria fraction, isolated mitochondria were slowly layered on top of a Percoll gradient and separated by one round of ultracentrifugation (80,000 x*g*, 45 min, 2°C; Graham, 2001). The post-mitochondrial fraction was centrifuged (130,000 x*g*, 1 h, 2°C) using 60 Ti fixed angle rotor (Beckman). The pellet (ER fraction) was dissolved in 3 ml of SEM buffer containing 2 mM of PMSF and dounced 10 times in homogenizer. The dounced solution was clarified (18,000 x*g*, 20 min, 2°C) and microsomes/ER fraction was collected from the supernatant. Proteins in whole-cell lysate, cytosol, and ER fractions were precipitated by TCA and finally dissolved in 2× sample buffer and incubated at 95°C for 10 min before SDS–PAGE analysis. Proteins of interest were visualized by immunodecoration using the indicated antibodies. Table S4 indicates the antibodies used in the current study.

Alkaline extraction

Isolated mitochondria (50 µg) were resuspended in 100 µl of 0.1 M Na_2CO_3 solution and incubated for 25 min at 4°C. Samples were centrifuged (94,000 x*g*, 30 min, 2°C), and the supernatant was collected and precipitated by TCA. Both pellets and precipitated proteins from the supernatant were dissolved in 40 µl of 2× sample buffer and heated at 95°C for 10 min before further analysis by SDS–PAGE.

Peptide scan assay

Cellulose membranes harboring 20-mer peptides covering the sequence of Om14 were activated in methanol for 1 min and washed twice with sterile water for 1 min. Then, membranes were equilibrated at room temperature with binding buffer (50 mM Tris-HCl and 150 mM NaCl, pH 7.5) for 2 h. After blocking with 1 µM BSA for 1 h, membranes were incubated overnight with 0.5 µM GST–Tom70–cytosolic domain. Next, the membranes were washed three times with binding buffer, and bound protein was visualized by immunodecoration using an antibody against GST.

Fluorescence microscopy

Yeast cultures were initially grown overnight in synthetic media with 2% galactose. Cultures were then diluted to OD_{600} of 0.2 and after further growth, cells were harvested at the logarithmic phase (3,000 x*g*, 5 min, RT). The collected cells were mixed with 1% (w/v) low melting point agarose in a 1:1 (v/v) ratio and were plated on a glass slide. Spinning disk microscope Zeiss Axio Examiner Z1 equipped with a CSU-X1 real-time confocal system (Visitron) and SPOT Flex charge-coupled device camera (Visitron) was used. Samples were observed using Objective Plan-Apochromat 63×/1.4 Oil DIC M27 (Zeiss) at room temperature. Images from three different channels (Brightfield, GFP, and RFP) were acquired using the AxioVision software (Visitron). Cropping and merging of microscope images were done using Fiji software.

Online supplemental material

Fig. S1 shows additional in vitro import assays of truncated Om14 variants. Fig. S2 shows the establishment of the proteolytic assay and its usage to monitor import into isolated mammalian mitochondria. Fig. S3 demonstrates that the central TMD of Mim1 can replace the native protein. Fig. S4 demonstrates that increasing the hydrophobicity of TMD1 does not affect the membrane integration of Om14. Table S1 contains a list of yeast strains used in this study. Table S2 contains a list of plasmids used in this study. Table S3 contains a list of primers used in this study. Table S4 contains a list of antibodies used in this study.

Acknowledgments

We thank E. Kracker for excellent technical assistance, K. Maruszczak and Elias Schermuly for help with some experiments, V. Kozjak-Pavlovic (University of Würzburg, Würzburg, Germany) for cells, and J. Nunnari (University of California Davis, Davis, CA) and T. Becker (University of Bonn, Bonn, Germany) for antibodies.

This work was supported by the Deutsche Forschungsgemeinschaft (grants RA 1028/7-2 and 10-2 to D. Rapaport and CRC 894 to M. Jung).

The authors declare no competing financial interests.

Author contributions: J. Zhou and K.S. Dimmer designed and conducted experiments, M. Jung prepared the peptide scan membranes, D. Rapaport designed experiments and analyzed data. J. Zhou and D. Rapaport wrote the manuscript. All authors read and approved the final manuscript.

Submitted: 6 December 2021
Revised: 26 January 2022
Accepted: 3 February 2022

References

Backes, S., Y.S. Bykov, T. Flohr, M. Räschle, J. Zhou, S. Lenhard, L. Krämer, T. Mühlhaus, C. Bibi, C. Jann, J.D. Smith, et al. 2021. The chaperone-binding activity of the mitochondrial surface receptor Tom70 protects the cytosol against mitoprotein-induced stress. *Cell Rep.* 35:108936. https://doi.org/10.1016/j.celrep.2021.108936

Becker, T., L.S. Wenz, V. Krüger, W. Lehmann, J.M. Müller, L. Goroncy, N. Zufall, T. Lithgow, B. Guiard, A. Chacinska, R. Wagner, et al. 2011. The mitochondrial import protein Mim1 promotes biogenesis of multi-spanning outer membrane proteins. *J. Cell Biol.* 194:387–395. https://doi.org/10.1083/jcb.201102044

Brix, J., S. Rüdiger, B. Bukau, J. Schneider-Mergener, and N. Pfanner. 1999. Distribution of binding sequences for the mitochondrial import receptors Tom20, Tom22, and Tom70 in a presequence-carrying preprotein and a non- cleavable preprotein. *J. Biol. Chem.* 274:16522–16530. https://doi.org/10.1074/jbc.274.23.16522

Burri, L., K. Vascotto, I.E. Gentle, N.C. Chan, T. Beilharz, D.I. Stapleton, L. Ramage, and T. Lithgow. 2006. Integral membrane proteins in the mitochondrial outer membrane of Saccharomyces cerevisiae. *FEBS J.* 273:1507–1515. https://doi.org/10.1111/j.1742-4658.2006.05171.x

Cohen, M.M.J., G.P. Leboucher, N. Livnat-Levanon, M.H. Glickman, and A.M.W. Weissman. 2008. Ubiquitin–Proteasome-dependent degradation of a mitofusin, a critical regulator of mitochondrial fusion. *Mol. Biol. Cell.* 19:2457–2464. https://doi.org/10.1091/mbc.E08

Coonrod, E.M., M.A. Karren, and J.M. Shaw. 2007. Ugo1p is a multipass transmembrane protein with a single carrier domain required for mitochondrial fusion. *Traffic.* 8:500–511. https://doi.org/10.1111/j.1600-0854.2007.00550.x

Daum, G., S.M. Gasser, and G. Schatz. 1982. Import of proteins into mitochondria. Energy-dependent, two-step processing of the intermembrane space enzyme cytochrome b2 by isolated yeast mitochondria. *J. Biol. Chem.* 257:13075–13080. https://doi.org/10.1016/s0021-9258(18)33624-x

Dimmer, K.S., D. Papić, B. Schumann, D. Sperl, K. Krumpe, D.M. Walther, and D. Rapaport. 2012. A crucial role for Mim2 in the biogenesis of mitochondrial outer membrane proteins. *J. Cell Sci.* 125:3464–3473. https://doi.org/10.1242/jcs.103804

Doan, K.N., A. Grevel, C.U. Mårtensson, L. Ellenrieder, N. Thornton, L.S. Wenz, Ł. Opaliński, B. Guiard, N. Pfanner, and T. Becker. 2020. The mitochondrial import complex MIM functions as main translocase for α-helical outer membrane proteins. *Cell Rep.* 31:107567. https://doi.org/10.1016/j.celrep.2020.107567

Drwesh, L., and D. Rapaport. 2020. Biogenesis pathways of α-helical mitochondrial outer membrane proteins. *Biol. Chem.* 401:677–686. https://doi.org/10.1515/hsz-2019-0440

Ellenrieder, L., M.P. Dieterle, K.N. Doan, C.U. Mårtensson, A. Floerchinger, M.L. Campo, N. Pfanner, and T. Becker. 2019. Dual role of mitochondrial porin in metabolite transport across the outer membrane and protein transfer to the inner membrane. *Mol. Cell.* 73:1056–1065.e7. https://doi.org/10.1016/j.molcel.2018.12.014

Friedman, J.R., L.L. Lackner, M. West, J.R. DiBenedetto, J. Nunnari, and G.K. Voeltz. 2011. ER tubules mark sites of mitochondrial division. *Science.* 334:358–362. https://doi.org/10.1126/science.1207385

Ghosh, S., D.M. Iadarola, W.B. Ball, and V.M. Gohil. 2019. Mitochondrial dysfunctions in Barth syndrome. *IUBMB Life.* 71:791–801. https://doi.org/10.1002/iub.2018

Graham, J.M. 2001. Isolation of lysosomes from tissues and cells by differential and density gradient centrifugation. *Curr. Protoc. Cell Biol.* 3:3.6. https://doi.org/10.1002/0471143030.cb0306s07

Hermann, G.J., J.W. Thatcher, J.P. Mills, K.G. Hales, M.T. Fuller, J. Nunnari, and J.M. Shaw. 1998. Mitochondrial fusion in yeast requires the transmembrane GTPase Fzo1p. *J. Cell Biol.* 143:359–373. https://doi.org/10.1083/jcb.143.2.359

Hoppins, S., J. Horner, C. Song, J.M. McCaffery, and J. Nunnari. 2009. Mitochondrial outer and inner membrane fusion requires a modified carrier protein. *J. Cell Biol.* 184:569–581. https://doi.org/10.1083/jcb.200809099

Jores, T., A. Klinger, L.E. Groß, S. Kawano, N. Flinner, E. Duchardt-Ferner, J. Wöhnert, H. Kalbacher, T. Endo, E. Schleiff, and D. Rapaport. 2016. Characterization of the targeting signal in mitochondrial β-barrel proteins. *Nat. Commun.* 7:12036. https://doi.org/10.1038/ncomms12036

Jores, T., J. Lawatscheck, V. Beke, M. Franz-Wachtel, K. Yunoki, J.C. Fitzgerald, B. Macek, T. Endo, H. Kalbacher, J. Buchner, and D. Rapaport. 2018. Cytosolic Hsp70 and Hsp40 chaperones enable the biogenesis of mitochondrial β-barrel proteins. *J. Cell Biol.* 217:3091–3108. https://doi.org/10.1083/jcb.201712029

Kolodziej, M.P., and V.A. Zammit. 1990. Sensitivity of inhibition of rat liver mitochondrial outer-membrane carnitine palmitoyltransferase by malonyl-CoA to chemical- and temperature-induced changes in membrane fluidity. *Biochem. J.* 272:421–425. https://doi.org/10.1042/bj2720421

Kozjak-Pavlovic, V., K. Ross, N. Benlasfer, S. Kimmig, A. Karlas, and T. Rudel. 2007. Conserved roles of Sam50 and metaxins in VDAC biogenesis. *EMBO Rep.* 8:576–582. https://doi.org/10.1038/sj.embor.7400982

Kreimendahl, S., J. Schwichtenberg, K. Günnewig, L. Brandherm, and J. Rassow. 2020. The selectivity filter of the mitochondrial protein import machinery. *BMC Biol.* 18:156. https://doi.org/10.1186/s12915-020-00888-z

Lauffer, S., K. Mäbert, C. Czupalla, T. Pursche, B. Hoflack, G. Rödel, and U. Krause-Buchholz. 2012. Saccharomyces cerevisiae porin pore forms complexes with mitochondrial outer membrane proteins Om14p and Om45p. *J. Biol. Chem.* 287:17447–17458. https://doi.org/10.1074/jbc.M111.328328

Lesnik, C., Y. Cohen, A. Atir-Lande, M. Schuldiner, and Y. Arava. 2014. OM14 is a mitochondrial receptor for cytosolic ribosomes that supports co-translational import into mitochondria. *Nat. Commun.* 5:5711. https://doi.org/10.1038/ncomms6711

Morgenstern, M., S.B. Stiller, P. Lübbert, C.D. Peikert, S. Dannenmaier, F. Drepper, U. Weill, P. Höß, R. Feuerstein, M. Gebert, M. Bohnert, et al. 2017. Definition of a high-confidence mitochondrial proteome at quantitative scale. *Cell Rep.* 19:2836–2852. https://doi.org/10.1016/j.celrep.2017.06.014

Neupert, W., and J.M. Herrmann. 2007. Translocation of proteins into mitochondria. *Annu. Rev. Biochem.* 76:723–749. https://doi.org/10.1146/annurev.biochem.76.052705.163409

Opaliński, Ł., J. Song, C. Priesnitz, L.S. Wenz, S. Oeljeklaus, B. Warscheid, N. Pfanner, and T. Becker. 2018. Recruitment of cytosolic J-proteins by TOM receptors promotes mitochondrial protein biogenesis. *Cell Rep.* 25:2036–2043.e5. https://doi.org/10.1016/j.celrep.2018.10.083

Otera, H., Y. Taira, C. Horie, Y. Suzuki, H. Suzuki, K. Setoguchi, H. Kato, T. Oka, and K. Mihara. 2007. A novel insertion pathway of mitochondrial outer membrane proteins with multiple transmembrane segments. *J. Cell Biol.* 179:1355–1363. https://doi.org/10.1083/jcb.200702143

Papić, D., K. Krumpe, J. Dukanovic, K.S. Dimmer, and D. Rapaport. 2011. Multispan mitochondrial outer membrane protein Ugo1 follows a unique Mim1-dependent import pathway. *J. Cell Biol.* 194:397–405. https://doi.org/10.1083/jcb.201102041

Paschen, S.A., T. Waizenegger, T. Stan, M. Preuss, M. Cyrklaff, K. Hell, D. Rapaport, and W. Neupert. 2003. Evolutionary conservation of biogenesis of β-barrel membrane proteins. *Nature.* 426:862–866. https://doi.org/10.1038/nature02208

Pfaller, R., N. Pfanner, and W. Neupert. 1989. Mitochondrial protein import: bypass of proteinaceous surface receptors can occur with low specificity and efficiency. *J. Biol. Chem.* 264:34–39.

Pfanner, N., B. Warscheid, and N. Wiedemann. 2019. Mitochondrial proteins: from biogenesis to functional networks. *Nat. Rev. Mol. Cell Biol.* 20:267–284. https://doi.org/10.1038/s41580-018-0092-0

Popov-Čeleketić, J., T. Waizenegger, and D. Rapaport. 2008. Mim1 functions in an oligomeric form to facilitate the integration of Tom20 into the mitochondrial outer membrane. *J. Mol. Biol.* 376:671–680. https://doi.org/10.1016/j.jmb.2007.12.006

Sakaue, H., T. Shiota, N. Ishizaka, S. Kawano, Y. Tamura, K.S. Tan, K. Imai, C. Motono, T. Hirokawa, K. Taki, N. Miyata, et al. 2019. Porin associates with Tom22 to regulate the mitochondrial protein gate assembly. *Mol. Cell.* 73:1044–1055.e8. https://doi.org/10.1016/j.molcel.2019.01.003

Sauerwald, J., T. Jores, M. Eisenberg-Bord, S.G. Chuartzman, M. Schuldiner, and D. Rapaport. 2015. Genome-wide screens in Saccharomyces cerevisiae highlight a role for cardiolipin in biogenesis of mitochondrial outer membrane multispan proteins. *Mol. Cell. Biol.* 35:3200–3211. https://doi.org/10.1128/mcb.00107-15

Sinzel, M., T. Tan, P. Wendling, H. Kalbacher, C. Özbalci, X. Chelius, B. Westermann, B. Brügger, D. Rapaport, and K.S. Dimmer. 2017. Mcp3 is a novel mitochondrial outer membrane protein that follows a unique IMP-dependent biogenesis pathway. *EMBO Rep.* 18:1869. https://doi.org/10.15252/embr.201745020

Sogo, L.F., and M.P. Yaffe. 1994. Regulation of mitochondrial morphology and inheritance by Mdm10p, a protein of the mitochondrial outer membrane. *J. Cell Biol.* 126:1361–1373. https://doi.org/10.1083/jcb.126.6.1361

Thomas, B.J., and R. Rothstein. 1989. Elevated recombination rates in transcriptionally active DNA. *Cell.* 56:619–630. https://doi.org/10.1016/0092-8674(89)90584-9

Vitali, D.G., L. Drwesh, B.A. Cichocki, A. Kolb, and D. Rapaport. 2020. The biogenesis of mitochondrial outer membrane proteins show variable dependence on import factors. *iScience.* 23:100779. https://doi.org/10.1016/j.isci.2019.100779

Vögtle, F.N., M. Keller, A.A. Taskin, S.E. Horvath, X.L. Guan, C. Prinz, M. Opalińska, C. Zorzin, M. van der Laan, M.R. Wenk, R. Schubert, et al. 2015. The fusogenic lipid phosphatidic acid promotes the biogenesis of mitochondrial outer membrane protein Ugo1. *J. Cell Biol.* 210:951–960. https://doi.org/10.1083/jcb.201506085

Waizenegger, T., T. Stan, W. Neupert, and D. Rapaport. 2003. Signal-anchor domains of proteins of the outer membrane of mitochondria: structural and functional characteristics. *J. Biol. Chem.* 278:42064–42071. https://doi.org/10.1074/jbc.M305736200

Walther, D.M., and D. Rapaport. 2009. Biogenesis of mitochondrial outer membrane proteins. *Biochim. Biophys. Acta.* 1793:42–51. https://doi.org/10.1016/j.bbamcr.2008.04.013

Walther, D.M., D. Papic, M.P. Bos, J. Tommassen, and D. Rapaport. 2009. Signals in bacterial β-barrel proteins are functional in eukaryotic cells for targeting to and assembly in mitochondria. *Proc. Natl. Acad. Sci. USA.* 106:2531–2536. https://doi.org/10.1073/pnas.0807830106

Wan, J., J. Steffen, M. Yourshaw, H. Mamsa, E. Andersen, S. Rudnik-Schöneborn, K. Pope, K.B. Howell, C.A. Mclean, A.J. Kornberg, J. Joseph, et al. 2016. Loss of function of SLC25A46 causes lethal congenital pontocerebellar hypoplasia. *Brain.* 139:2877–2890. https://doi.org/10.1093/brain/aww212

Wei, X., M. Du, J. Xie, T. Luo, Y. Zhou, K. Zhang, J. Li, D. Chen, P. Xu, M. Jia, H. Zhou, et al. 2020. Mutations in TOMM70 lead to multi-OXPHOS deficiencies and cause severe anemia, lactic acidosis, and developmental delay. *J. Hum. Genet.* 65:231–240. https://doi.org/10.1038/s10038-019-0714-1

Wimley, W.C., and S.H. White. 1996. Experimentally determined hydrophobicity scale for proteins at Membrane Interfaces. *Nat. Strut. Biol.* 3:842–848. https://doi.org/10.1038/nsb1096-842

Young, J.C., N.J. Hoogenraad, and F.U. Hartl. 2003. Molecular chaperones Hsp90 and Hsp70 deliver preproteins to the mitochondrial import receptor Tom70. *Cell.* 112:41–50. https://doi.org/10.1016/s0092-8674(02)01250-3

Supplemental material

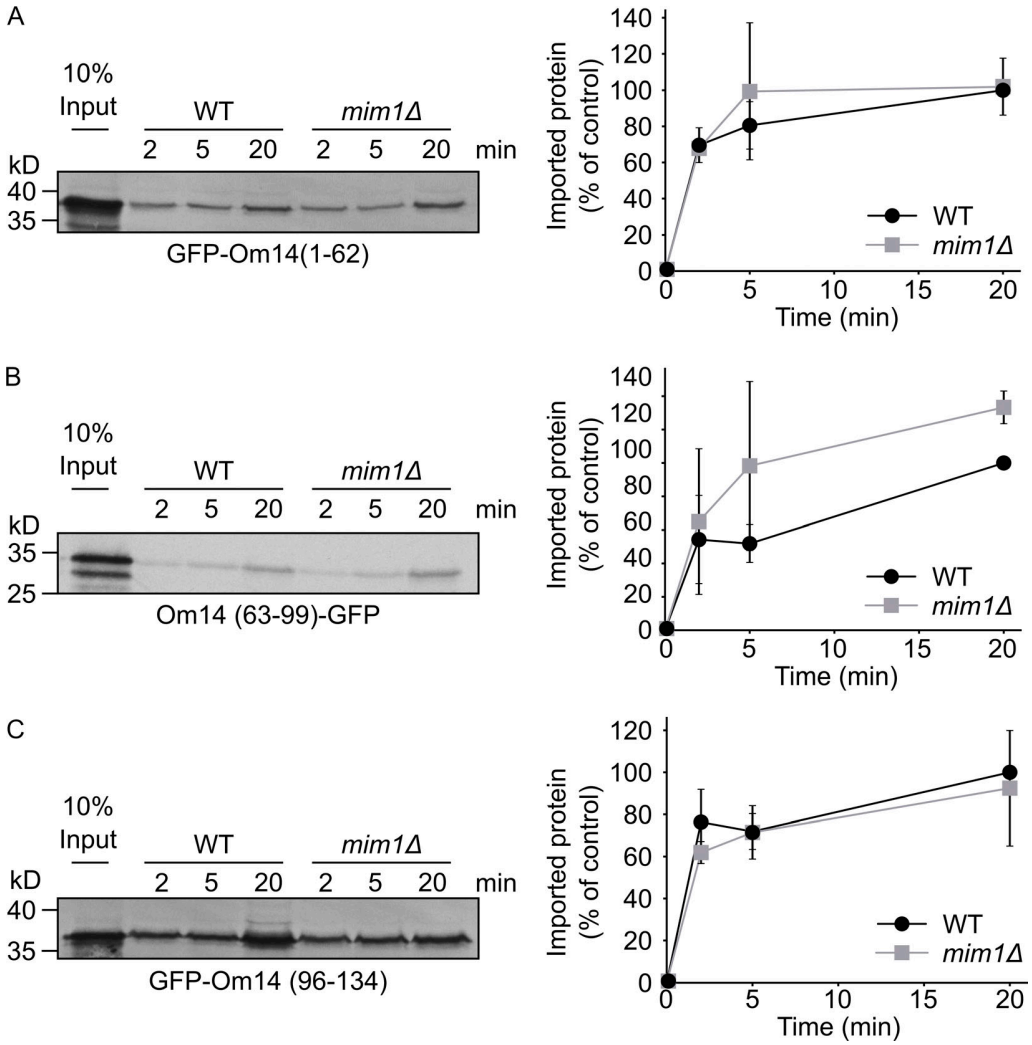

Figure S1. **The import of truncated Om14 variants is only mildly dependent on Mim1. (A–C)** Radiolabeled truncated variants of Om14 fused to GFP were incubated with mitochondria isolated from either WT or *mim1Δ* cells. At the end of the import reactions, samples were subjected to alkaline extraction and the pellets fractions were analyzed by SDS–PAGE and autoradiography. Right: Quantification of three independent experiments. The intensity of the band corresponding to import for 20 min into control organelles was set to 100%. Source data are available for this figure: SourceData FS1.

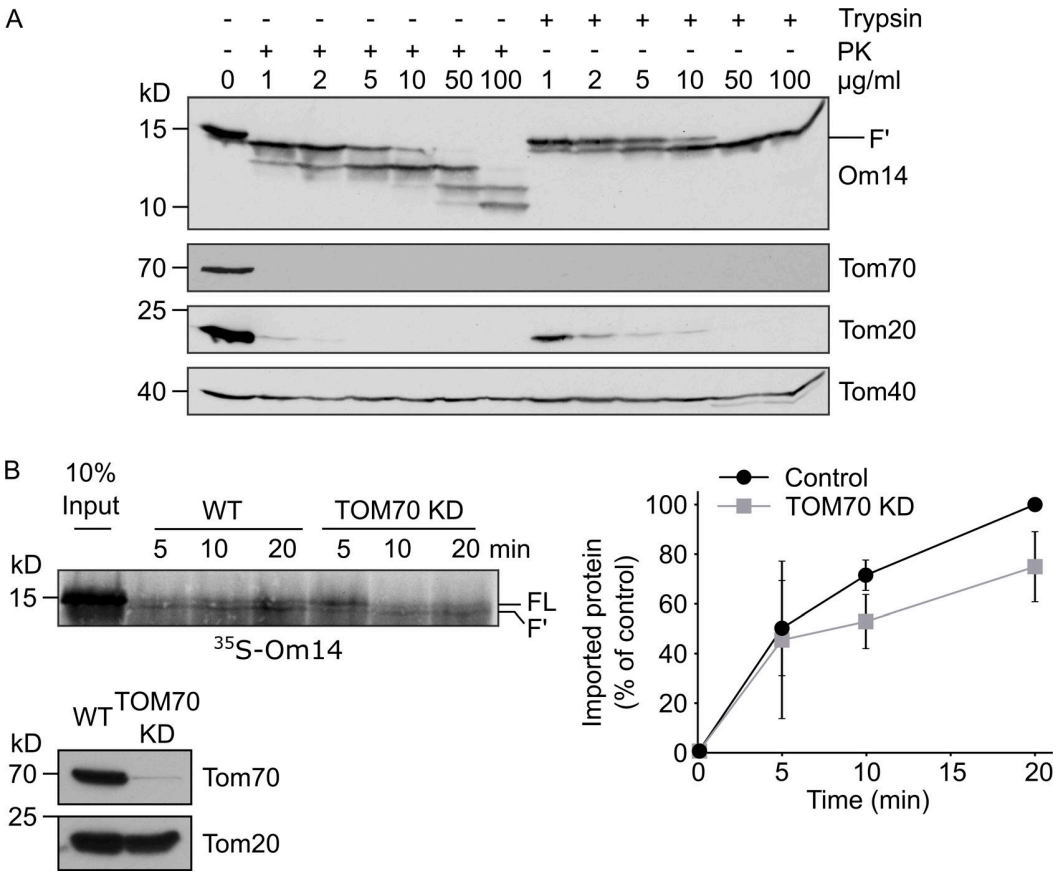

Figure S2. **TOM70 contributes to the import of Om14 into mammalian mitochondria. (A)** Isolated yeast mitochondria were treated with the indicated concentrations of either Proteinase K (PK) or trypsin. Mitochondrial proteins were then analyzed by SDS–PAGE and immunodecoration with the indicated antibodies. Tom20 and Tom70 are exposed on the surface of the organelle, whereas Tom40 is embedded within the membrane. **(B)** Radiolabeled Om14 was imported into mitochondria isolated from either control human HeLa cells or HeLa cells where Tom70 was knocked down. After the import, samples were treated with trypsin and analyzed and quantified as described in the legend to Fig. 2 B. The lower panel shows analysis of the isolated mitochondria by SDS–PAGE and Western blotting with the indicated antibodies. Note: TOM70 is hardly detected in the KD cells. Right: Quantification of the import efficiency was done as described in the legend to Fig. 2 B. Source data are available for this figure: SourceData FS2.

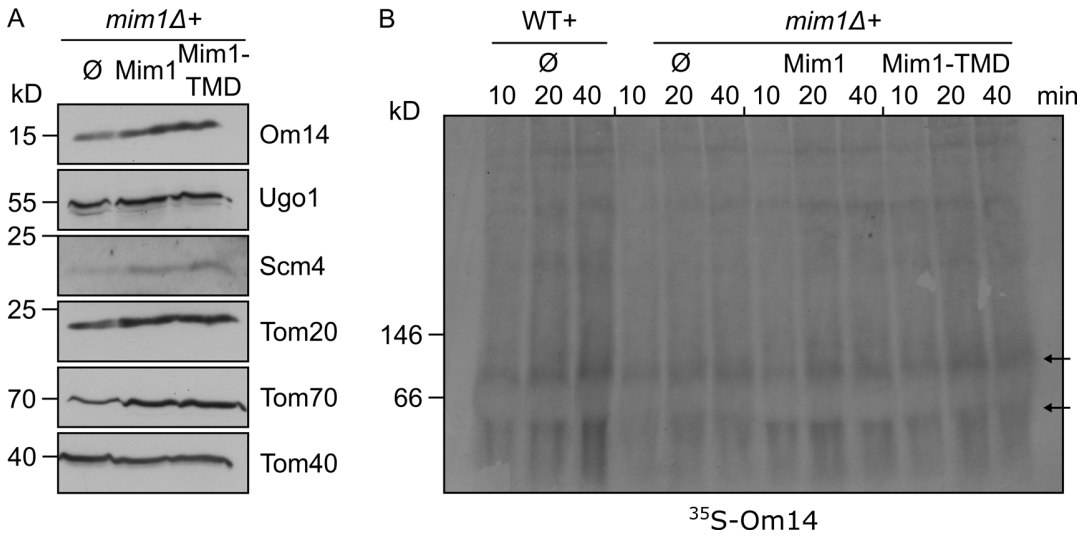

Figure S3. **The central TMD of Mim1 can replace the native protein. (A)** Mitochondria were isolated from mim1Δ cells harboring an empty vector (Ø) or a plasmid encoding either native Mim1 or its central TMD. The steady-state levels of known Mim1 substrates as well as of Tom40 (for comparison) were analyzed by SDS–PAGE and immunodecorated with the indicated antibodies. **(B)** Radiolabeled Om14 was imported into mitochondria isolated from the indicated cells and further analyzed by BN–PAGE and autoradiography. Both arrows mark oligomeric species of Om14. Source data are available for this figure: SourceData FS3.

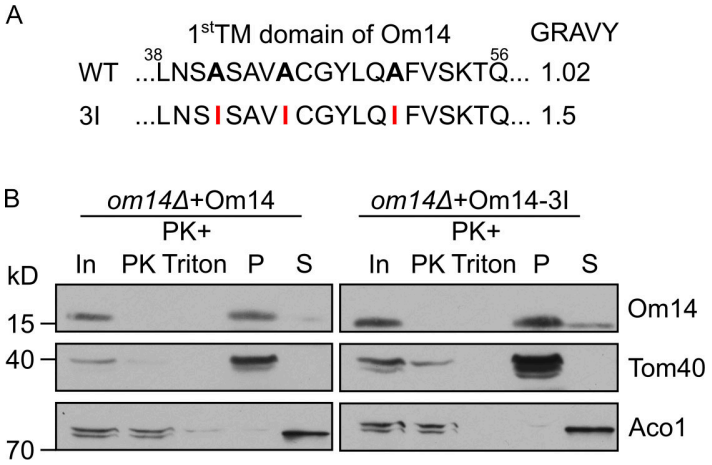

Figure S4. **Increasing the hydrophobicity of TMD1 does not affect the membrane integration of Om14. (A)** Amino acid sequence of the putative first TMD of both native Om14 (WT) and a variant with increased hydrophobicity due to the introduction of three Ile residues (3I). Mutated residues are in bold. **(B)** Mitochondria isolated from om14Δ cells expressing either native Om14 or the Om14-3I variant were subjected to Proteinase K treatment or alkaline extraction. Samples were further analyzed by SDS–PAGE and immunodecoration with the indicated antibodies. Source data are available for this figure: SourceData FS4

Provided online are Table S1, Table S2, Table S3, and Table S4. Table S1 lists the yeast strains used in this study. Table S2 lists the plasmids used in this study. Table S3 lists the primers used in this study. Table S4 lists the antibodies used in this study.

Table S1. Yeast strains used in this study.

Name	Mating type	Genetic background	Source of reference
W303a	MATa	*ade2-1 can1-1100 his3-11 leu2 3_112 trp1Δ2 ura3-52*	(Thomas and Rothstein, 1989)
W303α	MATα	*ade2-1 can1-1100 his3-11 leu2 3_112 trp1Δ2 ura3-52*	(Thomas and Rothstein, 1989)
mim1Δ	MATa	W303a; *mim1Δ::KanMX*	(Dimmer et al., 2012)
mim1Δ	MATα	W303α; *mim1Δ::KanMX*	(Dimmer et al., 2012)
tom70Δ/71Δ	MATα	W303α; *tom70Δ::KanMX tom71Δ::Nat*	(Jores et al., 2018)
por1Δ	MATα	W303α; *por1Δ::His3*	This study
om45Δ	MATα	W303α; *om45Δ::His3*	This study
om14Δ	MATa	W303a; *om14Δ::His3*	This study
por1Δ /mim1Δ	MATa	W303α; *por1Δ::His3 mim1Δ::KanMX*	This study

Dimmer, K.S., D. Papić, B. Schumann, D. Sperl, K. Krumpe, D.M. Walther, and D. Rapaport. 2012. A crucial role for Mim2 in the biogenesis of mitochondrial outer membrane proteins. J. Cell Sci. 125:3464–3473. 10.1242/jcs.103804

Jores, T., J. Lawatscheck, V. Beke, M. Franz-Wachtel, K. Yunoki, J.C. Fitzgerald, B. Macek, T. Endo, H. Kalbacher, J. Buchner, and D. Rapaport. 2018. Cytosolic Hsp70 and Hsp40 chaperones enable the biogenesis of mitochondrial β-barrel proteins. J. Cell Biol. 217:3091–3108. 10.1083/jcb.201712029

Thomas, B.J., and R. Rothstein. 1989. Elevated recombination rates in transcriptionally active DNA. Cell. 56:619–630. 10.1016/0092-8674(89)90584-9

Table S2. Plasmids used in this study.

Plasmid	Promoter	Coding Sequence(aa)	Markers	Source
pYX142	TPI	Ø	Amp^R, LEU2	#MBV026, Novagen
pYX142-eGFP	TPI	eGFP	Amp^R, LEU2	(Jores et al., 2016)
pYX142-eGFP-Om14	TPI	Om14 full length	Amp^R, LEU2	This study
pYX142-eGFP-Om14(1-62)	TPI	Om14(1-62)	Amp^R, LEU2	This study
pYX142-Om14(63-95)-eGFP	TPI	Om14(63-95)	Amp^R, LEU2	This study
pYX142-eGFP-Om14(96-134)	TPI	Om14(96-134)	Amp^R, LEU2	This study
pYX142-Om14(63-99)-eGFP	TPI	Om14(63-99)	Amp^R, LEU2	This study
pYX142-Om14-4A	TPI	Om14-4 alanine mutation	Amp^R, LEU2	This study
pYX142-Om14-3I	TPI	Om14-3 Ile mutation	Amp^R, LEU2	This study
pGEM4	SP6	Ø	Amp^R	P2161, Promega
pGEM4-Om14	SP6	Om14 full length	Amp^R	This study
pGEM4-Om14-4A	SP6	Om14-4 Ala mutation	Amp^R	This study
pGEM4-Ugo1-2HA	SP6	Ugo1	Amp^R	(Papić et al., 2011)
pGEM4-Porin-3HA	SP6	Porin	Amp^R	(Jores et al., 2018)

Jores, T., A. Klinger, L.E. Groß, S. Kawano, N. Flinner, E. Duchardt-Ferner, J. Wöhnert, H. Kalbacher, T. Endo, E. Schleiff, and D. Rapaport. 2016. Characterization of the targeting signal in mitochondrial β-barrel proteins. Nat. Commun. 7:12036. 10.1038/ncomms12036

Jores, T., J. Lawatscheck, V. Beke, M. Franz-Wachtel, K. Yunoki, J.C. Fitzgerald, B. Macek, T. Endo, H. Kalbacher, J. Buchner, and D. Rapaport. 2018. Cytosolic Hsp70 and Hsp40 chaperones enable the biogenesis of mitochondrial β-barrel proteins. J. Cell Biol. 217:3091–3108. 10.1083/jcb.201712029

Papić, D., K. Krumpe, J. Dukanovic, K.S. Dimmer, and D. Rapaport. 2011. Multispan mitochondrial outer membrane protein Ugo1 follows a unique Mim1-dependent import pathway. J. Cell Biol. 194:397–405. 10.1083/jcb.201102041

Table S3. Primers used in this study.

Primer name	Sequence (5′-3′)	Note
JZ020_GFPom14(96-134)_for	CCATGGATCCCATGAGATTCTTGAAGG	Amplification of the sequence encoding amino acids 96-134 of Om14, BamHI restriction site at 5’
JZ021_GFPom14(96-134)_rev	CCGGGTCGACTTATTTCTTGTCGTATC	Amplification of the sequence encoding amino acids 96-134 of Om14, SalI restriction site at 5’
JZ022_GFPom14(1-95)_for	CCATGGATCCCATGTCTGCAACTGC	Amplification of the sequence encoding amino acids 1-95 of Om14, BamHI restriction site at 5’
JZ023_GFPom14(1-95)_rev	CCGGGTCGACTTAGGCGTTGTGG	Amplification of the sequence encoding amino acids 1-95 of Om14, SalI restriction site at 5’
JZ032_Om14A45A51-I_for	GTGCATCAGCAGTCATTTGCGGCTACCTCCAAATTTTTGTCAGTAAGACGC	Site-directed mutagenesis
JZ033_Om14A45A51-I_rev	GCGTCTTACTGACAAAAATTTGGAGGTAGCCGCAAATGACTGCTGATGCAC	Site-directed mutagenesis
JZ034_Om14A41-I_for	CTGAAGGCACGGTTAAATAGTATTTCAGCAGTCATTTGCGGCTACC	Site-directed mutagenesis
JZ035_Om14A41-I_rev	GGTAGCCGCAAATGACTGCTGAAATACTATTTAACCGTGCCTTCAG	Site-directed mutagenesis
JZ036_GFPom14(1-62)_rev	CCGGGTCGACTTATACTTTGGCAAAGTC	Amplification of the sequence encoding amino acids 1-62 of Om14, SalI restriction site at 5’
JZ037_GFPom14(62-95)_for	CCATGGATCCCATGTGCTTTTTAGAACTTCAG	Amplification of the sequence encoding amino acids 63-95 of Om14, BamHI restriction site at 5’

JZ057_EcoRI om14TM2_for	CCTAGAATTCATGTGCTTTTTAGAA CTTCAG	Amplification of the sequence encoding amino acids 63-95 of Om14, EcoRI restriction site at 5’
JZ058_om14 TM2_KpnI_re v	CGCGGTACCGGCGTTGTGG	Amplification of the sequence encoding amino acids 63-95 of Om14, KpnI restriction site at 5’
JZ059_EcoRI _Om14TM2'_f or	CCATGAATTCATGGCCAAAGTATG C	Amplification of the sequence encoding amino acids 63-99 of Om14, EcoRI restriction site at 5’
JZ060_Om14 TM2'_KpnI_re v	CGCGGTACCCTTCAAGAATCTG	Amplification of the sequence encoding amino acids 63-99 of Om14, KpnI restriction site at 5’

Table S4. Antibodies used in this study.

Antibodies	Dilution	Source / Reference
polyclonal rabbit anti-GFP	1:2,000	TP401 (Torry Pines)
polyclonal rabbit anti-Tom70	1:2,000	Waizenegger et al., 2003
polyclonal rabbit anti-Tom40	1:5,000	Paschen et al., 2003
polyclonal rabbit anti-Tom20	1:2,000	Waizenegger et al., 2003
polyclonal rabbit anti-Mim1	1:500	Dimmer et al., 2012
polyclonal rabbit anti-Om14	1:2,000	Sauerwald et al., 2015
polyclonal rabbit anti-Aco1	1:10,000	Sauerwald et al., 2015
polyclonal rabbit anti-Hexokinase	1:3,000	100-4159, BioTrend
polyclonal mouse anti-AAC	1:5,000	Walther et al., 2009
polyclonal rabbit anti-Erv2	1:2,000	Sauerwald et al., 2015
polyclonal rabbit anti-Scm4	1:250	Becker et al., 2011
polyclonal rabbit anti-Porin	1:3,000	Sauerwald et al., 2015
polyclonal rabbit anti-Ugo1	1:2,000	Hoppins et al., 2009
monoclonal mouse anti-Tom70 (mammalian)	1:500	sc-390545, Santa Cruz Biotechnology
monoclonal mouse anti-Tom20 (mammalian)	1:500	sc-17764, Santa Cruz Biotechnology
Goat anti-rabbit IgG (H+L)-HRP conjugate	1:10,000	#1721019, Bio-Rad
Goat anti-mouse IgG (H+L)-HRP conjugate	1:2,500	#1721011, Bio-Rad

Becker, T., L.S. Wenz, V. Krüger, W. Lehmann, J.M. Müller, L. Goroncy, N. Zufall, T. Lithgow, B. Guiard, A. Chacinska, R. Wagner, et al. 2011. The mitochondrial import protein Mim1 promotes biogenesis of multispanning outer membrane proteins. J. Cell Biol. 194:387–395. 10.1083/jcb.201102044

Dimmer, K.S., D. Papić, B. Schumann, D. Sperl, K. Krumpe, D.M. Walther, and D. Rapaport. 2012. A crucial role for Mim2 in the biogenesis of mitochondrial outer membrane proteins. J. Cell Sci. 125:3464–3473. 10.1242/jcs.103804

Hoppins, S., J. Horner, C. Song, J.M. McCaffery, and J. Nunnari. 2009. Mitochondrial outer and inner membrane fusion requires a modified carrier protein. J. Cell Biol. 184:569–581. 10.1083/jcb.200809099

Paschen, S.A., T. Waizenegger, T. Stan, M. Preuss, M. Cyrklaff, K. Hell, D. Rapaport, and W. Neupert. 2003. Evolutionary conservation of biogenesis of β-barrel membrane proteins. Nature. 426:862–866. 10.1038/nature02208

Sauerwald, J., T. Jores, M. Eisenberg-Bord, S.G. Chuartzman, M. Schuldiner, and D. Rapaport. 2015. Genome-wide screens in Saccharomyces cerevisiae highlight a role for cardiolipin in biogenesis of mitochondrial outer membrane multispan proteins. Mol. Cell. Biol. 35:3200–3211. 10.1128/mcb.00107-15

Waizenegger, T., T. Stan, W. Neupert, and D. Rapaport. 2003. Signal-anchor domains of proteins of the outer membrane of mitochondria: structural and functional characteristics. J. Biol. Chem. 278:42064–42071. 10.1074/jbc.M305736200

Walther, D.M., D. Papic, M.P. Bos, J. Tommassen, and D. Rapaport. 2009. Signals in bacterial β-barrel proteins are functional in eukaryotic cells for targeting to and assembly in mitochondria. Proc. Natl. Acad. Sci. USA. 106:2531–2536. 10.1073/pnas.0807830106